Durham University

Durham E-Theses

Assessing trace metal pollution along the northeast and North Yorkshire coasts using brown algae

Eileen M Brendler-Spaeth

How to cite:

Brendler-Spaeth, Eileen M (2026) Assessing trace metal pollution along the northeast and North Yorkshire coasts using brown algae. Masters thesis, Durham University.

Use policy

The full-text may be used and/or reproduced, and given to third parties in any format or medium, without prior permission or charge, for personal research or study, educational, or not-for-profit purposes provided that:

- a full bibliographic reference is made to the original source
- a https://etheses.durham.ac.uk/id/eprint/16679/ is made to the metadata record in Durham E-Theses
- the full-text is not changed in any way

The full-text must not be sold in any format or medium without the formal permission of the copyright holders.

Please consult the full Durham E-Theses policy for further details.

Academic Support Office, The Palatine Centre, Durham University, Stockton Road, Durham, DH1 3LE
e-mail: e-theses.admin@durham.ac.uk Tel: +44 0191 334 6107
https://etheses.durham.ac.uk

Assessing trace metal pollution along the northeast and North Yorkshire coasts using brown algae

Eileen Marie Brendler-Spaeth

Department of Earth Sciences, Durham University

2025

This thesis is submitted in fulfilment of the requirements for the degree MScR Geological Sciences (F6A209).

Abstract

Sediments in the Tees Estuary are among the most metal-contaminated in the UK, reflecting a legacy of metal mining and industrial activity. Regular dredging and offshore disposal of these sediments may contribute to marine metal pollution, yet few studies have investigated bioavailable concentrations in this region. This study employed four species of brown algae (*Laminaria digitata*, *L. hyperborea*, *Fucus vesiculosus*, and *F. serratus*) as biological monitors to assess trace metal pollution along the northeast and North Yorkshire coastlines. Samples underwent acid digestion and were analysed for Fe, Zn, Mn, Cu, Ni, Cd, Cr, and Pb using inductively coupled plasma mass spectrometry (ICP-MS).

Overall, trace metal concentrations were comparable to background levels, indicating largely unpolluted conditions and minimal change since the late 1990s. Nevertheless, significant declines in macroalgal Fe, Cu, Zn, and Pb levels downstream of the Tees Estuary point to sediment disturbance as a potential source of contamination. Anomalously elevated Pb concentrations exhibited by two specimens from South Gare suggest transient inputs or fine particulate contamination of sample surfaces. Some trace metal concentrations at Cullercoats Beach were also relatively high compared to other sites, indicating possible influence from the Tyne Estuary. Interspecific and intrathallus variations were evident for several elements, with factors such as shore level, season, and year also likely affecting metal uptake. Despite these complexities, brown algae proved to be effective indicators of bioavailable trace metals, though their continued application requires tighter control of sampling variables and an improved understanding of uptake processes.

Table of contents

Statement of copyright

The copyright of this thesis (including any appendices or supplementary materials) rests with the author, unless otherwise stated.

Acknowledgements

I am grateful to the Fishmongers' Company's Fisheries Charitable Trust for their sponsorship, without which this research would not have been possible. I am especially grateful to my supervisor Prof. Darren Gröcke for his support and guidance throughout this project. I would also like to thank Freya Alldred, Jacqueline Pealing, and Prof. Rodney Forster (University of Hull) for their assistance with sample provision. Special thanks to Dr Gillian Taylor (Teesside University) and Dr Chris Ottley for their expertise and support with sample digestion and analysis.

1. Introduction

1.1. Trace metal pollution in marine environments

1.1.1. What are trace metals?

Trace metals, often referred to as heavy metals, are metals or metalloids with a density of at least 5.0 g/cm^3 (Huang *et al.*, 2025). Whilst some trace metals, such as Mn, Cu, and Zn, are essential for biological functions, they become toxic at elevated concentrations (e.g., Bryan, 1971; Chung and Lee, 1989; Ryan, McLoughlin and O'Donovan, 2012; Espinoza *et al.*, 2021). Others, including Cd, Pb, and Cr, are classed as non-essential elements and are toxic even at low concentrations (Espinoza *et al.*, 2021).

1.1.2. Sources of trace metal pollution

Trace metal pollution may occur naturally (e.g., via weathering of mineral deposits) or as a result of anthropogenic activities (Chung and Lee, 1989). Metals from anthropogenic sources may enter coastal and estuarine systems via fluvial transport, atmospheric deposition, waste dumping, and maritime activities (Bryan, 1980). Mining and industrial processes have led to the discharge of substantial quantities of trace metals into the marine environment (Bryan, 1971; Tomlinson *et al.*, 1980; Aboal *et al.*, 2023). In English fluvial and coastal systems, abandoned metal mines represent the largest sources of trace metal contamination (DEFRA, 2023). The UK's long legacy of metal mining has left thousands of abandoned metal mines across the country (Environment Agency, 2025a). In 2022, 1491 km of English rivers and estuaries were classified as polluted by mine-derived metals (Environment Agency, 2025a).

1.1.3. Why monitor trace metal pollution in marine environments?

Owing to their toxicity, persistence, and ability to bioaccumulate, trace metals, both essential and non-essential, pose a major threat to ecosystem structure and function (Aboal *et al.*, 2023). Bioaccumulated metals may also enter the human food chain via seafood consumption, presenting risks to human health. Chronic exposure to trace metals has been linked to a wide range of adverse outcomes, including

cognitive impairment, cardiovascular disease, renal dysfunction, and various cancers (García-Seoane *et al.*, 2018; Huang *et al.*, 2025).

Although there is evidence that global trace metal concentrations in marine environments have declined over the last 50 years (Aboal *et al.*, 2023), ongoing monitoring remains imperative. Effective management of estuarine and marine systems requires continuous assessment of trace metal pollution to support a wide range of sectors including industry, fisheries, harbour maintenance, conservation, and recreation (e.g., Phillips, 1977; Plater *et al.*, 1999; Sawidis *et al.*, 2001).

1.2. Monitoring trace metal pollution in marine environments

1.2.1. Limitations of seawater-based monitoring

Commonly used media for assessing marine trace metal pollution include seawater, sediment, and littoral biota (Phillips, 1977; Davies, Tomlinson and Stephenson, 1991; Giusti, Williamson and Mistry, 1999; Giusti, 2001). Trace metal concentrations in seawater are prone to considerable temporal and spatial variability due to transient factors such as tidal currents, marine circulation, freshwater inputs, and biochemical reactions (Phillips, 1977; Bryan, 1980; Tomlinson *et al.*, 1980; Davies, Tomlinson and Stephenson, 1991). Such variability complicates efforts to obtain representative measurements of overall pollution levels (Davies, Tomlinson and Stephenson, 1991). Mitigating these challenges requires repeated sampling over time, which is both resource-intensive and time-consuming (Phillips, 1977; Bryan, 1980; Tomlinson *et al.*, 1980; Stengel *et al.*, 2004). Furthermore, trace metal concentrations in seawater are typically very low, requiring high-sensitivity instrumentation or sample pre-concentration for accurate measurement (Tomlinson *et al.*, 1980).

1.2.2. Limitations of sediment-based monitoring

Sediment is often considered a more suitable indicator of marine trace metal pollution, as it reflects long-term accumulation of contaminants (Davies, Tomlinson and Stephenson, 1991). This temporal integration reduces the influence of short-term fluctuations that may otherwise produce misleading results (Sawidis *et al.*, 2001). Nevertheless, sediment-based monitoring presents its own challenges. For

example, variations in sedimentation rate and organic content may complicate interpretations (Phillips, 1977). Furthermore, trace metal levels in sediment or seawater do not necessarily reflect bioavailability, which refers to the proportion of contaminants accessible for uptake by organisms (Phillips, 1977; Bryan, 1980; Giusti, 2001). Since bioavailability is critical in assessing ecological and human health risks (Phillips, 1977), biotic materials such as macroalgae (seaweeds) may serve as more meaningful indicators of marine trace metal pollution.

1.2.3. Macroalgae as biomonitors

Macroalgae were first employed as biological monitors (biomonitors) of marine trace metal pollution in the early 1950s (Black and Mitchell, 1952) and their application has expanded in recent decades (García-Seoane *et al.*, 2018). Brown algae (Phaeophyceae), a class of macroalgae, are particularly suitable biomonitors of dissolved trace metal concentrations owing to the suite of polysaccharides present in their cell walls (Forsberg *et al.*, 1988; Davis, Volesky and Mucci, 2003; Stengel, McGrath and Morrison, 2005). These polysaccharides exhibit a strong affinity for divalent cations, including trace metals (Haug, 1961; Davis, Volesky and Mucci, 2003; Stengel, McGrath and Morrison, 2005).

Unlike other marine organisms, macroalgae cannot regulate their trace metal content, allowing them to accumulate metals to concentrations that are orders of magnitude higher than those in surrounding seawater (e.g., Black and Mitchell, 1952; Bryan, 1969; Fuge and James, 1973). This high accumulation capacity is advantageous for monitoring purposes, as it enables detection without the need for pre-concentration methods (Phillips, 1977; Tomlinson *et al.*, 1980).

Like sediment, macroalgal tissue concentrations reflect time-integrated values of ambient dissolved levels (Fuge and James, 1973, 1974; Foster, 1976; Phillips, 1977; Forsberg *et al.*, 1988; García-Seoane *et al.*, 2018). Their sedentary nature ensures that tissue concentrations are representative of local environmental conditions (Phillips, 1977; Tomlinson *et al.*, 1980; Stengel *et al.*, 2004; Viana *et al.*, 2010; Ryan, McLoughlin and O'Donovan, 2012; Chalkley *et al.*, 2019). Additionally, macroalgae are widely distributed and easily sampled (Fuge and James, 1974; Phillips, 1977; Tomlinson *et al.*, 1980; Stengel *et al.*, 2004; Viana *et al.*, 2010; Ryan, McLoughlin and O'Donovan, 2012; Chalkley *et al.*, 2019). They prove particularly

useful for identifying high-risk areas with anomalously elevated concentrations that warrant further investigation (Viana *et al.*, 2010; Chalkley *et al.*, 2019).

1.3. Research aim and objectives

Limited research has been conducted since the 1990s and early 2000s concerning trace metal pollution along the northeast and North Yorkshire coasts (Smurthwaite, 2006; Alderton, 2012). The majority of studies in this area have focused on trace metal concentrations in sediments, with few considering macroalgae (Giusti, 2001; Alderton, 2012). Whilst the Water Quality Archive (Environment Agency, 2025d) provides regularly updated data from numerous coastal and estuarine sampling points, trace metal monitoring is limited to a small subset of sites. Moreover, these measurements are restricted to water samples, which convey limited insight into metal bioavailability. This study aims to provide an updated, biologically relevant assessment of trace metal contamination along the northeast and North Yorkshire coastlines. This aim is addressed through the following research objectives:

1. Quantify the spatial distribution of trace metal concentrations along the northeast and North Yorkshire coastlines and use a metal pollution index to assess overall contamination levels.
2. Evaluate the relative state of trace metal pollution across the study area by comparison with background levels.
3. Assess temporal changes in trace metal concentrations by comparison with historical data.
4. Investigate the role of dredging and disposal of Tees Estuary sediments as a potential source of trace metal contamination across the study area.
5. Identify and explore non-pollution factors contributing to trace metal variability in macroalgae (e.g., species, season, thallus segment, site-specific conditions) and consider their implications for biomonitoring applications.

2. Background

2.1. The Tees Estuary

2.1.1. Tees catchment characteristics

The River Tees is one of the largest rivers in the northeast of England, alongside the Rivers Tyne and Humber, with a catchment area of approximately 1906 km^2 (Davies, Tomlinson and Stephenson, 1991; Hudson-Edwards, Macklin and Taylor, 1997; Jones and Turki, 1997). It rises on Cross Fell in the North Pennines and flows eastwards for approximately 160 km, before emptying into the North Sea between Hartlepool and Redcar (Jones and Turki, 1997) (Figure 1).

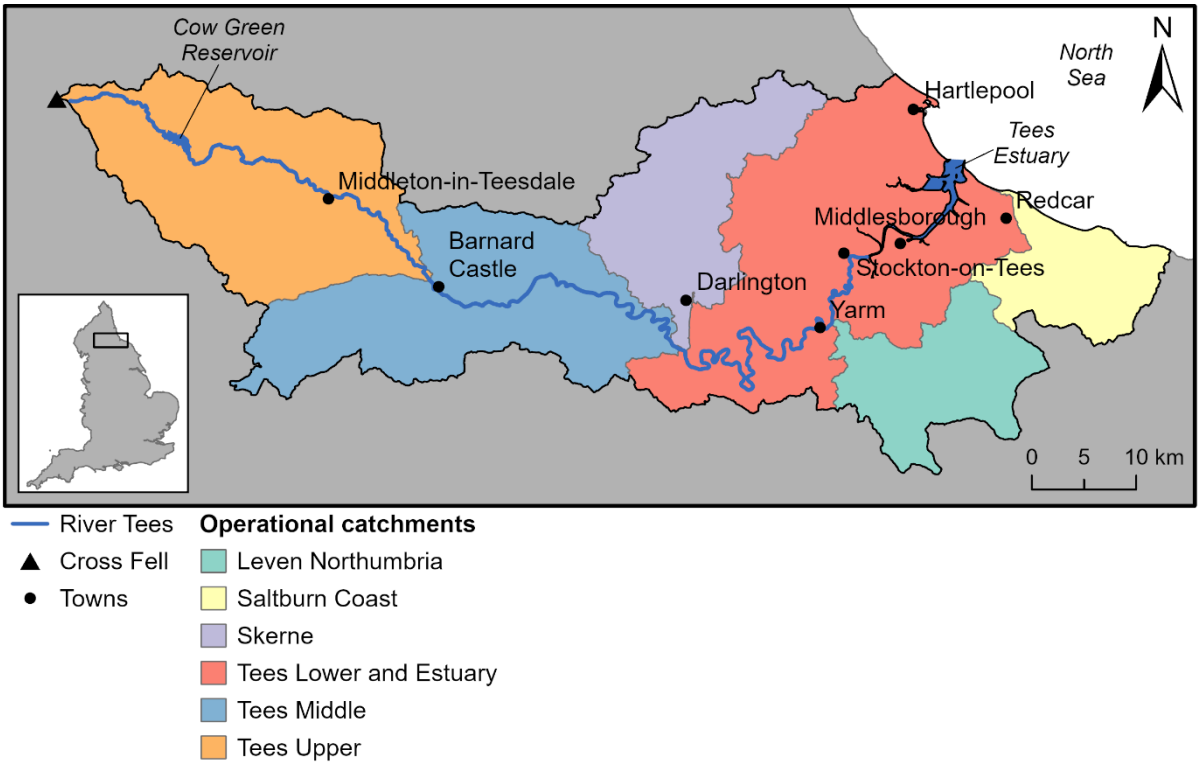

Figure 1 | The Tees catchment. The main river channel (blue line), its source at Cross Fell (black triangle), nearby towns (black circles), and other labelled features along its course. The management catchment (thick black line) encompasses six coloured operational catchments. Tributaries not shown. Inset: reference map of England.

The upland part of the Tees catchment is dominated by Carboniferous limestone, sandstone, and shale formations, intruded by a network of dolerite sills and dykes (Hudson-Edwards, Macklin and Taylor, 1997). The lowland areas are primarily underlain by Permian marl and limestone, as well as Triassic and Jurassic sandstone and mudstone strata (Hudson-Edwards, Macklin and Taylor, 1997; Giusti, 2001). The North Pennine Orefield, drained by the Tees and its tributaries, hosts a

diverse suite of metal-bearing minerals including galena, Cd-bearing sphalerite, chalcopyrite, cerussite, and smithsonite (Hudson-Edwards, Macklin and Taylor, 1997).

The Tees Estuary is narrow, stratified, and approximately 30 km in length (Hardy, Evans and Tremayne, 1993). It discharges at a rate of around 17 m^3/s and has a mean tidal range of 3.4 m (Davies, Tomlinson and Stephenson, 1991; Jones and Turki, 1997). Sediments in the estuary are mainly organic-rich clayey-silts (Jones and Turki, 1997). Outside the estuary, material is transported southwards along the coast (Eastabrook *et al.*, 2022).

2.1.2. Contamination of Tees Estuary sediments

The Tees Estuary contains some of the UK's most contaminated sediments with respect to trace metals (Davies, Tomlinson and Stephenson, 1991; Jones and Turki, 1997). These sediments record two distinct phases of contamination: far-field upland metal mining and more recent industrial activity flanking estuary margins (Berry and Plater, 1998; Plater *et al.*, 1999).

2.1.2.1. Mining in the upper Tees catchment

Whilst Pb extraction in the North Pennine Orefield can be traced back to Roman times, it did not become properly established until the early 1700s (Berry and Plater, 1998). Pb mining peaked between 1815–1880, declining thereafter (Hudson-Edwards, Macklin and Taylor, 1997; Berry and Plater, 1998). Small scale Zn extraction began in 1794, growing in scale following the decline of Pb mining (Berry and Plater, 1998). Zn mining peaked in 1883 and continued until 1918 (Berry and Plater, 1998). An estimated 2.6×10^5 tonnes of Pb and 435 tonnes of Zn were extracted from the area prior to the closure of the last metal mine (Hudson-Edwards, Macklin and Taylor, 1997).

Metal-bearing wastewater and fine rock particles derived from spoil tips and other mining processes have contaminated streams and rivers draining the area (Hudson-Edwards, Macklin and Taylor, 1997). Contaminated fluvial sediment from upland mining areas may be transported downstream with limited reworking, eventually depositing in the Tees Estuary (Hudson-Edwards, Macklin and Taylor, 1997).

2.1.2.2. Industry around the Tees Estuary

The Tees Valley industrial cluster, also referred to as the Teesside industrial cluster, is located along the Tees Estuary and spans the boroughs of Middlesborough, Stockton-on-Tees, Darlington, Hartlepool, and Redcar and Cleveland (IDRIC, 2022). It is home to the UK's largest freeport and Europe's second largest chemical complex (IDRIC, 2022). Teesside has a rich and varied industrial legacy with key sectors including chemicals, petrochemicals, steel, pharmaceuticals, oil and gas, cement, fertilisers, and metals (Giusti, 2001; IDRIC, 2022; Herman, Iskandarova and Sovacool, 2025).

Significant industrial growth along the Tees Estuary began in the 1800s, with further expansion occurring between 1930 and 1970 (Berry and Plater, 1998). During the latter period, industrial discharges into the estuary increased more than tenfold (Berry and Plater, 1998). Water quality was at its lowest during the early 1970s, when approximately 1.37×10^6 m^3 of industrial waste was discharged daily (Hardy, Evans and Tremayne, 1993; Jones and Turki, 1997). From the late 1970s to the mid-2000s, industrial activity at Teesside steadily declined following the collapse of the petrochemical, steel, and oil sectors (Herman, Iskandarova and Sovacool, 2025). Water quality improved during this time owing to reduced industrial discharges (Hardy, Evans and Tremayne, 1993; Jones and Turki, 1997; Giusti, 2001). Taylor (1982) reported that trace metal concentrations in Tees Estuary waters were unlikely to pose adverse effects on marine life. Efforts to revitalise the industrial cluster began in 2007, with further renewal initiatives launched in 2015 (Herman, Iskandarova and Sovacool, 2025).

Between 2009 and 2022, the Tees Estuary maintained a 'moderate' ecological status and 'fail' chemical status under the Water Framework Directive (Environment Agency, 2025b). However, when considering trace metals of interest only, each has consistently achieved either 'good' or 'high' status (Environment Agency, 2025b), indicating that industrial metal pollution is no longer as severe as in previous decades.

2.1.2.3. Trace metal concentrations in Tees Estuary sediments

Several studies have investigated trace metal concentrations in sediments from the Tees Estuary, although published research has markedly declined since the late 1990s to early 2000s.

Davies, Tomlinson and Stephenson (1991) reported that mean trace metal concentrations in sediment cores followed the order: Zn > Mn > Pb > Cu > Cr > Ni > Cd, with Zn, Pb, Cr, and Cd exceeding background levels by factors of 5–20. However, compared to earlier findings by Murrey and Norton (1979), concentrations of Zn, Pb, Cu, Cr, Ni, and Cd had declined, reflecting deindustrialisation and reduced discharges into the estuary. Jones and Turki (1997) corroborated many of these observations, with median sediment concentrations decreasing in a broadly similar order: Zn > Pb > Cr > Cu > Ni > Co > Cd. Enrichment of Zn, Pb, Cr, and Cd relative to background levels persisted at most sample sites, alongside Cu and Co.

Research by Berry and Plater (1998) and subsequently Plater *et al.* (1999) indicated that trace metal contamination in deeper sediment layers reflected far-field mining activity, whereas the shallow record corresponded primarily to industrial pollution from sources in and around the estuary. Berry and Plater (1998) measured peak metal concentrations up to ten times higher than those in deeper core layers, which was ascribed to the pronounced increase in industrial discharges between 1930 to 1970. Plater *et al.* (1999) identified Pb and Zn as the most abundant trace metals in sediments from the Tees Estuary, with a smaller contribution from Cu, and only minor amounts of As, Cr, and Ti.

Giusti (2001) found that Fe, Mn, and Zn were the most abundant trace metals in surface sediments from the Tees Estuary, and Ag the least. Elevated levels of Zn and Pb above background values were reported across all sample sites along the northeast coast. Ag enrichment was observed at one location in the Tees Estuary. However, with the exception of Ag at that site, trace metal concentrations within Tees Estuary sediments remained below thresholds typically associated with adverse biological effects.

2.1.3. Contaminated sediments as sources of water pollution

2.1.3.1. Metal speciation and bioavailability

Metal speciation governs environmental behaviour, including mobility and bioavailability (Jones and Turki, 1997; Morillo, Usero and Gracia, 2004; Zhang *et al.*, 2017). In Tees Estuary sediments, the dominant phases are the residual, oxidizable, and reducible fractions (Jones and Turki, 1997). The residual fraction contains metals bound within crystalline lattices, the oxidizable fraction those bound

to organic matter and sulphides, and the reducible fraction those bound to Fe and Mn oxides (Jones and Turki, 1997; Morillo, Usero and Gracia, 2004; Zhang *et al.*, 2017).

The residual fraction is relatively inactive, non-labile, and primarily lithogenic in origin (Jones and Turki, 1997; Morillo, Usero and Gracia, 2004; Zhang *et al.*, 2017). The oxidizable and reducible fractions, on the other hand, are derived mainly from anthropogenic sources and may become labile under changing environmental conditions such as pH, redox potential, and salinity (Jones and Turki, 1997; Morillo, Usero and Gracia, 2004; Zhang *et al.*, 2017). The reducible fraction is considered the most labile of the three, and the residual fraction the least, exerting little bioavailability (Jones and Turki, 1997; Zhang *et al.*, 2017). Jones and Turki (1997) found that in Tees Estuary sediments, Cd, Cr, Pb, and Zn are mainly hosted by the reducible, residual, and oxidizable fractions. Cu is primarily associated with the oxidizable and residual fractions, whilst Co and Ni occur at relatively low concentrations, mainly within the residual and reducible fractions.

2.1.3.2. Dredging and remobilisation of sedimentary trace metals

Trace metals can be remobilised into the water column when environmental conditions change. Metals in the reducible fraction are released into pore waters under anoxic conditions via microbially mediated reduction of Fe and Mn oxides during early diagenesis (Jones and Turki, 1997; Morillo, Usero and Gracia, 2004). These metals can subsequently reach the overlying water column via resuspension or diffusion (Jones and Turki, 1997). Metals in the oxidizable fraction may be liberated under oxic conditions via microbial oxidation of organic matter (Jones and Turki, 1997; Morillo, Usero and Gracia, 2004). Such conditions may arise when sediment is resuspended, either by natural means or anthropogenic activities such as dredging (Jones and Turki, 1997; Morillo, Usero and Gracia, 2004).

Dredging refers to the removal or relocation of seabed or riverbed material and falls into two categories: maintenance and capital (OSPAR Commission, 2008; MMO, 2019; Gibbon, 2023). Maintenance dredging is conducted routinely along navigational channels to keep them sufficiently deep for ships to pass through (Davies, Tomlinson and Stephenson, 1991; OSPAR Commission, 2008; MMO, 2019; Gibbon, 2023). Capital dredging, on the other hand, involves the removal of material to a depth that has not been dredged for at least a decade, typically to

deepen existing navigational channels, create new ones, or support construction projects (OSPAR Commission, 2008; MMO, 2019). In the UK, most dredged material is disposed of at designated offshore sites (OSPAR Commission, 2008; Gibbon, 2023).

The Tees Estuary is subject to regular maintenance dredging and, more recently, capital dredging associated with the ongoing Teesworks development (MMO, 2023a, 2023b). Dredged sediments are deposited at two offshore disposal sites (Figure 2), located approximately 6 and 9.5 km from the estuary mouth (MMO, 2023a, 2023b; Bolam *et al.*, 2024). Disturbance of contaminated sediments can remobilise vast quantities of bound metals, such that sediments transition from acting as a pollutant sink to a source, even long after mining and industrial discharges have ceased (Davies, Tomlinson and Stephenson, 1991; Jones and Turki, 1997; Zhang *et al.*, 2017). Once reintroduced into the water column, these metals may become bioavailable and be taken up by marine organisms.

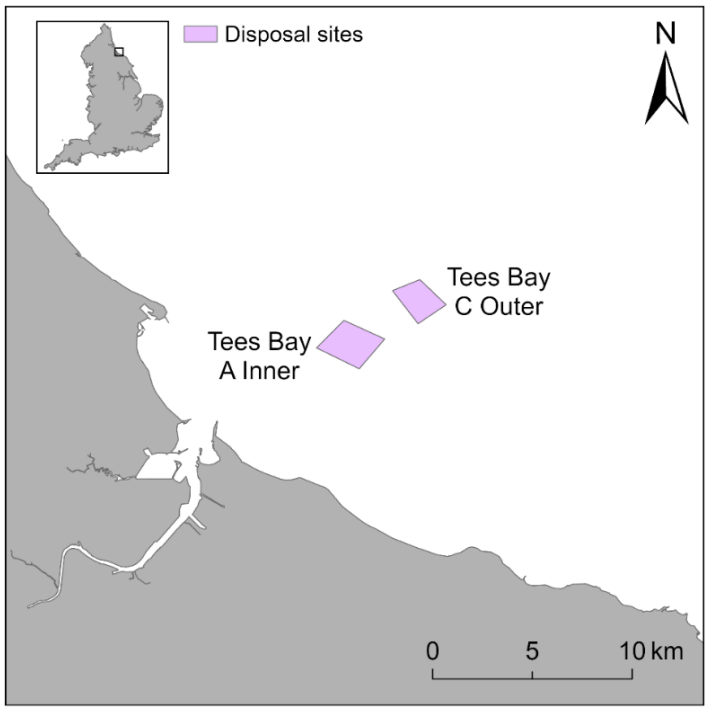

Figure 2 | Tees Bay disposal sites. Disposal sites for dredged material from the Tees Estuary (pink polygons, labelled), based on Bolam *et al.* (2024). Inset: reference map of England.

2.1.3.3. The 2021 mass crustacean mortalities

In the autumn of 2021, a series of mass crustacean mortalities occurred along the northeast and North Yorkshire coasts, stretching from Seaham to Scarborough (Eastabrook *et al.*, 2022; Ford, Fitzsimons and Halsall, 2024; Losada *et al.*, 2025). Mortalities were centred on the area encompassing Hartlepool, Teesmouth, and

Redcar (Eastabrook *et al.*, 2022). Multiple independent investigations were conducted into possible causal factors.

One proposed source was pyridine, an organic compound used as an industrial solvent with a long history of discharge into the Tees Estuary (Eastabrook *et al.*, 2022; Ford, Fitzsimons and Halsall, 2024; Losada *et al.*, 2025). A campaign of accelerated dredging was concurrent with the mass mortalities, and it was hypothesised that pyridine may have been liberated from the sediment into the water column and caused the deaths (Eastabrook *et al.*, 2022; Ford, Fitzsimons and Halsall, 2024; Losada *et al.*, 2025). Eastabrook *et al.* (2022) demonstrated that pyridine is toxic to brown crabs and that a pyridine plume may have extended to affected sites further down the coast. However, this hypothesis is highly contested with alternative proposed causes including an unknown, novel pathogen (Whitcombe and Forster, 2023) and/or an algal bloom, believed to have occurred off Teesside in September 2021 (Eastabrook *et al.*, 2022; Ford, Fitzsimons and Halsall, 2024). A definitive cause remains unidentified, and it is possible that a combination of factors may have also been responsible (Ford, Fitzsimons and Halsall, 2024).

Although pyridine is not the focus of this study, its potential contribution to these mortalities suggests a viable contamination pathway between sediment and the overlying water column. Such a mechanism could similarly facilitate the remobilisation of trace metals from contaminated Tees Estuary sediments, with possible ecological consequences. Furthermore, this incident highlights the importance of robust coastal pollution monitoring.

2.2. Phycology

2.2.1. Brown algae overview

Of the three classes of macroalgae (green, red, and brown), brown algae are the most globally abundant (Konstantin *et al.*, 2023). They are widespread in littoral zones across temperate to subpolar regions (Davis, Volesky and Mucci, 2003; Baweja *et al.*, 2016; Lee, 2018). Within this class, the orders Laminariales (kelps) and Fucales are commonly used in studies of marine trace metal pollution (Chung and Lee, 1989; García-Seoane *et al.*, 2018). This study employed four representative species: *L. digitata* and *L. hyperborea* (Laminariales, Laminariaceae), and *F. vesiculosus* and *F. serratus* (Fucales, Fucaceae) (Table 1).

Species	Habitat	Growth rate (cm/day)*	Lifespan (years)	Characteristics	Ref
L. digitata	Sublittoral to lower eulittoral, 1–20 m depth	1.3	4–6	• Broad, digitate, glossy fronds lacking midribs • Smooth, flexible, oval stipe • Shallow, domed holdfast	[1–3]
L. hyperborea	1–36 m depth, typically ~8 m	0.94	11–20	• Broad, digitate, glossy fronds lacking midribs • Rough, stiff, circular, tapered stipe, often covered by epiphytes • Conical holdfast	[2–4]
F. vesiculosus	Mid to upper eulittoral	0.05–0.14	2–5	• Dichotomously branched fronds bearing distinct midribs and smooth edges • Spherical, paired air bladders • Inflated tips (receptacles) when fertile	[5, 6]
F. serratus	Lower to mid eulittoral	0.1–0.2	2–5	• Dichotomously branched fronds bearing distinct midribs and serrated edges • No air bladders • Sterile border around receptacles	[6, 7]

Table 1 | Morphological and ecological attributes of brown algal species investigated.

* Growth rate during season of maximum growth.

[1] Hill (2008).

[2] Lee (2018).

[3] Raab, Stengel and Feldmann (2025).

[4] Tyler-Walters (2007).

[5] White (2008).

[6] Catarino, Silva and Cardoso (2018).

[7] Jackson (2008).

2.2.2. Anatomy and growth

2.2.2.1. Laminariales

Laminariales comprise three main anatomical components: holdfasts (also known as haptera), stipes (also known as stems), and flat bodies composed of blades (also known as fronds or laminae) (Baweja *et al.*, 2016; Lee, 2018; Raab, Stengel and Feldmann, 2025) (Figure 3). The term thallus may refer either to the main body of the macroalga or, more broadly, to the entire specimen including stipe and holdfast. In this study, the latter definition is adopted.

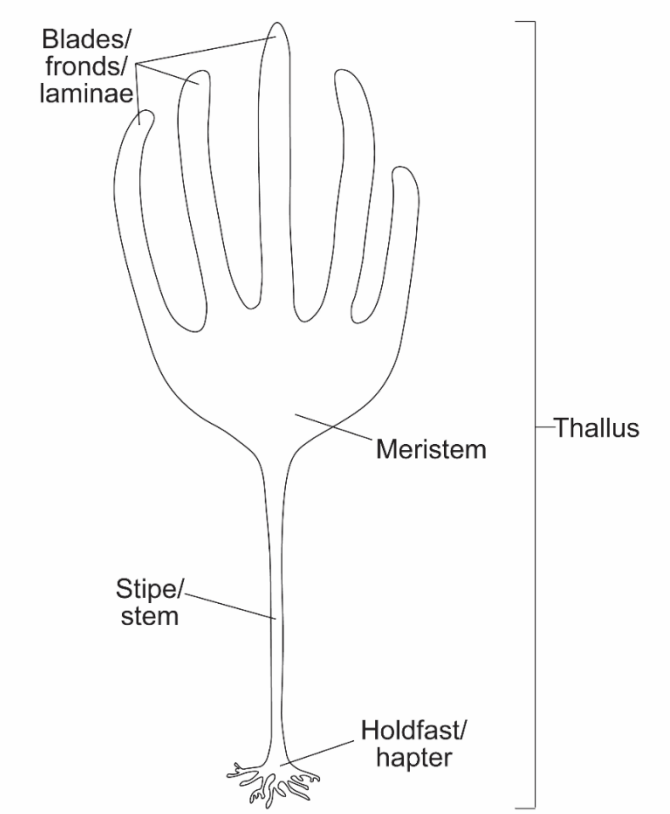

Figure 3 | Laminariale anatomy.

Laminariales may reach lengths of up to 4 m, growing from an intercalary meristem between the stipe and blade body (Figure 3), which adds tissue to both (Adams *et al.*, 2011; Lee, 2018; Raab, Stengel and Feldmann, 2025). Growth rate is high between winter and early summer and declines from late summer into autumn (Bartsch *et al.*, 2008; Hill, 2008; Lee, 2018).

2.2.2.2. Fucales

Fucales are characterised by the dichotomous branching of their thallus into flattened fronds, or blades (Catarino, Silva and Cardoso, 2018; Lee, 2018) (Figure 4). Fronds consist of a central midrib flanked by wings either side and may bear fertile receptacles at their tips and oval gas vesicles (also known as gas or air bladders) along their lengths (White, 2008; Baweja *et al.*, 2016; Catarino, Silva and Cardoso, 2018; Lee, 2018). Gas vesicles may be absent in small specimens or those subjected to intense wave action in exposed areas (White, 2008; Lee, 2018). The base of the thallus includes a short narrow stipe and discoid holdfast (Catarino, Silva and Cardoso, 2018; Lee, 2018).

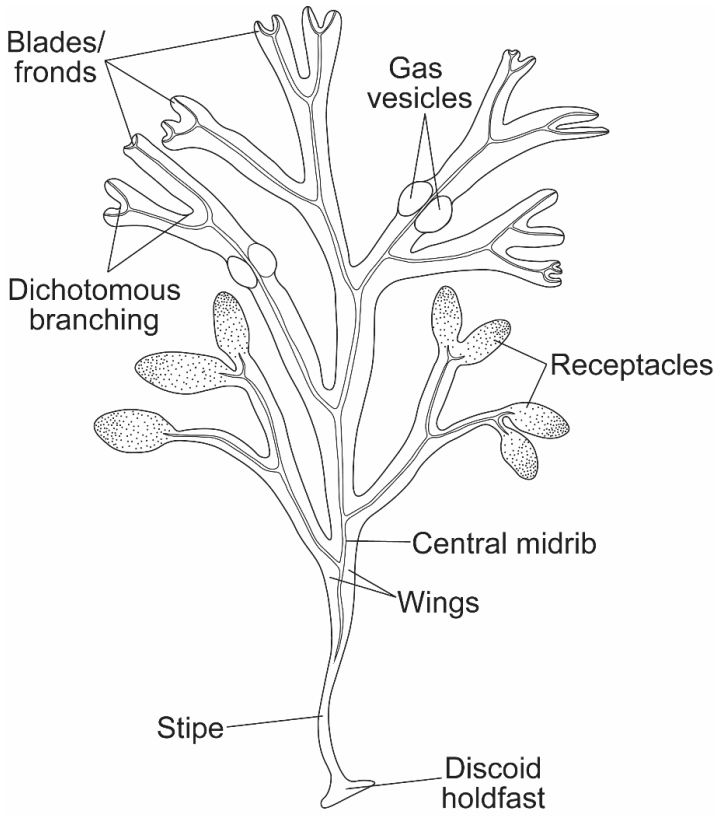

Figure 4 | Fucale anatomy. After Birkemeyer *et al.* (2019).

In Fucales, growth occurs from an apical cell at the frond tip, and individuals typically reach a maximum length of 30–50 cm (Baweja *et al.*, 2016; Lee, 2018). The apical cell undergoes multiple divisions annually, forming dichotomous branches (forks) (Lee, 2018; García-Seoane *et al.*, 2021). When not dividing, it stimulates division in adjacent cells (Lee, 2018). In most Fucales, growth rate peaks in late spring to early summer and declines from late autumn through spring (Carlson, 1991).

2.2.3. Trace metal uptake by brown algae via biosorption

2.2.3.1. Cell wall structure and extracellular polysaccharides

Brown algae share a similar cell structure with other macroalgal classes but are distinguished by their high extracellular polysaccharide content (Lee, 2018). Extracellular refers to components bound to the outside of the cell wall and membrane (Vázquez-Arias *et al.*, 2023). The cell wall is composed of at least two layers: an inner microfibrillar skeleton and an outer amorphous embedding matrix (Figure 5), which are attached to one another via hydrogen bonds (Davis, Volesky and Mucci, 2003).

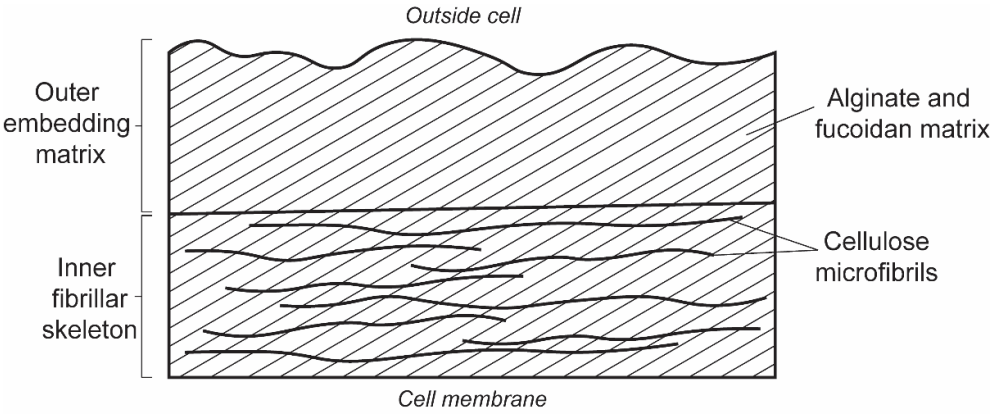

Figure 5 | Brown algal cell wall. After Davis, Volesky and Mucci (2003).

2.2.3.1.1. Inner microfibrillar skeleton

The microfibrillar skeleton (Figure 5) provides rigidity and structure to the cell wall and, in brown algae, is mainly made of cellulose (Davis, Volesky and Mucci, 2003; Baweja *et al.*, 2016; Lee, 2018). Cellulose is an uncharged, unbranched polysaccharide comprising 2–20% of the dry weight in brown algae (Davis, Volesky and Mucci, 2003). It consists of (1→4)-linked β-D-glucose units (Figure 6) and, in the cell wall, forms a network of curved, flattened microfibrils (Davis, Volesky and Mucci, 2003) (Figure 5).

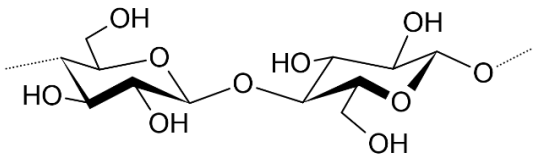

Figure 6 | Chemical structure of cellulose in brown algae. Two (1→4)-linked β-D-glucose monomers. Dotted bonds represent repeating units along polymer axis. After Rowbotham *et al.* (2012).

2.2.3.1.2. Outer embedding matrix

The embedding matrix (Figure 5) is primarily composed of alginic acid (or its salt, alginate), with fucoidan present in smaller amounts (Chung and Lee, 1989; Davis, Volesky and Mucci, 2003; Baweja *et al.*, 2016; Lee, 2018). These polysaccharides impart strength and flexibility to cell walls and, more pertinently to the present study, play a crucial role in trace metal biosorption (Davis, Volesky and Mucci, 2003; Catarino, Silva and Cardoso, 2018).

2.2.3.1.2.1. Fucoidan

Fucoidan is a polysaccharide rich in sulphated L-fucose (Li *et al.*, 2008; Stiger-Pouvreau, Bourgougnon and Deslandes, 2016). It has been reported to make up 5–20% of the dry weight in brown algae (Davis, Volesky and Mucci, 2003). Its structure varies between species and even across seasons due to differences in biosynthesis (Li *et al.*, 2008; Stiger-Pouvreau, Bourgougnon and Deslandes, 2016; van Weelden *et al.*, 2019). However, it always contains a linear backbone of sulphated α-L-fucose units, which may be exclusively (1→3)-linked or alternate between (1→3)- and (1→4)-linkages (Li *et al.*, 2008; Stiger-Pouvreau, Bourgougnon and Deslandes, 2016; Catarino, Silva and Cardoso, 2018; van Weelden *et al.*, 2019).

Fucoidan may also contain branches of uronic acids, acetyl groups, proteins, and additional sugars, including further fucose residues (Li *et al.*, 2008; Stiger-Pouvreau, Bourgougnon and Deslandes, 2016; Catarino, Silva and Cardoso, 2018; van Weelden *et al.*, 2019). Sulphation and branching typically occur at C-2, and sometimes at C-3 and C-4 (Li *et al.*, 2008; Stiger-Pouvreau, Bourgougnon and Deslandes, 2016; van Weelden *et al.*, 2019). Metal biosorption in fucoidan occurs mainly via sulphate groups (Davis, Volesky and Mucci, 2003).

In *F. vesiculosus*, fucoidan consists of alternating (1→3)-linked and (1→4)-linked α-L-fucose units, with sulphation primarily at C-2 and sometimes C-3 (Li *et al.*, 2008; Catarino, Silva and Cardoso, 2018; van Weelden *et al.*, 2019) (Figure 7a). In *F. serratus*, the backbone is similarly linked but is more branched, with sulphation mainly at C-2 and sometimes C-4 (Li *et al.*, 2008; Catarino, Silva and Cardoso, 2018; van Weelden *et al.*, 2019) (Figure 7b). In contrast, the fucoidan backbone in *L. digitata* comprises exclusively (1→3)-linked α-L-fucose units, with sulphation at C-2 and C-4 (Stiger-Pouvreau, Bourgougnon and Deslandes, 2016) (Figure 7c).

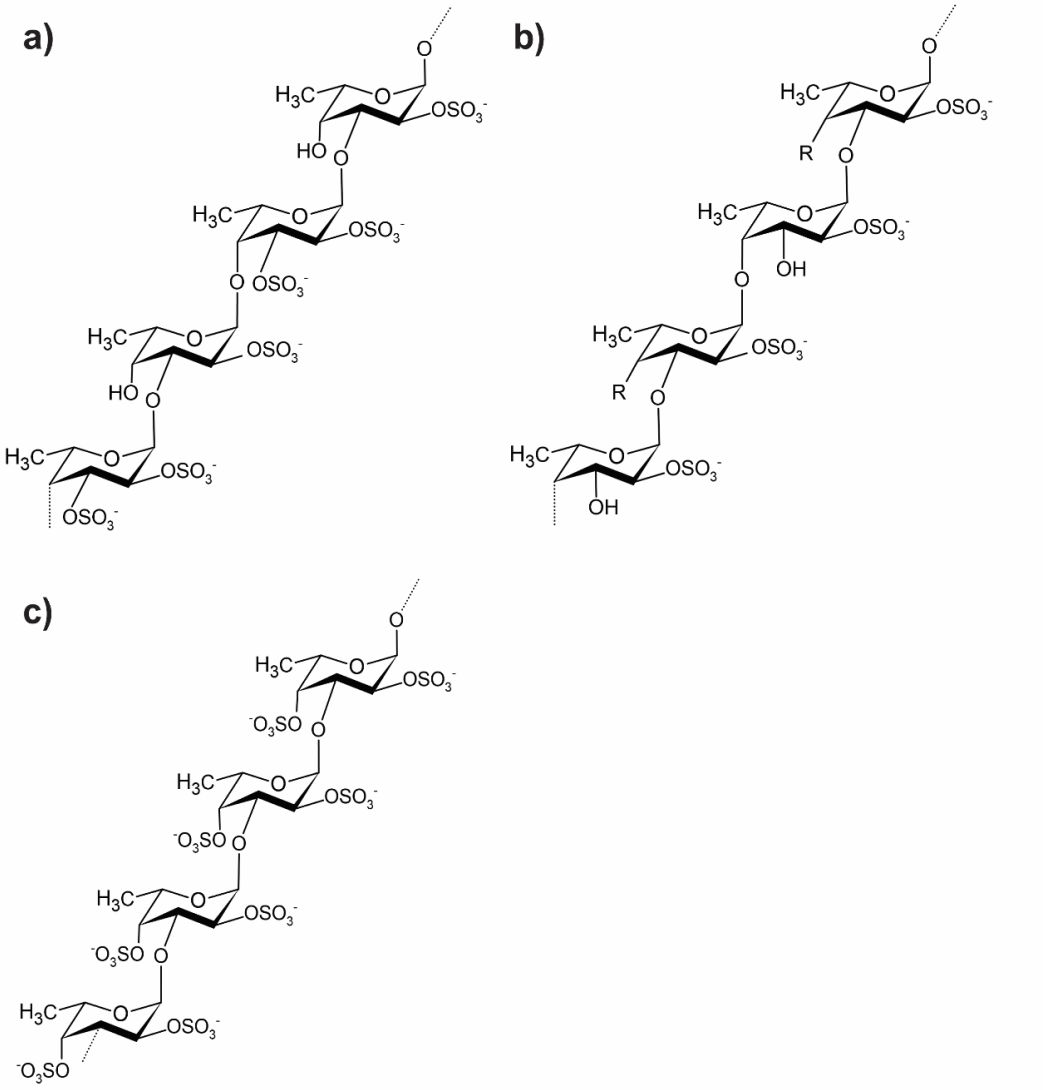

Figure 7 | Chemical structures of fucoidan. a) Fucoidan in *F. vesiculosus*: Alternating (1→3)-linked and (1→4)-linked α-L-fucose backbone with sulphation occurring mainly at C-2 and sometimes C-3. **b)** Fucoidan in *F. serratus*: Alternating (1→3)-linked and (1→4)-linked α-L-fucose backbone with sulphation occurring mainly at C-2. R represents branches of sulphate groups, uronic acids, acetyl groups, or additional sugars. **c)** Fucoidan in *L. digitata*: (1→3)-linked α-L-fucose backbone with sulphation at C-2 and C-4. Dotted bonds represent repeating units along polymer backbone. After Catarino, Silva and Cardoso (2018) and van Weelden *et al.* (2019).

2.2.3.1.2.2. Alginic acid

Alginic acid constitutes 10–40% of the dry weight in brown algae (Davis, Volesky and Mucci, 2003; Schiener *et al.*, 2015; Rowbotham, Greenwell and Dyer, 2021), although contents as high as 59% have been reported in *F. vesiculosus* (Catarino, Silva and Cardoso, 2018). It is a linear polysaccharide composed of (1→4)-linked monomers of α-L-guluronic acid (G) (Figure 8a) and β-D-mannuronic acid (M) (Figure 8b) (Davis, Volesky and Mucci, 2003; Catarino, Silva and Cardoso, 2018;

Lee, 2018; Cao *et al.*, 2020; Rowbotham, Greenwell and Dyer, 2021). These monomers may be arranged into homopolymeric (G-block or M-block) or heteropolymeric (MG-block) sequences (Davis, Volesky and Mucci, 2003; Catarino, Silva and Cardoso, 2018; Cao *et al.*, 2020) (Figure 8c).

M-blocks are characterised by their flexibility and flat, ribbon-like structures, whereas G-blocks form buckled chains with greater structural rigidity (Davis, Volesky and Mucci, 2003; Catarino, Silva and Cardoso, 2018; Rowbotham, Greenwell and Dyer, 2021). The buckled structure of G-blocks, coupled with their anionic nature, creates electron-rich cavities conducive to divalent cation binding (Rowbotham, Greenwell and Dyer, 2021). In alginate, carboxylate groups are primarily responsible for metal biosorption (Davis, Volesky and Mucci, 2003).

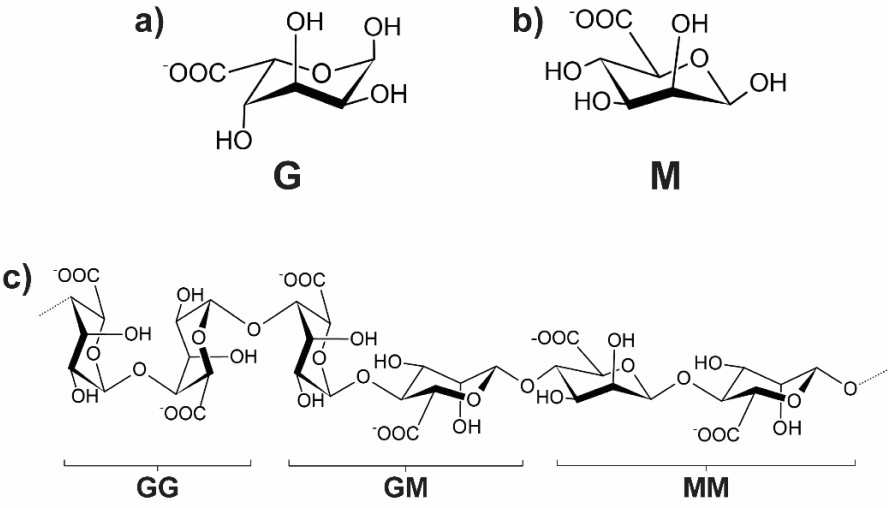

Figure 8 | Chemical structure of alginate. a) α-L-guluronic acid (G) monomer. **b)** β-D-mannuronic acid (M) monomer. **c)** Alginate polymer of (1→4)-linked G and M monomers forming polyguluronic (GG), heteropolymeric (GM), and polymannuronic (MM) acid sequences. Dotted bonds represent repeating units along polymer axis. After Davis, Volesky and Mucci (2003), Rowbotham *et al.* (2013), Catarino, Silva and Cardoso (2018), and Rowbotham, Greenwell and Dyer (2021).

2.2.3.2. The egg-box model

One proposed mechanism for divalent cation binding in alginate is known as the egg-box model, first described by Grant *et al.* (1973). In this model, two antiparallel G-block chains align to form an 'egg-box' cavity that accommodates a divalent cation (Catarino, Silva and Cardoso, 2018; Cao *et al.*, 2020; Rowbotham, Greenwell and Dyer, 2021) (Figure 9a). The cation is chelated by five oxygen atoms from each G-block, resulting in a di-pentadentate coordination complex (Rowbotham, Greenwell and Dyer, 2021). Dimerization proceeds along the paired G-block chains until

interrupted by an M-block (Davis, Volesky and Mucci, 2003) (Figure 9b). Alginate gelation occurs when multiple chains become interconnected through lateral cross-linking of these dimers (Davis, Volesky and Mucci, 2003; Cao *et al.*, 2020) (Figure 9c).

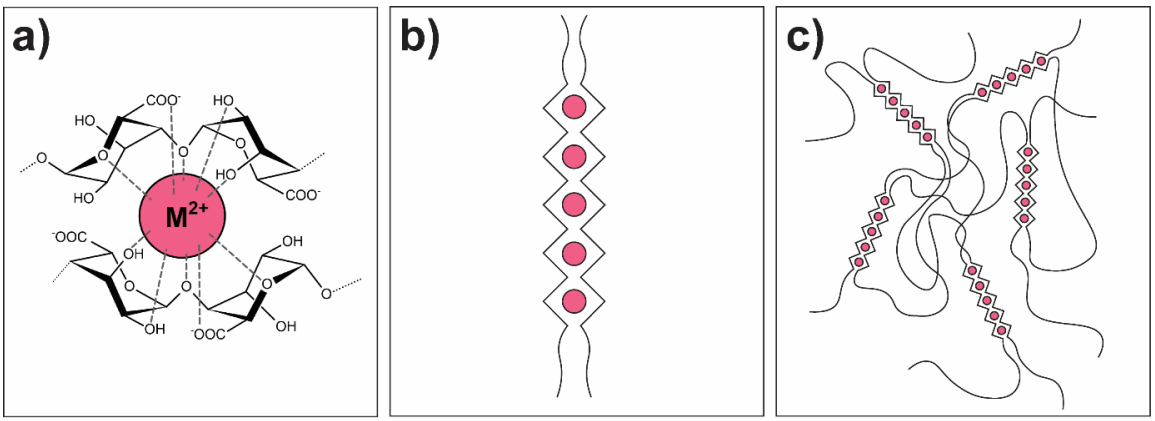

Figure 9 | Egg-box model. a) Egg-box cavity: Two antiparallel polyguluronic acid chains (G-blocks) chelating a divalent cation (M^{2+}, pink circle) in a di-pentadentate configuration (dashed lines). Dotted bonds represent repeating units along polymer axes. **b)** Egg-box dimers: Binding of divalent cations (pink circles) to egg-box cavities along paired G-blocks (illustrated by zig-zag chains). **c)** Alginate gelation: Cross-linking of egg-box dimers. After Davis, Volesky and Mucci (2003), Cao *et al.* (2020), and Rowbotham, Greenwell and Dyer (2021).

2.2.3.2.1. Alginate selectivity

Alginate exhibits strong binding selectivity between cations (Davis, Volesky and Mucci, 2003). For example, Ca^{2+} ions promote gelation more readily than Mg^{2+} ions due to their size and shape being more compatible with binding cavities (Rowbotham, Greenwell and Dyer, 2021). The approximate sequence of preferential metal binding in alginate, from highest to lowest affinity, is as follows: $Pb^{2+} > Cu^{2+} > Cd^{2+} > Ba^{2+} > Sr^{2+} > Ca^{2+} > Co^{2+} > Ni^{2+} > Mn^{2+} > Mg^{2+}$ (Haug, 1961).

2.2.4. Are there challenges associated with using macroalgae as biomonitors of trace metal pollution?

The use of macroalgae as biomonitors over water or sediment sampling introduces a biological dimension that complicates data interpretation (Phillips, 1977). Trace metal concentrations in macroalgae may vary due to species, specimen age, thallus segment, season, and environmental conditions (e.g., light, salinity, and temperature), as opposed to changing pollution levels (Black and

Mitchell, 1952; Tomlinson *et al.*, 1980; Stengel *et al.*, 2004; Stengel, McGrath and Morrison, 2005; Chalkley *et al.*, 2019; Huang *et al.*, 2025). A lack of standardization across these variables restricts interstudy comparisons and undermines the reliability of conclusions (García-Seoane *et al.*, 2021). Ensuring consistency requires sampling specimens of the same species, age, season, and shore level (Phillips, 1977; Sawidis *et al.*, 2001). Where this is not feasible due to logistical constraints (e.g., limited access or availability), such factors must at least be accounted for during sampling and analysis. Surface contamination by fine particulate material may also lead to overestimation of bioavailable concentrations (Barnett and Ashcroft, 1985; Viana *et al.*, 2010; García-Seoane *et al.*, 2021).

2.2.4.1. Interspecific variation in trace metal concentrations

Interspecific variation in trace metal concentrations can arise from morphological, physiological, and ecological differences (Ryan, McLoughlin and O'Donovan, 2012).

2.2.4.1.1. Morphology

Traits such as surface area and thallus morphology may influence trace metal uptake. Species with higher surface area to volume ratios tend to accumulate greater trace metal concentrations due to increased contact with surrounding water and enhanced nutrient uptake (Sawidis *et al.*, 2001; Stengel *et al.*, 2004; Huang *et al.*, 2025). Furthermore, thin-sheeted and filamentous macroalgae have been reported to exhibit higher Zn levels than thick, leathery forms (Stengel *et al.*, 2004). However, all species sampled in the present study fall within the latter category (Stengel *et al.*, 2004), such that any observed interspecific differences in trace metal concentrations are unlikely to be heavily driven by morphological variations.

2.2.4.1.2. Physiology

Physiological factors influencing trace metal accumulation include variations in growth rate, photosynthetic response, nutrient uptake, metal-binding affinity, and life cycle type (Sawidis *et al.*, 2001; Ryan, McLoughlin and O'Donovan, 2012; Huang *et al.*, 2025). Species with higher growth rates often exhibit lower trace metal concentrations due to a dilution effect, whereby rapid biomass accumulation

reduces metal content per unit mass (Sawidis *et al.*, 2001). Therefore, *Laminaria* spp. may be expected to contain lower trace metal concentrations than *Fucus* spp., given their comparatively higher growth rates (Table 1).

Variations in polysaccharide content may contribute to differences in trace metal concentrations between species. *F. vesiculosus* has been reported to contain higher levels of alginate and fucoidan than *F. serratus* (Fletcher *et al.*, 2017; Catarino, Silva and Cardoso, 2018), potentially enhancing its affinity for trace metals. The composition of these polysaccharides may also play an important role. Haug and Smidsrød (1965) demonstrated that alginate in *L. hyperborea* exhibits a lower M:G ratio than in *L. digitata*, resulting in a greater abundance of G-blocks and egg-box binding sites. Alginates in *Fucus* spp. contain fewer G-blocks than those in *L. hyperborea* (Catarino, Silva and Cardoso, 2018), suggesting a lower metal-binding capacity, contrary to expectations based solely on growth rate.

2.2.4.1.3. Ecology

Ecological differences in trace metal uptake may arise from growth at different tidal elevations. Shore level governs not only the duration of submersion, but also light exposure, temperature, and desiccation stress, all of which affect metabolic rates and, consequently, metal uptake (Bryan and Hummerstone, 1973; Stengel *et al.*, 2004). Longer submersion promotes greater element uptake from seawater, whereas increased air exposure can enhance elemental loss via desiccation and oxidative stress (Ownsworth *et al.*, 2019).

Bryan and Hummerstone (1973) reported higher concentrations of Pb, Mn, and Fe in *F. vesiculosus* collected from the lower shore compared to upper shore specimens. Similarly, Fuge and James (1973) found higher Zn levels in *F. serratus* than *F. vesiculosus*, attributing this to the former's growth at lower tidal elevations and longer submersion periods. However, the same study reported the opposite trend for Fe, with higher concentrations in *F. vesiculosus*, whilst Tomlinson *et al*. (1980) found no significant differences in metal concentrations between the two species.

Despite their faster growth, *Laminaria* spp. may be expected to accumulate higher trace metal concentrations than *Fucus* spp., given their growth at lower shore levels (Table 1). However, Stengel *et al.* (2004) found that whilst Zn concentrations

were indeed higher in lower and mid-shore species such as *F. serratus* and *F. vesiculosus* compared to the upper shore *F. spiralis*, *L. digitata* exhibited lower Zn concentrations than both *F. vesiculosus* and *F. serratus*. Similarly, Biancarosa *et al.* (2018) reported generally lower trace metal levels in *L. digitata* compared to *F. vesiculosus* and *F. serratus*, particularly for Mn and Cd, with mean concentrations more than an order of magnitude lower. Trace metal levels appear relatively consistent between *L. digitata* and *L. hyperborea* (Schiener *et al.*, 2015; Raab, Stengel and Feldmann, 2025), perhaps reflecting their growth at similar tidal elevations (Table 1).

2.2.4.2. Intrathallus variation in trace metal concentrations

Intrathallus variation in trace metal concentrations has been linked to differences in tissue age, metabolic activity (e.g., photosynthesis), growth rate, and polysaccharide content (e.g., alginate) (Bryan and Hummerstone, 1973; Stengel, McGrath and Morrison, 2005; García-Seoane *et al.*, 2021). In *F. vesiculosus*, trace metal concentrations typically increase with thallus age, with higher levels reported in older tissues compared to growing tips (Barnett and Ashcroft, 1985; Forsberg *et al.*, 1988). However, Tomlinson *et al.* (1980) observed higher Cu concentrations in the fronds of *F. serratus* relative to their stipes, whilst García-Seoane *et al.* (2021) found higher Cd concentrations in younger tissues of *F. vesiculosus*. The latter was ascribed to higher growth rates in younger tissues providing greater availability of binding sites, thereby enhancing metal uptake. This effect appeared metal-specific though, as opposite trends were observed for Fe, Ni, Pb, and Zn in the same study.

In *L. digitata*, Zn concentrations are elevated in distal blade sections compared to growing regions, a pattern explained by biomass dilution effects (Bryan, 1969). Fe concentrations are highest in holdfasts and lowest in meristems and young blades, attributed to Fe limitation in fast growing tissue (Stengel, McGrath and Morrison, 2005). Similarly, Mn concentrations are highest in holdfasts and increase from stipe to blade, a trend linked to gradients in photosynthetic activity and biomass dilution (Stengel, McGrath and Morrison, 2005). In contrast, Cu concentrations are highest in meristems and young blades and lowest in stipes and distal blades (Stengel, McGrath and Morrison, 2005). This was ascribed to an elevated demand for Cu-binding enzymes in fast growing tissues (Stengel, McGrath and Morrison, 2005).

Concentrations of As in *L. digitata* were reported to increase from stipes to blade tips which was attributed to higher fucoidan content in blade tissues (Sim *et al.*, 2023). Black (1950) found higher alginic acid levels in stipes compared to holdfasts in both *L. digitata* and *L. hyperborea*. Despite previous findings, holdfasts may therefore exhibit lower trace metal concentrations than other thallus segments. Differences in the ratio of M:G units in alginate across thallus regions (Davis, Volesky and Mucci, 2003) may also have implications for metal-binding capacity.

2.2.4.3. Seasonal variation in trace metal concentrations

Seasonal fluctuations in trace metal concentrations are closely associated with changes in environmental conditions such as temperature, precipitation, salinity, pH, and light regime (Phillips, 1977; García-Seoane *et al.*, 2021). These factors exert a dual influence: they affect metal bioavailability in the environment (e.g., via weathering and runoff) and modulate biological processes governing metal uptake, including metabolic activity, growth rate, and polysaccharide production (Fuge and James, 1973; Phillips, 1977; García-Seoane *et al.*, 2021). For example, lower growth rates in *Fucus* spp. during winter promote trace metal accumulation, whereas higher growth rates in spring and summer result in biomass dilution and a progressive decline in tissue concentrations (Fuge and James, 1973; Phillips, 1977; Stengel, McGrath and Morrison, 2005; García-Seoane *et al.*, 2021). Seasonal variation in alginate content also plays a role, with levels peaking in winter and decreasing through summer (García-Seoane *et al.*, 2021).

Consistent with these mechanisms, seasonal variation has been widely documented. In northwest France and northwest Spain, *F. serratus* and *F. vesiculosus* exhibited peak trace metal concentrations in winter and minima in summer (Miramand and Bentley, 1992; García-Seoane *et al.*, 2021). In west Wales, Fuge and James (1973) reported spring maxima and autumn minima for both species, whilst *L. digitata* generally demonstrated elevated concentrations in winter and lowest levels between June and August (Adams *et al.*, 2011).

2.2.5. Trace metal concentrations in brown algae

2.2.5.1. Background concentrations of trace metals in brown algae

Typical background concentrations of trace metals in brown algae are summarised in Table 2. Of the four species studied here, *F. vesiculosus* is the most frequently reported in the literature, with comparatively fewer data available for *L. digitata*, *L. hyperborea*, and *F. serratus* (Aboal *et al.*, 2023).

2.2.5.2. Previous study of trace metal concentrations in brown algae along the northeast coast

Giusti (2001) investigated trace metal concentrations in *F. vesiculosus* and intertidal sediments along the Northumberland and Durham coastlines. In *F. vesiculosus*, the most abundant trace metals were Fe, Mn, Zn, and Cu, whilst Cd and Ag were the least abundant. Samples collected around the Tees Estuary exhibited some of the lowest trace metal levels compared to other sites, with mean concentrations of Cr, Mn, Fe, Ni, Cu, Zn, Cd, and Pb ranging between 0.9–2.4, 18.8–136.2, 67.5–658.8, 0.6–2.9, 8.4–15.8, 23.6–62.9, 0.0–0.2, and 0.5–4.9 mg/kg dry weight, respectively. These values are comparable to those at the designated control site (Table 2, reference 6) and fall within ranges reported for *F. vesiculosus* from unpolluted locations and *Fucus* spp. across the UK (Table 2). Samples collected from sites further north of the Tees Estuary exhibited substantially higher concentrations, with Cd levels up to 50 times greater and indicative of anthropogenic pollution. Collectively, these findings suggest that relative to other stretches of the northeast coastline, the Tees Estuary exhibits comparatively low levels of trace metal contamination.

Species	Metal concentration (mg/kg dw)								Ref
	Cr	Mn	Fe	Ni	Cu	Zn	Cd	Pb	
L. digitata	0.4–2.9	9–100	138–1570	1.4–8.2	5–120	59–148		2–20	[1]
L. digitata	1.3 ± 0.4		47 ± 37	1.0 ± 0.1	2.9 ± 1.0	20 ± 6	0.4 ± 0.1	7.1 ± 4.9	[2]
L. digitata	0.56–0.92	1.6–4.1	36–55	0.32–0.63	0.57–1.9	6.1–15	0.17–0.89	0.041–0.068	[3]
L. digitata	0.7–1.3	4–12	41–199	0.3–0.6	2–17	33–49		0.1–0.6	[4]
L. hyperborea	0.9–1.5	10–30	159–314	0.9–2.0	14–30	59–136		10–26	[1]
L. hyperborea	0.5–2.8	0–38	51–702	0.0–4.3	1–7	1–54		0.0–0.6	[4]
F. vesiculosus	1.5–1.8	102–116	221–730	3.8–5.9	7–10	60–105		2–7	[1]
F. vesiculosus	0.6		33–77		2.1–5.3	7.2–10.2	0.5–2.1	0.4	[5]
F. vesiculosus	0.8–1.8	276.2–778.4	65.0–616.1	0.3–0.7	4.8–9.4	12.9–17.7	0.2–0.5	0.1–1.1	[6]
F. vesiculosus	0.3	149.1		3.6	1.4	25	0.4	0.7	[7]
F. serratus	0.7–2.6	120–800	320–717	1.6–4.5	5–11	63–79		4–21	[1]
Fucus sp.	0.4 ± 0.1	45.0 ± 9.0	53.0 ± 17.3	1.2 ± 0.4	3.8 ± 0.4	73.7 ± 7.3	0.5 ± 0.2	1.3 ± 0.7	[8]
Fucus spp.		33–190	56–1517	1.8–18.0	1.7–28.4	42–962	0.4–20.8	0.5–9.0	[9]

Table 2 | Background trace metal concentrations in brown algae. Trace metal concentrations (mg/kg dry weight) reported for species relevant to the present study, collected from unpolluted or

control sites (except reference [9], which provides UK-wide values). Collection sites, sampling periods, and reporting formats are as follows:

[1] Black and Mitchell (1952). Isle of Seil, Scotland. Jul and Oct 1948, Jan and May 1949, Jun 1950. Reported as concentration ranges.

[2] Sharp, Samant and Vaidya (1988). Nova Scotia, Canada. Jun and Aug 1983. Reported as mean concentrations ± standard deviations.

[3] Ahn *et al.* (2004). Svalbard, Norway. Jul–Aug 2003. Reported as concentration ranges.

[4] Schiener *et al.* (2015). Isle of Seil, Scotland. Aug 2010–Oct 2011. Reported as concentration ranges.

[5] Riget, Johansen and Asmund (1997). Nuup Kangerlua, Greenland. Summer 1980–1982. Reported as (ranges of) geometric mean concentrations.

[6] Giusti (2001). Holy Island, northeast England. Winter 1997–1998. Reported as concentration ranges.

[7] Ryan, McLoughlin and O'Donovan (2012). Wexford, Ireland. May 2008. Reported as mean concentrations.

[8] Tomlinson *et al.* (1980). East coast of Ireland. Mid-winter (year not specified). Reported as mean concentrations ± standard deviations.

[9] Preston *et al.* (1972). UK coastline. 1970 (month/season not specified). Reported as concentration ranges.

2.3. Metal pollution index (MPI)

Absolute metal concentrations do not always provide an accurate or meaningful indication of pollution status (Karaouzas *et al.*, 2021). Multi-element metal pollution indices (MPIs) offer a simple, integrative measure of overall contamination by condensing multiple metals into a single metric (Tomlinson *et al.*, 1980; Brady *et al.*, 2015; Kowalska *et al.*, 2018; Karaouzas *et al.*, 2021). They are useful for visualising spatial and temporal trends in general pollution load and for communicating results to decision-makers and the public (Tomlinson *et al.*, 1980; Karaouzas *et al.*, 2021). MPIs have been widely applied across water, soil, and sediment quality assessments (e.g., Brady *et al.*, 2015; Kowalska *et al.*, 2018; Karaouzas *et al.*, 2021), as well as in macroalgal biomonitoring studies (e.g., Tomlinson *et al.*, 1980; Giusti, 2001; Chalkley *et al.*, 2019).

Despite their utility, MPIs have several limitations. They require an appropriate background reference value, and using baselines from outside the study area may produce misleading results if natural, non-pollution factors (e.g., local geology) differ substantially (Brady *et al.*, 2015; Kowalska *et al.*, 2018). Nevertheless, absolute concentrations face the same challenge, as their interpretation also relies on

comparison with a background value. MPIs may mask cases where a single metal is highly enriched in an otherwise pristine system, potentially obscuring significant ecological risks (Tomlinson *et al.*, 1980; Brady *et al.*, 2015; Karaouzas *et al.*, 2021). Although weighting schemes can account for such disproportionate enrichment, or indeed differences in metal toxicity, these are not applied in all MPIs (Tomlinson *et al.*, 1980; Brady *et al.*, 2015; Karaouzas *et al.*, 2021). MPIs also overlook potential synergistic or antagonistic interactions among metals (Tomlinson *et al.*, 1980), summarising only their individual concentrations. Furthermore, different indices may yield inconsistent pollution classifications due to differences in their underlying parameters and thresholds (Brady *et al.*, 2015; Karaouzas *et al.*, 2021). This complicates interstudy comparisons, even when similar indices are used, as they may differ in metal selection, background values, and/or threshold criteria.

3. Methodology

3.1. Sample collection

A total of 54 brown algal specimens (19 *L. hyperborea*, 14 *L. digitata*, 16 *F. vesiculosus*, and 5 *F. serratus*) were collected from 10 sites along the northeast and North Yorkshire coasts (Figure 10). Of these sites, six were clustered around the Tees Estuary, three were located further south, and one further north. Further details are provided in Appendix A.

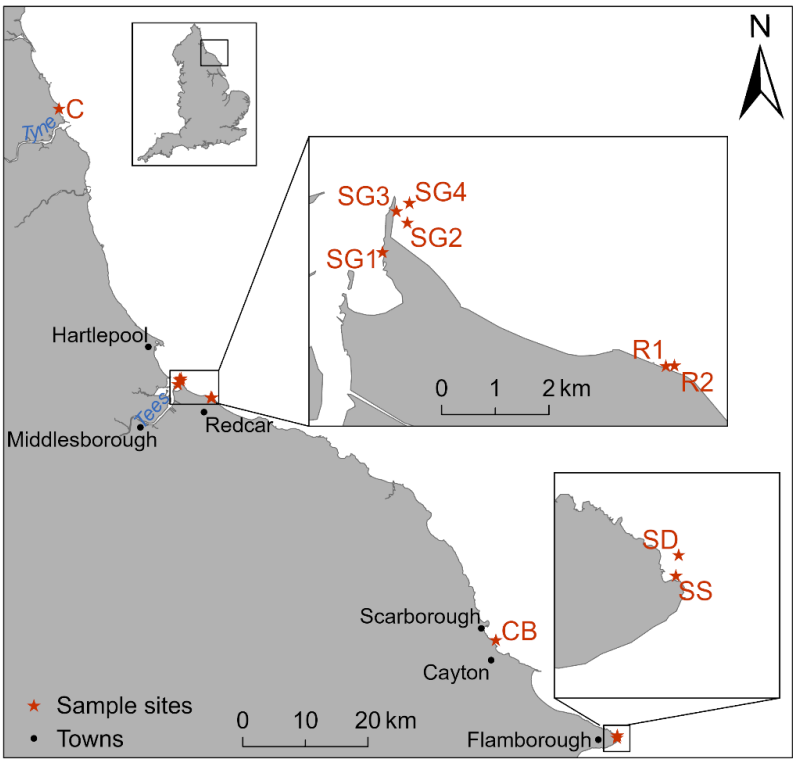

Figure 10 | Sample sites. Insets: reference map of England and enlarged views of the South Gare area and Selwicks Bay. Enlarged maps are presented at the same scale. Sample sites (red stars) are labelled as follows: C = Cullercoats Beach, SG1–4 = South Gare 1–4, R1–2 = Redcar Beach 1–2, CB = Cayton Bay, SD = Selwicks Bay Deep, SS = Selwicks Bay Shallow. Nearby towns (black circles) and the Rivers Tyne and Tees are also labelled.

3.1.1. *Laminaria* spp. collection

Whole *Laminaria* spp. specimens were collected by hand from Cullercoats Beach, Selwicks Bay, Cayton Bay, and South Gare, either at low tide or by diving. Collections from Selwicks Bay, Cayton Bay, and South Gare were made during spring and summer 2024 and stored frozen in individual polyethylene bags. Specimens from Cullercoats Beach were collected in winter 2025 and refrigerated in individual polyethylene bags until processing. At all sites, specimens were

collected *in situ*, except for *L. hyperborea* from Cullercoats Beach, which were obtained as wash-ups.

3.1.2. *Fucus* spp. collection

Whole specimens of *Fucus* spp. were collected by hand from the intertidal zone at Cullercoats Beach, South Gare, and Redcar Beach during winter and spring 2025. Specimens were placed in individual polyethylene bags and refrigerated until processing. Only specimens growing *in situ* were selected. Specimens were collected at the same tidal elevation within each site.

3.2. Sample preparation

Three sample sets were prepared to account for differences in morphology and analytical objectives. These are hereafter referred to as thallus-segmented (or simply segmented), composite, and blade-only samples. For data analysis, composite and blade-only samples were grouped together and are referred to collectively as blade/composite samples.

3.2.1. Cullercoats Beach, South Gare 1 and 2, and Redcar Beach samples

Specimens were rinsed with tap water to remove particulate matter such as sand. *Laminaria* spp. were subsampled to assess intrathallus variation in trace metal concentrations, whereas *Fucus* spp. were processed for bulk concentration analysis. These objectives required different subsampling techniques, outlined below. In both cases, subsamples were cut on a glass slab using a stainless-steel razor blade, placed into individual, open, 50 mL polypropylene tubes, and oven-dried at 80 °C for 48 h.

3.2.1.1. *Laminaria* spp. preparation (thallus-segmented samples)

Once rinsed with tap water, specimens were divided into main anatomical components (holdfast, stipe, and frond body). Each component was rinsed with ultrapure water, brushed with a toothbrush to remove particulate material, and blotted dry. Epiphytes and bryozoans, particularly abundant on *L. hyperborea* stipes, were scraped off. Subsampling techniques varied by anatomical component (Figure 11).

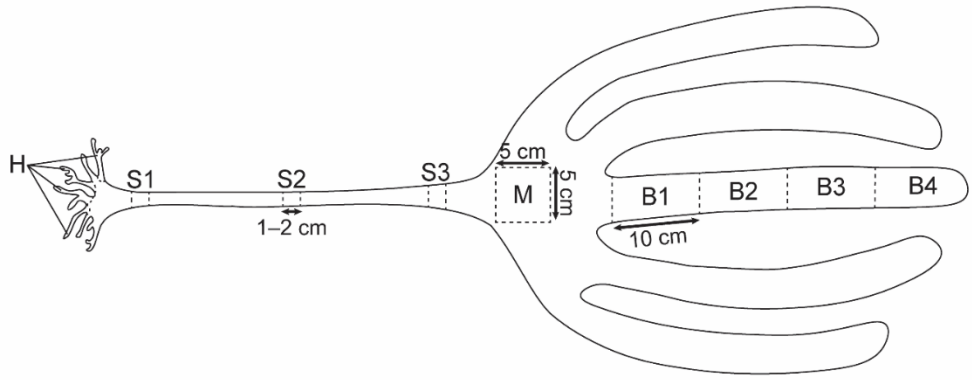

Figure 11 | *Laminaria* spp. preparation. Schematic illustrating the subsampling approach applied to *Laminaria* spp. specimens in the thallus-segmented sample set (dashed lines, annotations). Segments are labelled as follows: H = holdfast, S1–3 = stipe 1–3, M = meristem, B1–4 = blade 1–4.

3.2.1.1.1. Holdfasts

Individual root-like projections were removed from three to five randomly selected locations and cut into <1 cm pieces (Figure 11). Where substrate could not be removed by brushing, it was cut away. One specimen lacked a holdfast, and two others had only very small holdfasts, which were not sampled.

3.2.1.1.2. Stipes

Stipes were subsampled at the base, middle, and top (Figure 11). At each point, 1–2 cm thick cross-sections were cut and further divided into smaller pieces to better facilitate drying. Two specimens had only very short stipes, which were not sampled.

3.2.1.1.3. Meristems

Meristems were sampled by removing an area of approximately 5 x 5 cm adjacent to the top of the stipe (Figure 11), which was subsequently cut into smaller strips. In specimens with very long meristems, these were divided into

approximately 10 x 5 cm sections. Sample IDs were assigned in sequence, with meristem 1 corresponding to the youngest section nearest the top of the stipe and higher numbers representing progressively older sections.

3.2.1.1.4. Blades

The central blade of each specimen was removed and sectioned into approximately 10 cm segments, typically yielding four blade samples per specimen (Figure 11). However, one specimen provided only a single sample, whilst six were obtained from another. Sample IDs were assigned in sequence, with blade 1 corresponding to the youngest section adjacent to the meristem and higher numbers representing progressively older, more distal sections. Blade segments were further cut into smaller pieces or strips.

3.2.1.2. *Fucus* spp. preparation (composite samples)

Following rinsing with tap water, 8–10 cm long undamaged frond sections were cut from five randomly selected locations to form a composite subsample for each specimen (Figure 12). Fronds were rinsed with ultrapure water, brushed with a toothbrush to remove particulate material, and blotted dry before being shredded into approximately 1 x 1 cm strips. Reproductive receptacles and air bladders were excluded from composite subsamples, as their tissue composition differs from that of vegetative tissue (Lee, 2018).

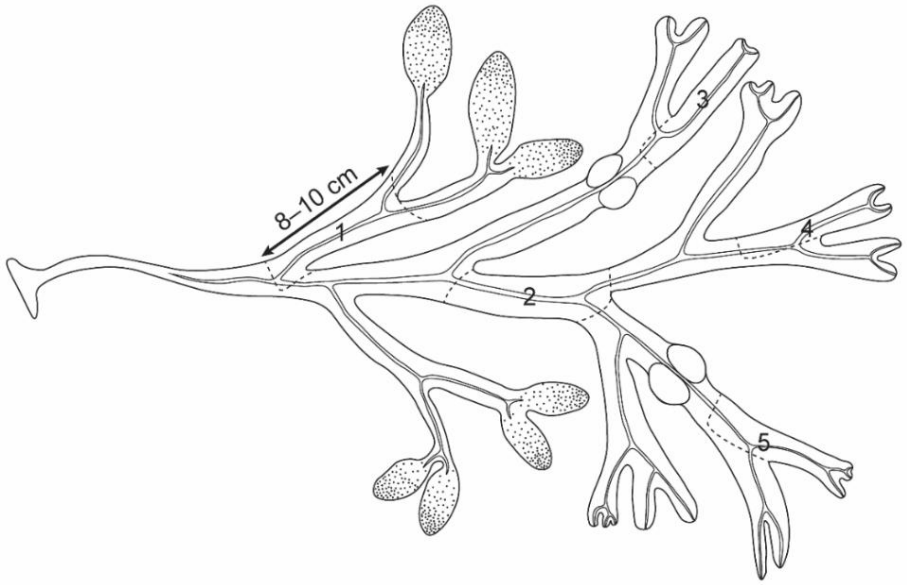

Figure 12 | *Fucus* spp. preparation. Schematic illustrating the subsampling approach applied to *Fucus* spp. specimens. Five 8–10 cm frond sections (dashed outlines, labelled 1–5) were pooled into one composite subsample per specimen.

3.2.2. Selwicks Bay, Cayton Bay, and South Gare 3 and 4 samples (blade-only samples)

Specimens were thawed overnight, after which central blades were removed on a glass slab using a stainless-steel razor blade. Epiphytes and bryozoans were scraped off, and particulate material was removed by rinsing with ultrapure water. Blades were blotted dry, shredded into smaller strips, placed in a glass beaker, and oven-dried at 80 °C for 24 h.

3.3. Sample digestion

Two digestion methods were employed. Most thallus-segmented samples were digested at the National Horizons Centre, Teesside University, via closed-vessel microwave-assisted acid digestion, whilst a small number were digested in the Department of Earth Sciences, Durham University, via closed-vessel hot plate acid digestion. One sample was digested using both methods. All blade-only and composite samples were digested via the hot plate method.

3.3.1. Closed-vessel microwave-assisted acid digestion

Approximately 100 mg of dried sample were weighed into a PTFE digestion vessel, and 8 mL of 70% HNO_3 was added. Digestion was carried out in a microwave system (Milestone ETHOS UP MAXI-14 rotor, National Horizons Centre, Teesside University) using a programme optimised for calcium alginate: 10 min at 160 °C and 850 W, 15 min at 200 °C and 850 W, 20 min cool down. Digests were then diluted to 30 mL with ultrapure water.

3.3.2. Closed-vessel hot plate acid digestion

Dried samples were ground in a food processer for 1–2 min in 30 s bursts. Approximately 100 mg of ground sample were weighed into a PTFE vial, and 2.5 mL of 69% HNO_3 was added. Vials were sealed and heated on a hot plate at 125 °C for 3–5 h, then left to digest further at room temperature for 48–72 h. Digests were subsequently diluted to 50 mL with ultrapure water.

3.4. ICP-MS analysis

Prior to analysis, digests were further diluted 1:5 with 3% HNO_3. Concentrations of Cr, Mn, Fe, Ni, Cu, Zn, Cd, and Pb were determined by ICP-MS (Thermo Scientific iCAP TQe, Department of Earth Sciences, Durham University).

3.5. Quality control measures

- Procedural blanks were prepared for both digestion techniques and treated identically to samples.
- Replicate digestions were performed on randomly selected samples.
- For hot plate digestions, the same sample was included in each batch as an internal standard.
- Multi-element calibration standards were prepared at different concentrations and analysed periodically throughout sample runs to monitor instrumental drift.
- High-purity reagents were used, including Milli-Q ultrapure (18.2 MΩ·cm) water and reagent grade HNO_3, and clean laboratory practices were consistently maintained.
- Method detection limits (MDLs) for each trace metal were calculated for every digestion batch as the mean concentration of procedural blanks plus three standard deviations. For microwave-assisted digestion, where only one procedural blank was used, the standard deviation from instrument replicates was applied instead.

3.6. Data processing and analysis

3.6.1. Raw data processing

Raw data were first corrected for instrumental drift, dilution, and sample mass to yield trace metal concentrations in mg/kg dry weight. For microwave-assisted digestion results, an additional correction was applied to account for elevated procedural blank concentrations. This was not necessary for hot plate digestion results due to minimal background contamination. Adjusted sample concentrations and procedural blank concentrations are presented in Appendix B.

Prior to sample mass adjustment, concentrations (in ppb) were compared against MDLs. None of the hot plate results fell below MDLs, whereas many microwave results did, due to high blank concentrations. To account for variable sample masses, sample-specific MDLs (in mg/kg dry weight) were calculated for each metal. Values falling below their respective MDLs were substituted with half the MDL. However, most substituted values for Cu and Pb were negative, and these elements were therefore excluded from further analysis in the thallus-segmented dataset. One sample also yielded a negative Cr concentration following substitution. As it was a duplicate, the replicate value was retained without averaging.

3.6.2. MPI calculation

To assess overall trace metal contamination between sites, MPI was calculated for each using the blade/composite dataset and the following equation (Giusti, 2001; Chalkley *et al.*, 2019):

$$MPI = (M_1 \times M_2 \times M_3 \times \ldots \times M_n)^{\frac{1}{n}}$$

where M = concentration of a metal (in mg/kg dry weight) and n = number of metals included.

This is a simple geometric mean and does not incorporate weighting for extreme enrichment of individual metals or for differences in toxicity. Results are therefore interpreted in conjunction with absolute concentrations. In addition to using background concentrations derived from distant unpolluted sites, results are also interpreted against UK-wide reference values (Table 2). This is to mitigate some of the issues associated with using baselines from outside the study area.

3.6.3. Figure generation

Spatial maps were produced using Esri ArcGIS Pro (version 3.3.0). An England boundary shapefile was sourced from the Open Geography Portal (Office for National Statistics, 2025) and Tees catchment shapefiles from the Catchment Data Explorer (Environment Agency, 2023). Box plots were generated in Microsoft Excel, chemical structure drawings in ACD ChemSketch, and schematic illustrations in Adobe Illustrator.

3.6.4. Statistical analyses

All statistical analyses were conducted in Posit RStudio (version 2025.05.1+513). Analyses were performed separately on the segmented and blade/composite datasets. Normality of trace metal concentration data was assessed using Shapiro–Wilk tests. All metals, except Zn in the segmented dataset, exhibited non-normal distributions ($p < 0.05$) (Appendix C), and non-parametric methods were therefore employed.

Spearman's rank correlation coefficients were calculated to evaluate trends in trace metal concentrations along the coastline (blade/composite data) and along the thallus (segmented data). Relative position indices were applied in both cases. For downcoast analyses, South Gare 1 was assigned a value of 0 and Selwicks Bay Shallow a value of 8. Thallus trends were evaluated in two parts: from holdfast to meristem 1 and from meristem 1 to blade tip, with relative position indices assigned accordingly (e.g., holdfast = 0, meristem 1 = 4). Dunn's test was applied to compare trace metal concentrations across thallus segments. Pairwise *p*-values were adjusted using the Benjamini–Hochberg correction to control false discovery rate. Wilcoxon rank-sum tests were performed to assess interspecific and depth-related differences in trace metal concentrations. Statistical significance was defined as $p < 0.05$. Full test results are presented in Appendix D.

4. Results and discussion

4.1. Comparison with background levels

The vast majority of trace metal concentrations fall within or below background and UK ranges (Table 3). Only a small number of samples exceed these levels for one or two metals (mainly Cr, Ni, Cd, and Pb), with a few values anomalously high relative to other samples. These are discussed later in detail. Overall, sample concentrations generally reflect unpolluted conditions along the northeast and North Yorkshire coasts relative to background levels.

Sample set	Metal concentration (mg/kg dw)		
	Cr	**Mn**	**Fe**
All samples	**0.03–74.00 *(1.51)***	**0.95–318.62 *(27.53)***	**14.79–931.95 *(134.01)***
Blade/composite	**0.06–0.48 *(0.17)***	**3.82–142.22 *(40.24)***	**21.94–931.95 *(129.13)***
C	0.06–0.11 *(0.09)*	45.72–142.22 *(89.41)*	45.36–109.34 *(71.31)*
F. vesiculosus	0.09–0.11 *(0.10)*	83.24–142.22 *(117.24)*	86.84–109.34 *(93.66)*
F. serratus	0.06–0.10 *(0.08)*	45.72–88.68 *(67.14)*	45.36–67.54 *(53.42)*
SG1	0.28–0.37 *(0.33)*	58.53–112.21 *(91.75)*	146.63–194.70 *(164.61)*
SG3	0.19–0.48 *(0.28)*	10.26–18.70 *(14.19)*	361.28–931.95 *(573.04)*
SG4	0.14–0.28 *(0.22)*	9.74–16.47 *(14.02)*	66.79–468.66 *(201.70)*
SG2	0.10–0.12 *(0.11)*	61.31–92.92 *(74.53)*	119.94–128.56 *(123.11)*
R1	0.07–0.09 *(0.08)*	28.14–48.56 *(41.01)*	34.24–53.96 *(41.14)*
R2	0.07–0.09 *(0.08)*	17.31–35.59 *(27.78)*	30.07–56.44 *(45.30)*
CB	0.10–0.31 *(0.17)*	3.82–36.69 *(11.44)*	21.94–55.77 *(37.41)*
L. digitata	0.10–0.31 *(0.18)*	3.82–5.27 *(4.79)*	37.35–55.77 *(44.65)*
L. hyperborea	0.12–0.24 *(0.17)*	7.34–36.69 *(18.10)*	21.94–41.44 *(30.16)*
SD	0.18–0.24 *(0.22)*	26.05–37.45 *(30.61)*	65.45–103.31 *(78.42)*
SS	0.12–0.21 *(0.17)*	8.55–21.11 *(14.32)*	29.00–93.71 *(55.16)*
Thallus-segmented	**0.03–74.00 *(2.80)***	**0.95–318.62 *(15.32)***	**14.79–539.18 *(138.69)***
L. digitata	0.04–74.00 *(4.13)*	0.95–318.62 *(13.99)*	17.44–539.18 *(169.98)*
Holdfast	0.84	318.62	186.87
Stipe	0.16–74.00 *(12.76)*	0.95–6.00 *(2.31)*	25.82–385.26 *(93.75)*
Meristem	0.04–23.54 *(2.61)*	1.27–5.48 *(3.28)*	17.44–520.21 *(127.35)*
Blade	0.41–8.62 *(1.91)*	2.08–13.97 *(5.49)*	68.87–539.18 *(227.77)*
L. hyperborea	0.03–1.27 *(0.45)*	1.00–112.56 *(17.70)*	14.79–212.32 *(83.07)*
Holdfast	0.35–1.27 *(0.81)*	51.87–112.56 *(82.21)*	98.08–203.87 *(150.98)*
Stipe	0.13–1.09 *(0.55)*	1.59–46.09 *(22.21)*	17.05–212.32 *(95.70)*
Meristem	0.03–0.21 *(0.12)*	1.00–1.75 *(1.38)*	14.79–16.95 *(15.87)*
Blade	0.12–0.95 *(0.36)*	1.21–3.74 *(2.27)*	33.65–181.04 *(73.41)*
Background	**0.3–2.9**	**0–800**	**33–1570**
UK		**33–190**	**56–1517**

Sample set	Metal concentration (mg/kg dw)		
	Ni	**Cu**	**Zn**
All samples	**0.17–100.24** ***(3.38)***	**0.86–5.77** ***(2.44)***	**3.99–88.42** ***(33.39)***
Blade/composite	**0.17–5.71** ***(1.60)***	**0.86–5.77** ***(2.44)***	**16.52–88.42** ***(38.99)***
C	1.78–4.28 *(2.92)*	1.93–2.81 *(2.25)*	40.12–66.55 *(52.64)*
F. vesiculosus	3.18–4.82 *(3.95)*	2.06–2.45 *(2.26)*	41.24–51.43 *(47.42)*
F. serratus	1.78–2.56 *(2.10)*	1.93–2.81 *(2.23)*	40.12–66.55 *(56.82)*
SG1	0.65–2.71 *(1.90)*	4.42–5.77 *(5.11)*	40.40–88.42 *(68.51)*
SG3	0.27–0.43 *(0.33)*	2.84–4.17 *(3.45)*	32.78–56.02 *(42.70)*
SG4	0.19–0.29 *(0.24)*	1.94–4.58 *(3.00)*	27.48–42.49 *(37.33)*
SG2	4.25–5.71 *(4.74)*	2.54–3.26 *(2.78)*	47.93–70.76 *(57.73)*
R1	2.50–4.29 *(3.60)*	1.94–2.29 *(2.15)*	36.99–50.42 *(44.28)*
R2	1.61–3.71 *(2.87)*	1.42–2.34 *(1.99)*	23.68–44.95 *(37.39)*
CB	0.17–0.67 *(0.32)*	0.86–2.32 *(1.54)*	16.52–35.14 *(22.89)*
L. digitata	0.17–0.24 *(0.20)*	1.79–2.32 *(1.96)*	22.53–35.14 *(28.09)*
L. hyperborea	0.21–0.67 *(0.44)*	0.86–1.43 *(1.12)*	16.52–19.19 *(17.69)*
SD	0.52–1.23 *(0.87)*	1.73–4.02 *(2.76)*	23.62–37.39 *(29.71)*
SS	0.28–0.49 *(0.39)*	1.36–1.80 *(1.64)*	17.17–21.50 *(20.18)*
Thallus-segmented	**0.25–100.24** ***(5.09)***		**3.99–47.73** ***(28.00)***
L. digitata	0.25–100.24 *(7.23)*		8.06–41.01 *(27.05)*
Holdfast	2.53		12.42
Stipe	0.29–51.75 *(8.94)*		8.06–39.57 *(21.17)*
Meristem	0.25–100.24 *(10.55)*		11.32–37.14 *(25.31)*
Blade	0.40–34.15 *(4.65)*		16.66–41.01 *(31.54)*
L. hyperborea	0.27–8.16 *(1.28)*		3.99–47.73 *(29.69)*
Holdfast	0.56–8.16 *(4.36)*		3.99–5.97 *(4.98)*
Stipe	0.34–3.70 *(1.30)*		22.08–36.57 *(29.52)*
Meristem	0.36–0.47 *(0.42)*		27.43–33.29 *(30.36)*
Blade	0.27–1.33 *(0.72)*		25.32–47.73 *(35.83)*
Background	**0.0–8.2**	**0.57–120**	**1–148**
UK	**1.8–18.0**	**1.70–28**	**42–962**

Sample set	Metal concentration (mg/kg dw)	
	Cd	**Pb**
All samples	**0.01–1.60 *(0.24)***	**0.16–41.98 *(2.53)***
Blade/composite	**0.03–0.87 *(0.27)***	**0.16–41.98 *(2.53)***
C	0.32–0.87 *(0.57)*	0.31–0.67 *(0.44)*
F. vesiculosus	0.32–0.47 *(0.41)*	0.33–0.63 *(0.45)*
F. serratus	0.52–0.87 *(0.70)*	0.31–0.67 *(0.44)*
SG1	0.15–0.29 *(0.21)*	1.62–2.68 *(2.15)*
SG3	0.03–0.04 *(0.04)*	3.31–7.55 *(5.01)*
SG4	0.03–0.22 *(0.13)*	1.61–41.98 *(24.03)*
SG2	0.44–0.70 *(0.56)*	0.43–0.57 *(0.52)*
R1	0.40–0.52 *(0.45)*	0.16–0.32 *(0.24)*
R2	0.22–0.28 *(0.26)*	0.17–0.31 *(0.26)*
CB	0.03–0.20 *(0.09)*	0.21–0.65 *(0.39)*
L. digitata	0.03–0.03 *(0.03)*	0.28–0.50 *(0.35)*
L. hyperborea	0.08–0.20 *(0.14)*	0.21–0.65 *(0.43)*
SD	0.21–0.36 *(0.29)*	0.85–2.08 *(1.24)*
SS	0.14–0.20 *(0.17)*	0.29–0.67 *(0.44)*
Thallus-segmented	**0.01–1.60 *(0.21)***	
L. digitata	0.01–0.45 *(0.10)*	
Holdfast	0.09	
Stipe	0.03–0.28 *(0.10)*	
Meristem	0.01–0.45 *(0.20)*	
Blade	0.01–0.16 *(0.04)*	
L. hyperborea	0.05–1.60 *(0.40)*	
Holdfast	0.55–1.00 *(0.78)*	
Stipe	0.11–0.91 *(0.33)*	
Meristem	0.39–1.60 *(1.00)*	
Blade	0.05–0.59 *(0.22)*	
Background	**0.17–0.89**	**0.0–26**
UK	**0.40–20.80**	**0.5–9**

Table 3 | Summary statistics. Minimum–maximum *(mean)* trace metal concentrations (mg/kg dry weight) across all samples and pooled subsets. Data are summarised for blade/composite and thallus-segmented sets, and further by site, species, and thallus segment where relevant. Site abbreviations: C = Cullercoats Beach, SG1–4 = South Gare 1–4, R1–2 = Redcar Beach 1–2, CB = Cayton Bay, SD = Selwicks Bay Deep, SS = Selwicks Bay Shallow. Background and UK reference ranges (minimum–maximum), derived from Table 2, are included for context.

4.2. Blade/composite results

4.2.1. Spatial trends in trace metal concentrations

Whilst MPI provides a useful overview of the spatial distribution of trace metal pollution (Figure 13), investigating how individual trace metal concentrations change along the coastline (Figure 14) offers a more detailed perspective and can reveal differences in metal behaviour.

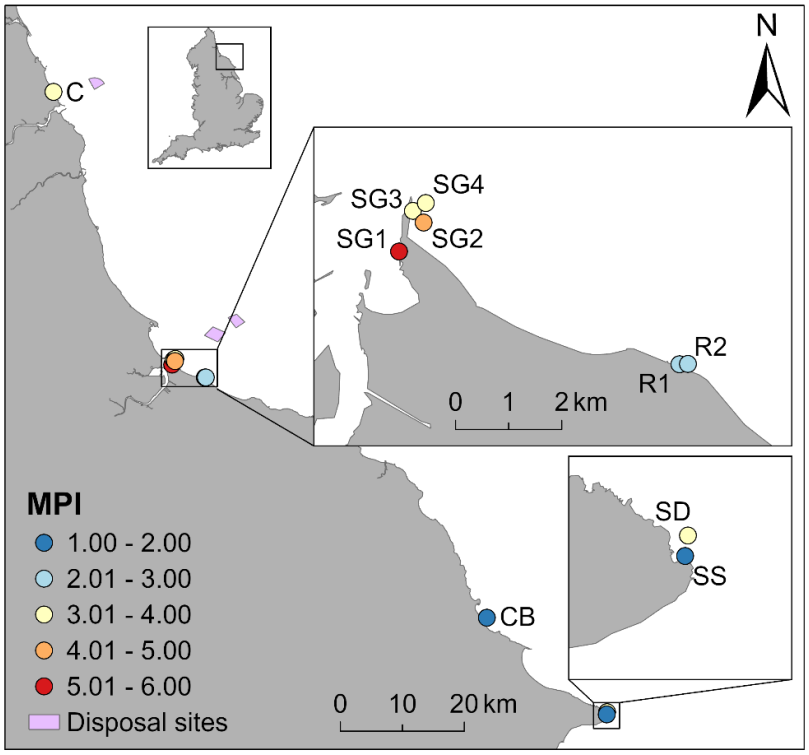

Figure 13 | MPI along the northeast and North Yorkshire coastlines. Insets: reference map of England and enlarged views of the South Gare area and Selwicks Bay. Enlarged maps are presented at the same scale. Sample sites are labelled as follows: C = Cullercoats Beach, SG1–4 = South Gare 1–4, R1–2 = Redcar Beach 1–2, CB = Cayton Bay, SD = Selwicks Bay Deep, SS = Selwicks Bay Shallow. Offshore disposal sites for material dredged from the Tees and Tyne Estuaries are also shown (pink polygons), based on Bolam *et al.* (2023, 2024).

4.2.1.1. Overview

MPI is highest at South Gare 1 and declines down the coast, reaching a minimum at Cayton Bay (Figure 13). Significant downward trends from South Gare 1 are observed for Fe ($p < 0.001$), Cu ($p < 0.001$), Zn ($p < 0.001$), and Pb ($p = 0.003$) (Table 3 and Figure 14).

Overall, MPI values are low (Figure 13). A threshold indicative of background conditions can be estimated using maximum trace metal concentrations reported

for brown algae from unpolluted sites (Table 3), yielding a value of 43. All MPI values fall well below this limit. When compared to a ‘typical’ UK MPI (83), derived using the same approach, the present values are also substantially lower.

Mean concentrations of individual trace metals fall within ranges typical of brown algae from unpolluted sites (Table 3 and Figure 14). The same is generally true when compared to UK reference values (Table 3), with the exception of mean Pb at South Gare 4. Two samples from this site exhibited Pb levels approximately three- and five-fold higher than values reported by Preston *et al.* (1972).

4.2.1.2. South Gare 1

Elevated MPI at South Gare 1 may reflect proximity to trace metal inputs, potentially associated with sediment dredging upstream of the Tees Estuary mouth. The site’s location within the estuary breakwaters may limit mixing of dredged material with open coastal waters, concentrating metals locally and leading to the higher overall MPI observed. Elevated trace metal concentrations in *F. vesiculosus* growing in sheltered environments such as harbours have previously been reported (Fuge and James, 1973).

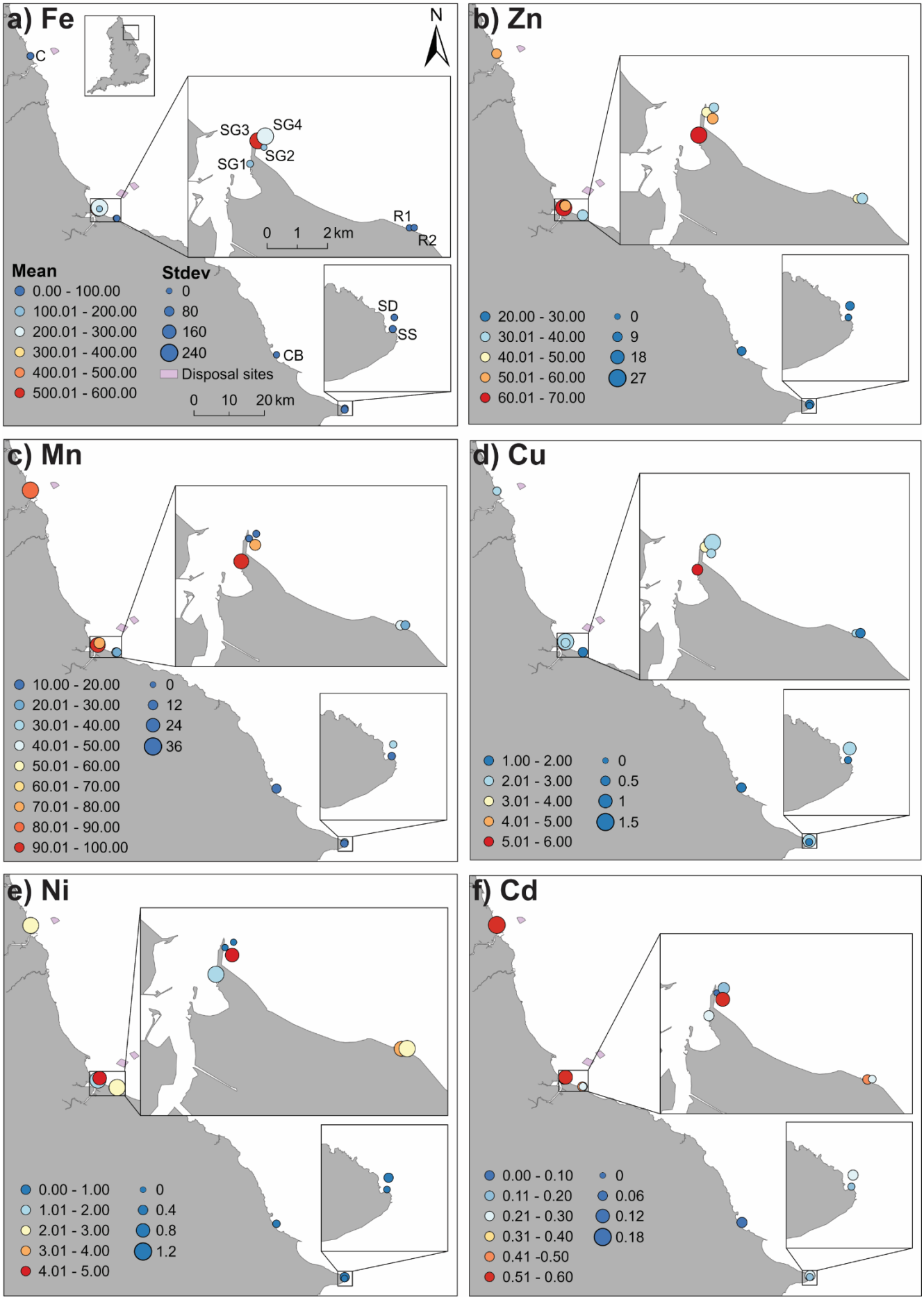
a) Fe
N
C
SG3
SG4
SG2
SG1
R1
R2
0 1 2 km
SD
SS
CB
Mean
0.00 - 100.00
100.01 - 200.00
200.01 - 300.00
300.01 - 400.00
400.01 - 500.00
500.01 - 600.00
Stdev
0
80
160
240
Disposal sites
0 10 20 km
b) Zn
20.00 - 30.00
30.01 - 40.00
40.01 - 50.00
50.01 - 60.00
60.01 - 70.00
0
9
18
27
c) Mn
10.00 - 20.00
20.01 - 30.00
30.01 - 40.00
40.01 - 50.00
50.01 - 60.00
60.01 - 70.00
70.01 - 80.00
80.01 - 90.00
90.01 - 100.00
0
12
24
36
d) Cu
1.00 - 2.00
2.01 - 3.00
3.01 - 4.00
4.01 - 5.00
5.01 - 6.00
0
0.5
1
1.5
e) Ni
0.00 - 1.00
1.01 - 2.00
2.01 - 3.00
3.01 - 4.00
4.01 - 5.00
0
0.4
0.8
1.2
f) Cd
0.00 - 0.10
0.11 - 0.20
0.21 - 0.30
0.31 - 0.40
0.41 -0.50
0.51 - 0.60
0
0.06
0.12
0.18

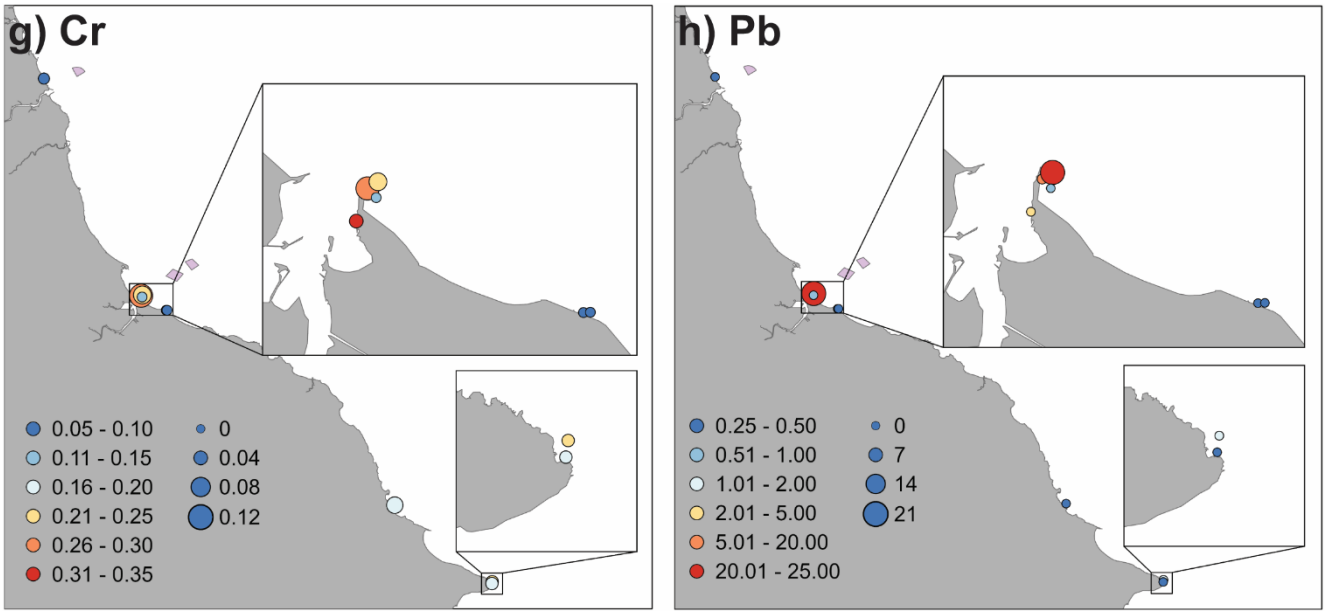

Figure 14 | Trace metal concentrations along the northeast and North Yorkshire coastlines. Insets in all panels show enlarged views of the South Gare area and Selwicks Bay. Panel a) additionally includes a reference map of England. Enlarged maps are presented at the same scale. Scale bars and sample site labels in panel a) apply across all panels. Sample sites are labelled as follows: C = Cullercoats Beach, SG1–4 = South Gare 1–4, R1–2 = Redcar Beach 1–2, CB = Cayton Bay, SD = Selwicks Bay Deep, SS = Selwicks Bay Shallow. Mean metal concentrations (mg/kg dry weight) are illustrated by coloured circles, with circle size representing standard deviation (Stdev). Each panel displays the range of concentrations and standard deviations. Note the variable bin widths for Pb concentrations. Circle sizing is consistent across the full coastline map and insets in each panel. Offshore disposal sites for material dredged from the Tees and Tyne Estuaries are also shown (pink polygons), based on Bolam *et al.* (2023, 2024).

4.2.1.3. South Gare 2, 3, and 4

MPI values at South Gare 2, 3, and 4 are relatively high (Figure 13). Although disposal sites for dredged material are located several kilometres offshore, Eastabrook *et al.* (2022) demonstrated that a modelled pyridine plume released during sediment dredging and disposal could reach the South Gare area within days, carrying elevated concentrations. This, combined with the sites' proximity to the estuary mouth, may account for the relatively high MPI values observed.

4.2.1.3.1. South Gare 2 versus 3 and 4

MPI at South Gare 2 is higher than at South Gare 3 and 4 (Figure 13). This observation appears to be driven primarily by Mn, Ni, and Cd (Table 3 and Figure

14). These metals even occur at higher concentrations at Redcar Beach compared to South Gare 3 and 4, despite these sites being further downcoast.

One possible explanation for these disparities is temporal variability. Samples from South Gare 3 and 4 were collected in 2024, whereas those from South Gare 2 were collected in 2025. Dredging intensity, perhaps linked to the ongoing Teesworks development, may have increased between these years.

Interspecific variation may be another reason. *F. vesiculosus* was collected at South Gare 2, whereas *L. digitata* and *L. hyperborea* were collected at South Gare 3 and 4, respectively. *Laminaria* spp. typically exhibit higher growth rates than *F. vesiculosus* (Table 1), resulting in stronger biomass dilution and consequently lower trace metal concentrations (Sawidis *et al.*, 2001).

Seasonal differences in sampling may have further amplified these growth-related effects. *F. vesiculosus* from South Gare 2 was collected in March, in contrast to April for South Gare 3, and May and July for South Gare 4. Whilst these differences in collection timing are modest, seasonal growth rates vary between species. In most Fucales, growth rates peak between late spring and early summer, whereas in Laminariales, growth rates may be high from winter onwards (Bartsch *et al.*, 2008; Hill, 2008; Lee, 2018). Therefore, *F. vesiculosus* from South Gare 2 may not have reached peak growth yet, whereas *Laminaria* spp. from South Gare 3 and 4 could have been undergoing fast growth for several months already, compounding the disparity in biomass dilution.

However, the opposite could also be argued. Since *Laminaria* spp. typically grow at lower tidal elevations than *F. vesiculosus* (Table 1), they are submerged for longer periods and would therefore be expected to accumulate higher trace metal concentrations (Bryan and Hummerstone, 1973; Fuge and James, 1973; Stengel *et al.*, 2004; Ownsworth *et al.*, 2019). Nevertheless, lower trace metal levels have been reported in *L. digitata* compared to *Fucus* spp., despite growing at lower tidal elevation (Stengel *et al.*, 2004; Biancarosa *et al.*, 2018). Differences in subsampling strategy between *F. vesiculosus* (composite) and *Laminaria* spp. (blade-only) may have also contributed.

In contrast to Mn, Ni, and Cd, mean Fe levels are higher at South Gare 3 and 4 compared to South Gare 2 (Table 3 and Figure 14). South Gare 3, in particular, exhibits an exceptionally elevated mean Fe concentration, far exceeding those

recorded at all other sites. South Gare 3 and 4 show large standard deviations and wide concentration ranges for Fe. Duplicate samples show consistent results, suggesting genuine environmental variation.

It has previously been shown that Fe in water samples from the Tees Estuary occurs mainly in particulate form, with relatively minor proportions present in the soluble phase (Taylor, 1982). The role of fine sediment particles in influencing metal concentrations in brown algae, including Fe, has been well-documented (García-Seoane *et al.*, 2021). Barnett and Ashcroft (1985) reported high Fe concentrations in *F. vesiculosus* at several sites along the Humber Estuary, attributing these values to surface contamination by fine particulate matter, despite thorough cleaning. Although Fe levels in this study are substantially lower than those observed in the Humber Estuary, the pronounced variability and relatively elevated concentrations at South Gare 3 and 4 may similarly reflect surface contamination by fine particulate material.

4.2.1.3.2. Pb concentrations at South Gare 4

Pb concentrations are highly variable, with mean levels spanning two orders of magnitude across all sites. South Gare 4 has an unusually high mean Pb concentration and standard deviation. Two of the three *L. hyperborea* samples collected here have consistent duplicates with elevated Pb (24.74–42.99 mg/kg dry weight), whereas the third is markedly lower (1.61 mg/kg dry weight). This discrepancy may be explained by differences in collection timing, as the lower Pb sample was obtained two months after the two high Pb samples.

One possibility is that a transient influx of dissolved Pb occurred prior to the collection of the first two samples but had dissipated before the third. Assuming a maximal growth rate of 0.94 cm/day for *L. hyperborea* (Table 1), approximately 54 cm of new biomass could have grown in two months, enough to produce a new blade. If this hypothetical Pb pulse ceased shortly after the first collection, lower Pb concentrations would be observed in the later sample.

However, the extent of Pb enrichment in the first two South Gare 4 samples raises the question of why similarly high levels were not observed in *L. digitata* from South Gare 3, located nearby and sampled only two weeks earlier. Based on the same growth rate assumption for *L. hyperborea* from South Gare 4, around 13 cm

of new biomass could have grown in that time, enough for around half a blade. This suggests that a dissolved Pb influx may have occurred between the South Gare 3 and first South Gare 4 collections. The timing could even place the onset of the influx just prior to South Gare 3 sampling, as these *L. digitata* samples also exhibited relatively elevated Pb levels (3.31–7.55 mg/kg dry weight) compared to other sites.

This hypothesis, however, rests on several assumptions, and the potential source of Pb remains unknown. If a period of intensive sediment dredging and disposal was responsible for the Pb pulse, one would expect the first two South Gare 4 samples to be highly enriched in multiple metals and the third to be uniformly lower, patterns which are not supported by the data. Furthermore, the assumption of maximal growth rates is unsuitable, given that collections were conducted in late spring and summer, when growth rates in Laminariales typically begin to decline (Bartsch *et al.*, 2008; Hill, 2008; Lee, 2018).

Surface contamination by fine particulate material presents another possible explanation for the observed Pb distribution. Pb is highly abundant in Tees Estuary sediments (Davies, Tomlinson and Stephenson, 1991; Jones and Turki, 1997; Plater *et al.*, 1999; Giusti, 2001) and predominantly occurs in particulate form in the estuary waters (Taylor, 1982). Like Fe, Pb concentrations in brown algae are known to be influenced by fine sediment particles on the thallus surface (García-Seoane *et al.*, 2021). Suspended sediment loads may have been higher during the collection of the first two South Gare 4 samples, and despite thorough cleaning, residual fine particles may have remained on blade surfaces, leading to anomalously elevated Pb concentrations.

4.2.1.4. Selwicks Bay

Moving down the coastline, MPI increases at Selwicks Bay sites (Figure 13), which may be attributed to local hydrodynamics. Selwicks Bay appears more enclosed than Cayton Bay, which could lead to reduced mixing with open coastal waters. Additionally, the coastline changes shape just south of Selwicks Bay, which may influence sediment deposition patterns and, in turn, dissolved trace metal availability.

Selwicks Bay Deep exhibits a particularly elevated MPI, even relative to Selwicks Bay Shallow, despite sites sharing the same collection date and species.

Concentrations at Selwicks Bay Deep are higher in all metals compared to Selwicks Bay Shallow (Figure 15). Significant differences are found for Mn, Ni, Zn, Cd, and Pb (p = 0.02 for all). This difference may reflect a depth effect, since samples at Selwicks Bay Deep were collected 4 m deeper than their shallow counterparts, and at the lowest tidal elevation across all sites. Lower tidal elevations can lead to longer submersion periods and greater potential for element uptake (Bryan and Hummerstone, 1973; Fuge and James, 1973; Stengel *et al.*, 2004; Ownsworth *et al.*, 2019).

4.2.1.5. Cullercoats Beach

MPI is relatively high at Cullercoats Beach (Figure 13), comparable to some South Gare sites. Mn, Zn, Ni, and Cd concentrations are particularly elevated and often accompanied by high standard deviations (Figure 14). This may reflect an influence from the River Tyne as opposed to the Tees, as the River Tyne discharges into the sea just south of Cullercoats Beach.

The Tyne shares a similar mining and industrial legacy with the Tees, draining the North Pennine Orefield (Hudson-Edwards *et al.*, 1996) and once hosting extensive iron, steel, shipbuilding, coke, and tar industries along its estuary (Hardy, Evans and Tremayne, 1993; Giusti, 2001). At the height of industrial discharges during the 1970s, the estuary received 68 x 10^4 m^3 of waste per day (Hardy, Evans and Tremayne, 1993). Elevated Pb, Zn, and Cr concentrations in estuarine sediments have been attributed to these industrial sources as well as erosional products from the North Pennines (Rowlatt and Lovell, 1994).

More recently, water sampling between 2022 and 2024 found the entire lower and estuary catchment polluted relative to environmental quality standards, linked to contamination from abandoned metal mines (Environment Agency, 2025c). As in the Tees Estuary, sediments are regularly dredged and disposed of offshore, approximately 5 km from the estuary mouth (Bolam *et al.*, 2023) (Figures 13 and 14). Comparable levels of metal pollution may therefore be expected in the Tyne area, which may explain the relatively high MPI observed at Cullercoats Beach.

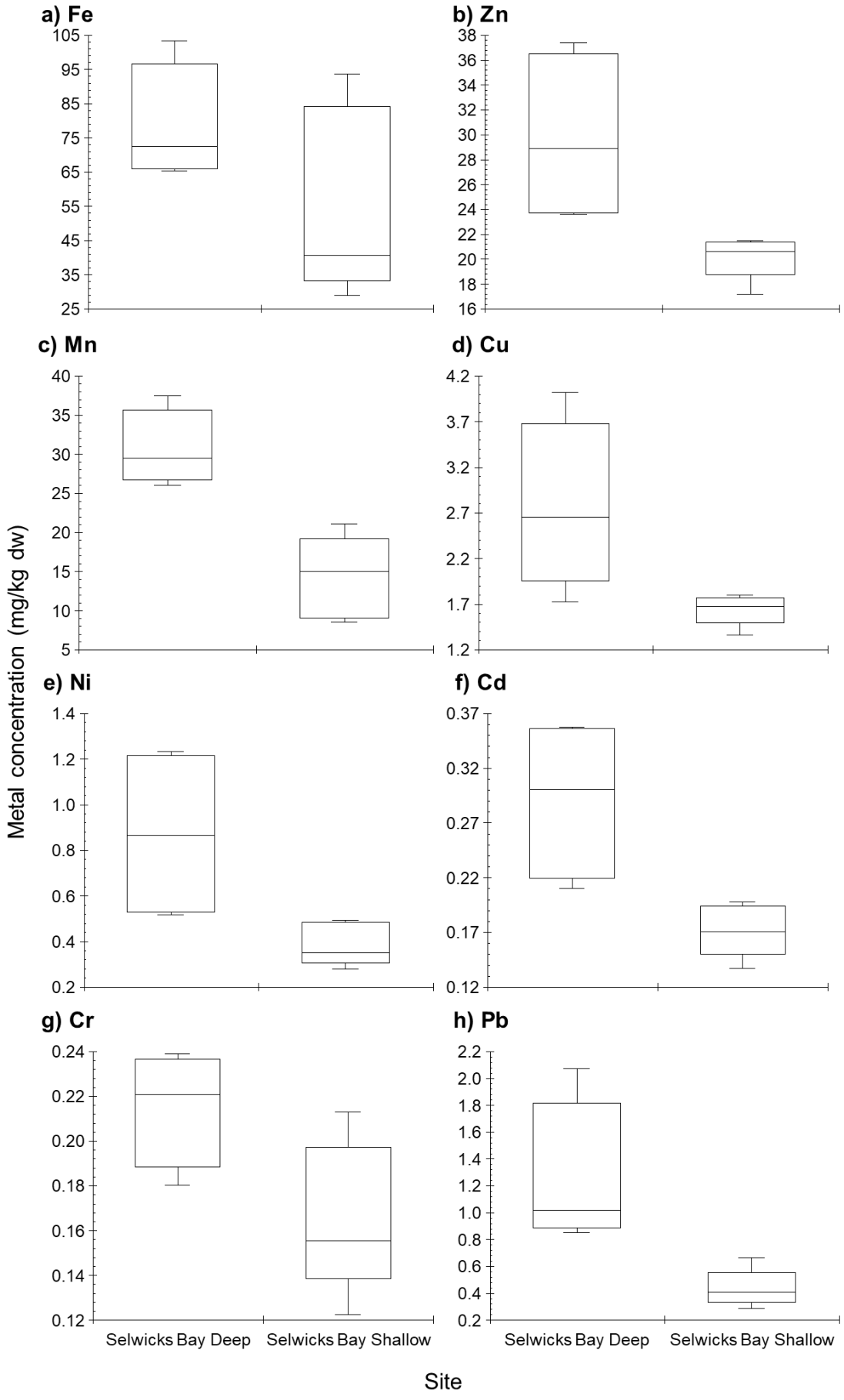

Figure 15 | Trace metal concentrations at different depths. Box plots comparing trace metal concentrations (mg/kg dry weight) in *L. hyperborea* from Selwicks Bay Deep (*n* = 4) and Selwicks Bay Shallow (*n* = 5).

4.2.1.6. Comparison with previous study

Five of the sites in Giusti (2001) were located in the same area as South Gare sites in the present study. MPI values are similar across both studies (Figure 16), although the range across Giusti's sites is more than double that observed here. Mean trace metal concentrations are comparable (Figure 17), although Fe, Zn, Ni, Cd, and Pb levels may be slightly higher in the present study compared to Giusti (2001), and vice versa for Mn, Cu, and Cr. Additionally, the present study shows greater ranges in mean Zn, Ni, Cd, and Pb concentrations, whilst Fe, Mn, Cu, and Cr levels appear more variable in Giusti (2001).

Possible reasons for these slight variations include differences in species, collection timing, pollution levels, and methods. Giusti (2001) only sampled *F. vesiculosus*, whereas *F. vesiculosus*, *L. digitata*, and *L. hyperborea* were collected from South Gare in the present study. The inclusion of multiple species could account for the higher variability demonstrated by some metals in the present study.

Giusti (2001) collected samples during winter whereas collections in the present study were conducted in spring and summer. The range of months, and even years, in the present study could also contribute to the larger variability in concentrations demonstrated by some metals. Additionally, Giusti's collection in winter could account for the higher Mn, Cu, and Cr levels observed, as trace metal concentrations are typically higher during this season due to slower growth in *F. vesiculosus* (Fuge and James, 1973; García-Seoane *et al.*, 2021).

Differences in observed concentrations may also be due to variations in sampling strategy and analysis. Giusti (2001) collected composite samples at each site by combining 8–10 cm of the most distal frond tips of 20–30 specimens. Samples were ashed, digested with aqua regia on a hot plate, and analysed by atomic absorption spectrophotometry.

Furthermore, these studies were conducted approximately 25 years apart, and differences in trace metal concentrations could simply reflect changes in pollution levels. It is important to note, nevertheless, that despite this interim, any changes in trace metal concentrations were fairly minor.

More broadly, Giusti (2001) reported an increasing trend in MPI down the northeast coast from Holy Island to Easington, followed by a decline towards the Tees area. The present study suggests a continued net decrease in MPI further down the coast, although the overall range in MPI values remains relatively modest (1.52–5.92).

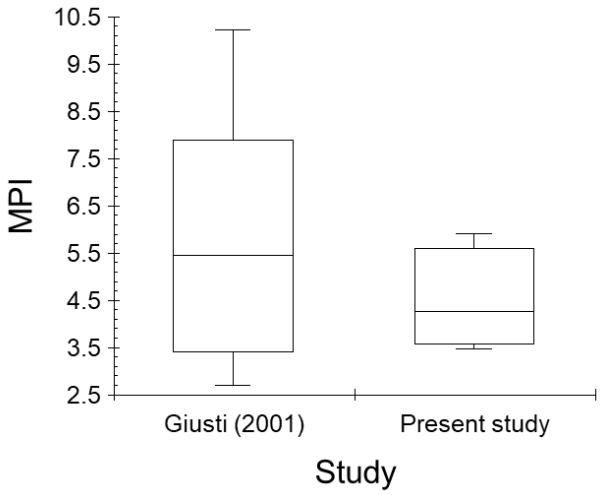

Figure 16 | MPI values at South Gare across two studies. Box plots comparing MPI values at South Gare sample sites between Giusti (2001) (*n* = 5) and the present study (*n* = 4).

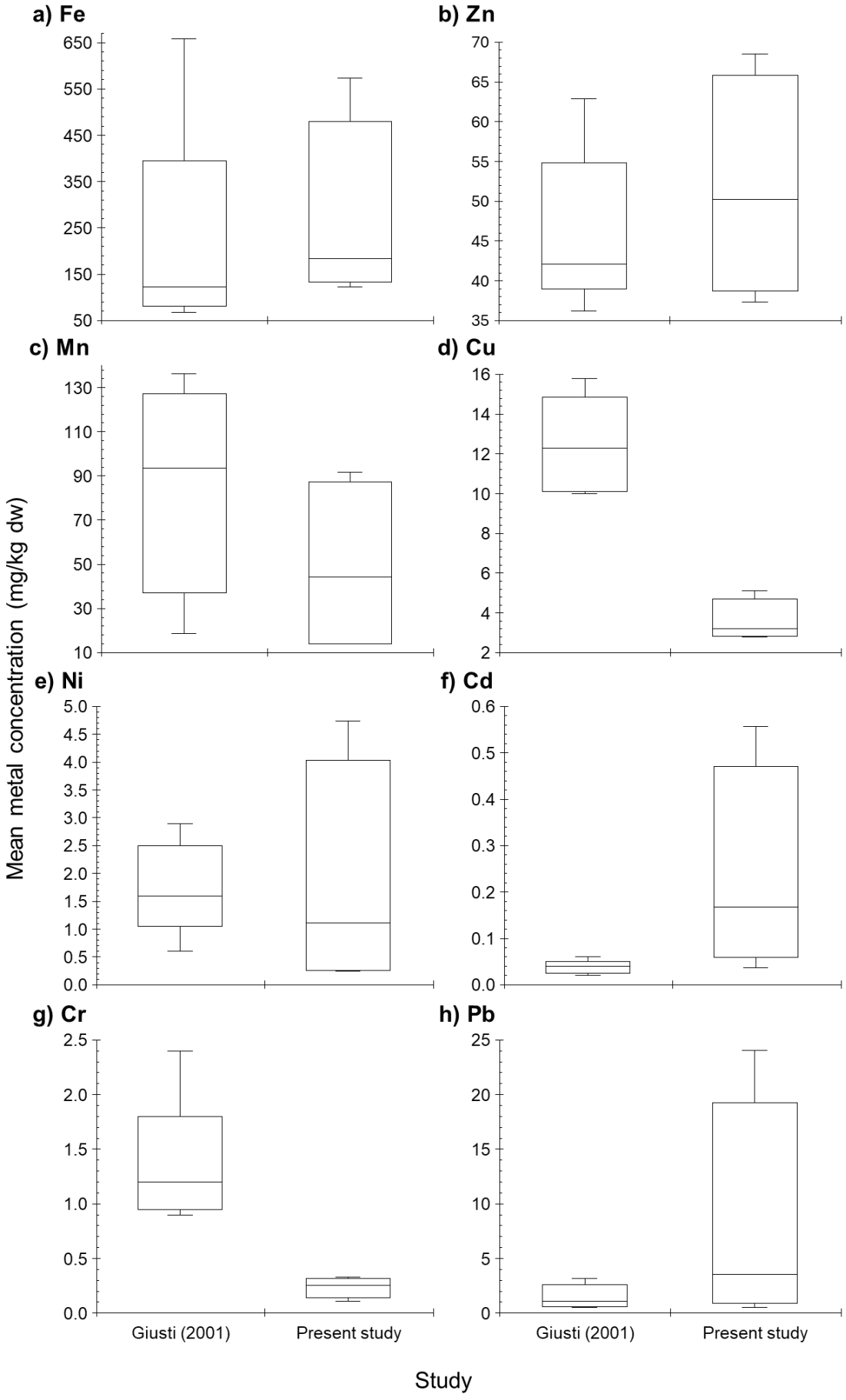

Figure 17 | Trace metal concentrations at South Gare across two studies. Box plots comparing mean trace metal concentrations (mg/kg dry weight) at South Gare sample sites between Giusti (2001) (n = 5) and the present study (n = 4).

4.2.2. Interspecific variation

Interspecific variation cannot be comprehensively assessed in this study, as not all four species were collected from one site. Other factors, such as pollution levels, local environmental conditions (e.g., temperature, salinity, pH), and collection timing, could be responsible for observed differences in trace metal concentrations, making it impossible to isolate interspecific effects. However, comparisons between *L. digitata* and *L. hyperborea* from Cayton Bay (Figure 18) and between *F. vesiculosus* and *F. serratus* from Cullercoats Beach (Figure 19) can be made.

4.2.2.1. Interspecific variation between *Laminaria* spp.

Significant differences in trace metal concentrations between *L. digitata* and *L. hyperborea* from Cayton Bay are found for Mn (p = 0.01), Fe (p = 0.04), Ni (p = 0.05), Cu (p = 0.01), Zn (p = 0.01), and Cd (p = 0.01). *L. hyperborea* exhibits higher levels of Mn, Ni, and Cd, whereas Fe, Cu, and Zn concentrations are higher in *L. digitata* (Figure 18). The higher Mn, Ni, and Cd concentrations in *L. hyperborea* may be linked to its lower alginate M:G ratio (Haug and Smidsrød, 1965), lower growth rate, longer lifespan, and slightly lower tidal elevation (Table 1).

Garcia-Vaquero *et al.* (2021) similarly reported contrasting behaviour in metal concentrations between *L. digitata* and *L. hyperborea*. Fe, Cu, Zn, Mn, and Ni levels tended to be higher in *L. digitata*, whilst Cd, Cr, and Pb concentrations were typically higher in *L. hyperborea*. These trends align with the present findings for Fe, Cu, Zn, and Cd, but not the other elements. Other studies have found little difference in trace metal content between the two species (Schiener *et al.*, 2015; Raab, Stengel and Feldmann, 2025). Interspecific variation in trace metal concentrations is therefore not universally consistent and perhaps reflects a more complex interplay of other factors, such as local contamination levels and environmental conditions, rather than physiological or ecological traits alone.

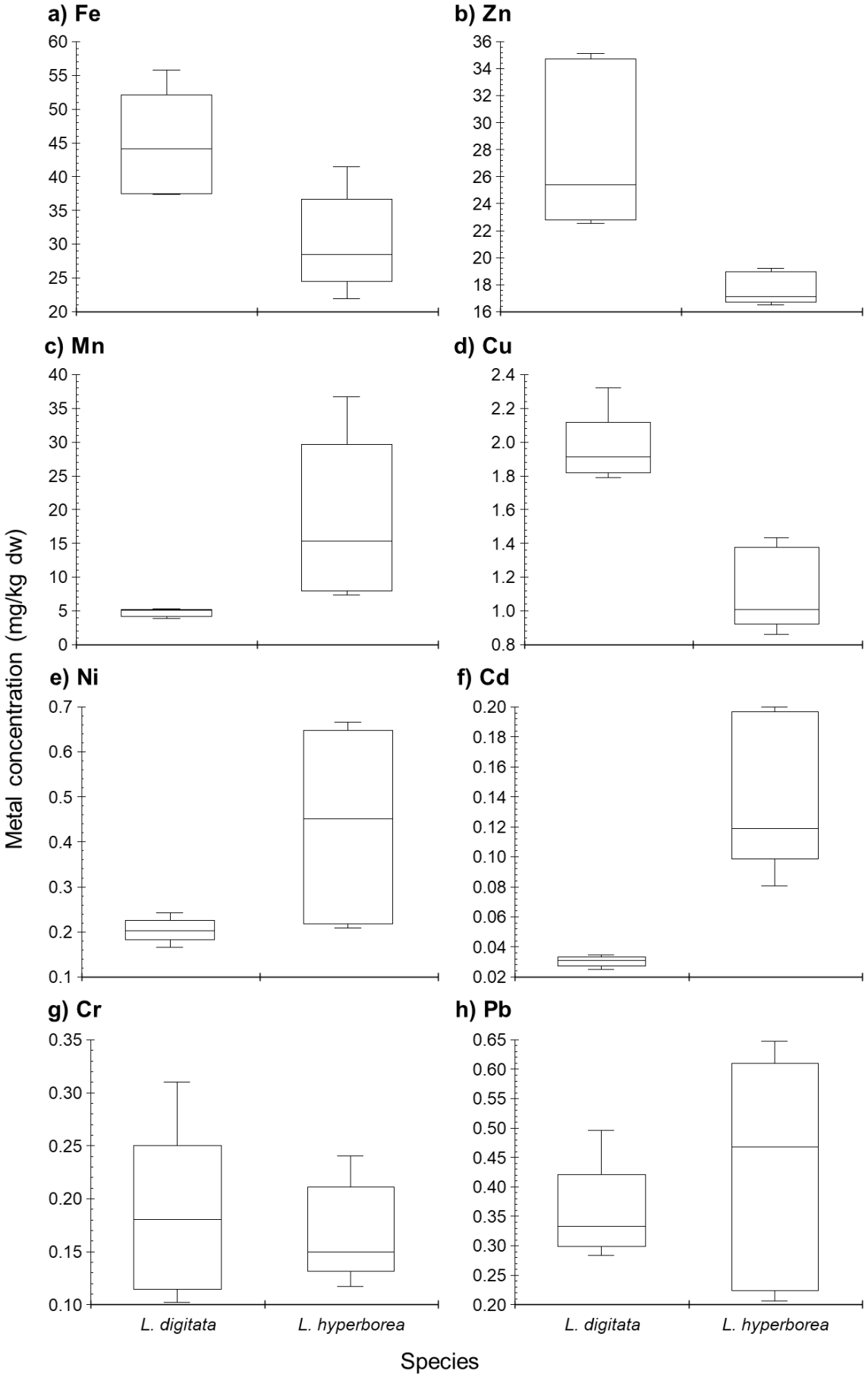

Figure 18 | Interspecific variation in trace metal concentrations between *Laminaria* spp. from Cayton Bay. Box plots comparing trace metal concentrations (mg/kg dry weight) between *L. digitata* (*n* = 5) and *L. hyperborea* (*n* = 5).

4.2.2.2. Interspecific variation between *Fucus* spp.

Significant differences in Mn (p = 0.04), Fe (p = 0.02), Ni (p = 0.02), and Cd (p = 0.02) concentrations are observed between *F. vesiculosus* and *F. serratus* from Cullercoats Beach. Mn, Fe, and Ni levels are higher in *F. vesiculosus,* whereas Cd concentrations are higher in *F. serratus* (Figure 19). *F. vesiculosus* exhibits a slightly lower growth rate (Table 1) and higher alginate and fucoidan content than *F. serratus* (Fletcher *et al.*, 2017; Catarino, Silva and Cardoso, 2018), which could account for the higher Mn, Fe, and Ni concentrations. Conversely, *F. serratus* grows at a lower tidal elevation than *F. vesiculosus*, which could explain the higher Cd levels.

Fuge and James (1973) reported lower Zn and higher Fe levels in *F. vesiculosus* relative to *F. serratus*. No significant differences in Zn concentrations were observed in the present study, but the same result was found for Fe. Other authors have reported no significant variations in trace metal content between these species (Tomlinson *et al.*, 1980; Stengel *et al.*, 2004; Biancarosa *et al.*, 2018). As discussed for *Laminaria* spp. from Cayton Bay, such inconsistencies between observations may reflect modulation of interspecific variation by other factors, resulting in complex interactions between species traits and site-specific conditions.

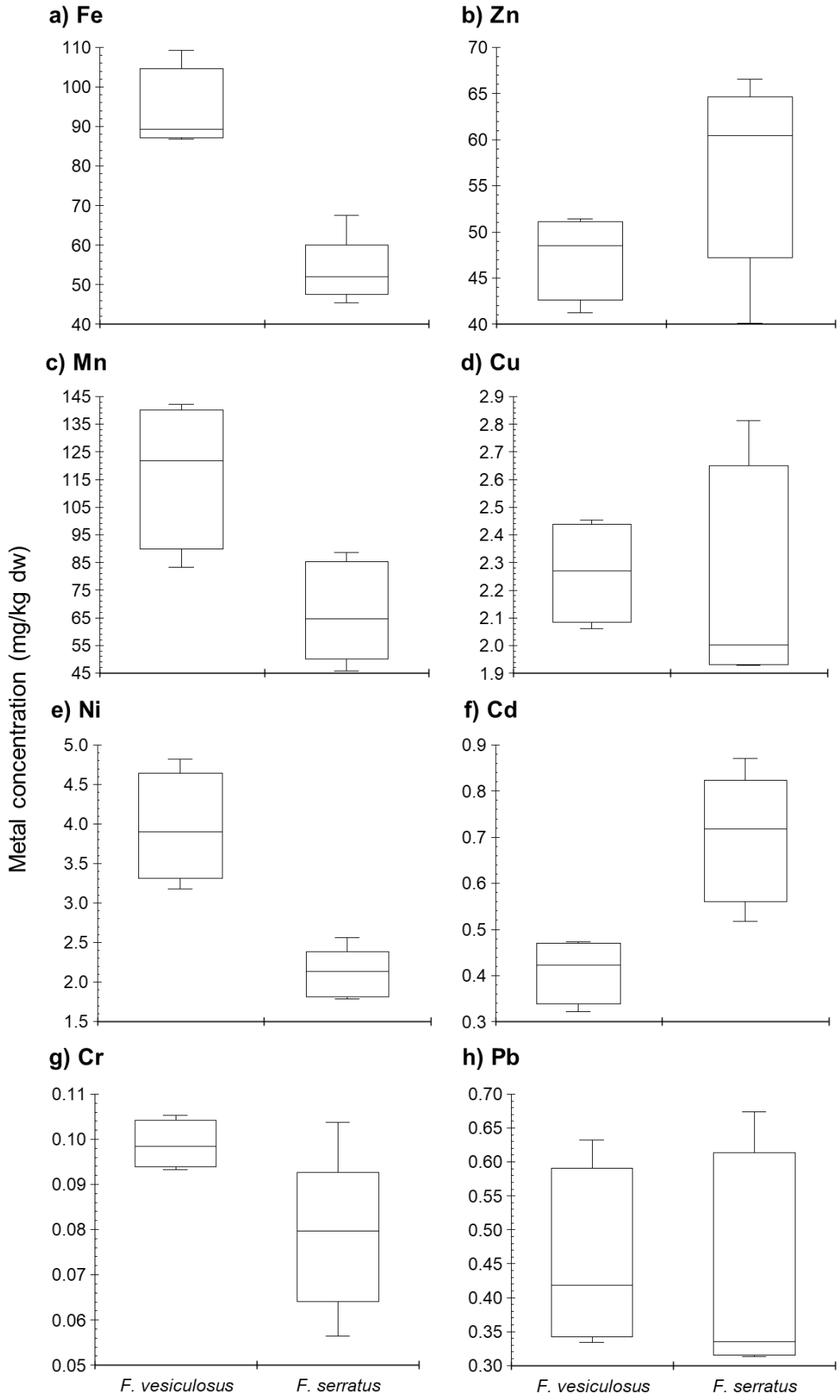

Figure 19 | Interspecific variation in trace metal concentrations between *Fucus* spp. Box plots comparing trace metal concentrations (mg/kg dry weight) between *F. vesiculosus* (*n* = 4) and *F. serratus* (*n* = 5) from Cullercoats Beach.

4.3. Thallus-segmented results

4.3.1. Intrathallus variation

Significant differences in Mn, Zn, and Cd concentrations are observed between thallus segments (Figure 20). Gradients in trace metal concentrations along the thallus are also evident, with Cr, Mn, Fe, Ni, Zn, and Cd showing significant trends away from growing regions.

4.3.1.1. Mn

Mn levels are significantly higher in holdfasts than in meristems (p = 0.01), stipes (p = 0.02), and blades (p = 0.02) (Figure 20). Concentrations increase significantly from meristems to holdfasts (p = 0.001) and from meristems to blade tips (p = 0.01). These findings align well with previous reports of Mn in *L. digitata*, where concentrations were approximately an order of magnitude higher in holdfasts and increased from stipes to distal blades (Bryan, 1969; Stengel, McGrath and Morrison, 2005). Elevated levels in holdfasts were attributed to longer metal exposure and greater retention in older tissue and the trend from stipe to blade to gradients in biomass dilution and photosynthetic activity (Stengel, McGrath and Morrison, 2005).

4.3.1.2. Zn

Zn concentrations are significantly higher in blades than in holdfasts (p = 0.01) (Figure 20). Zn levels also show a significant increase from meristems to blade tips (p = 0.03). This mirrors earlier findings in *L. digitata*, which were ascribed to reduced biomass dilution in slower-growing tissues (Bryan, 1969).

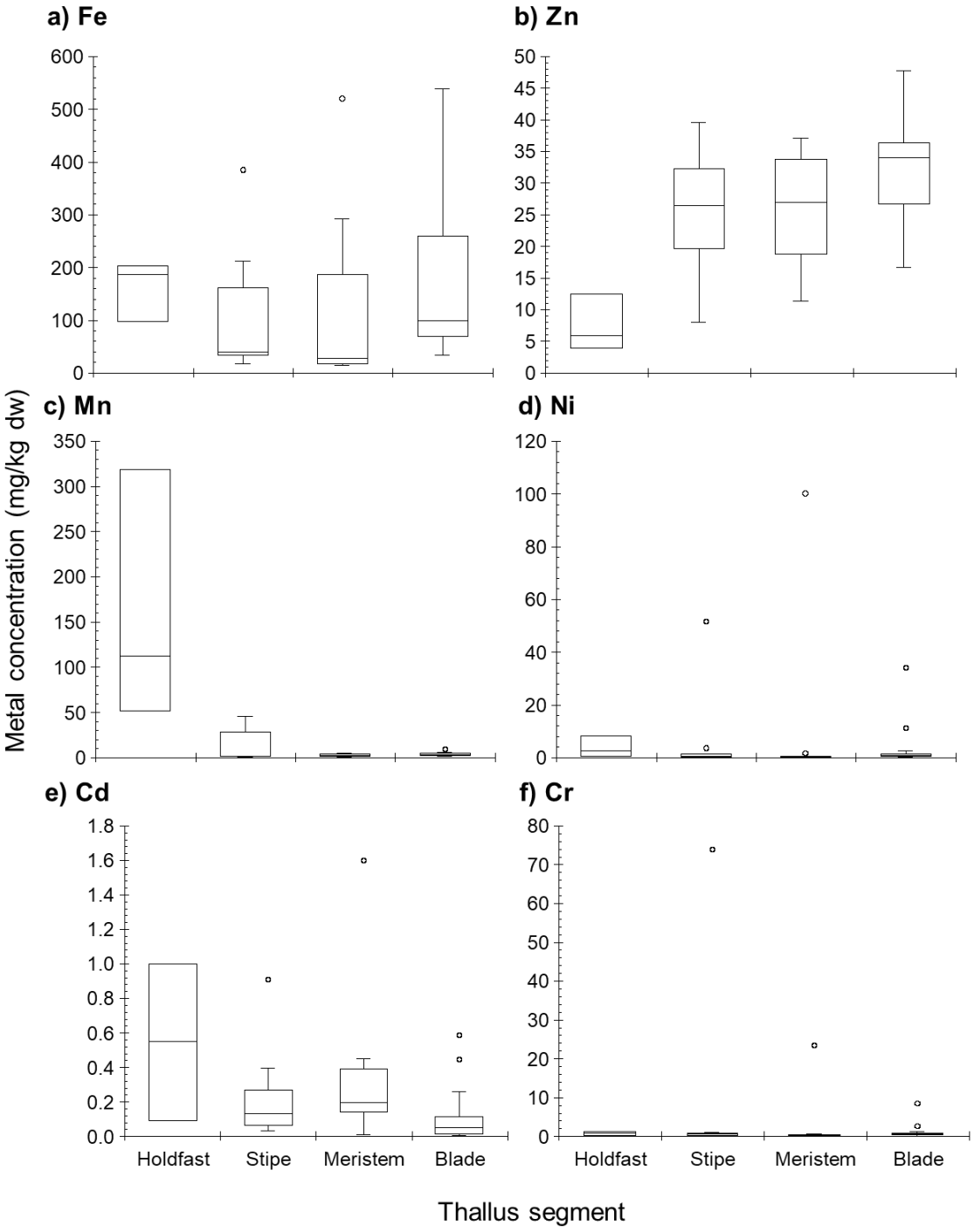

Figure 20 | Intrathallus variation in trace metal concentrations. Box plots comparing trace metal concentrations (mg/kg dry weight) between holdfasts (n = 3), stipes (n = 12), meristems (n = 12), and blades (n = 23) of *L. digitata* and *L. hyperborea* from Cullercoats Beach.

4.3.1.3. Cd

Significant differences in Cd concentrations are found between blades and meristems (p = 0.02) and between blades and holdfasts (p = 0.05), with both meristems and holdfasts exhibiting higher levels than blades (Figure 20). Higher concentrations in holdfasts may reflect longer metal exposure and greater retention

in older tissues, as with Mn (Stengel, McGrath and Morrison, 2005). Unlike other metals, Cd displays a decreasing trend from meristems to blade tips ($p < 0.001$). A similar pattern was reported for Cu in *L. digitata*, where concentrations peaked in meristems and young blades and were lowest in stipes and distal blades (Stengel, McGrath and Morrison, 2005). This was linked to an increased abundance of Cu-binding enzymes in growing regions. A similar mechanism may underlie the observed Cd distribution, although this is less likely given that Cd is a non-essential element (Espinoza *et al*., 2021). García-Seoane *et al.* (2021) reported higher Cd levels in younger tissues, suggesting that higher growth rates may increase the availability of binding sites for Cd uptake. However, this mechanism appears to be metal-specific, as opposite trends were observed for other metals, consistent with present findings.

4.3.1.4. Cr, Fe, and Ni

Cr, Fe, and Ni concentrations increase significantly from meristems to holdfasts ($p < 0.001$, $p < 0.001$, and $p = 0.01$, respectively) and from meristems to blade tips ($p < 0.001$ for all). Bryan (1969) also reported increasing Fe concentrations along *L. digitata* blades with distance from the meristem. Stengel, McGrath and Morrison (2005) similarly observed the lowest Fe levels in meristems and young blades. Fe limitation in growing tissues was proposed as a contributing factor in the latter study. A similar mechanism may apply to Ni, although this is less likely for Cr, which is a non-essential element (Espinoza *et al.*, 2021). Greater biomass dilution in growing regions could also account for these distributions (Bryan, 1969; Stengel, McGrath and Morrison, 2005).

4.3.2. Interspecific variation

Fewer metals exhibit significant differences between *L. digitata* and *L. hyperborea* in this sample set (Figure 21) compared to samples from Cayton Bay (Figure 18). This may be due to the added complexity of intrathallus variation potentially obscuring interspecific trends. Only Cr and Cd exhibit significant differences, with Cr concentrations higher in *L. digitata* ($p = 0.01$) and Cd higher in *L. hyperborea* ($p < 0.001$) (Figure 21). The elevated Cd concentrations in *L. hyperborea* are consistent with findings from Cayton Bay and Garcia-Vaquero *et al.*

(2021). As previously discussed, higher metal accumulation in *L. hyperborea* may be linked to its lower growth rate, longer lifespan, lower alginate M:G ratio, and growth at a slightly lower tidal elevation compared to *L. digitata*.

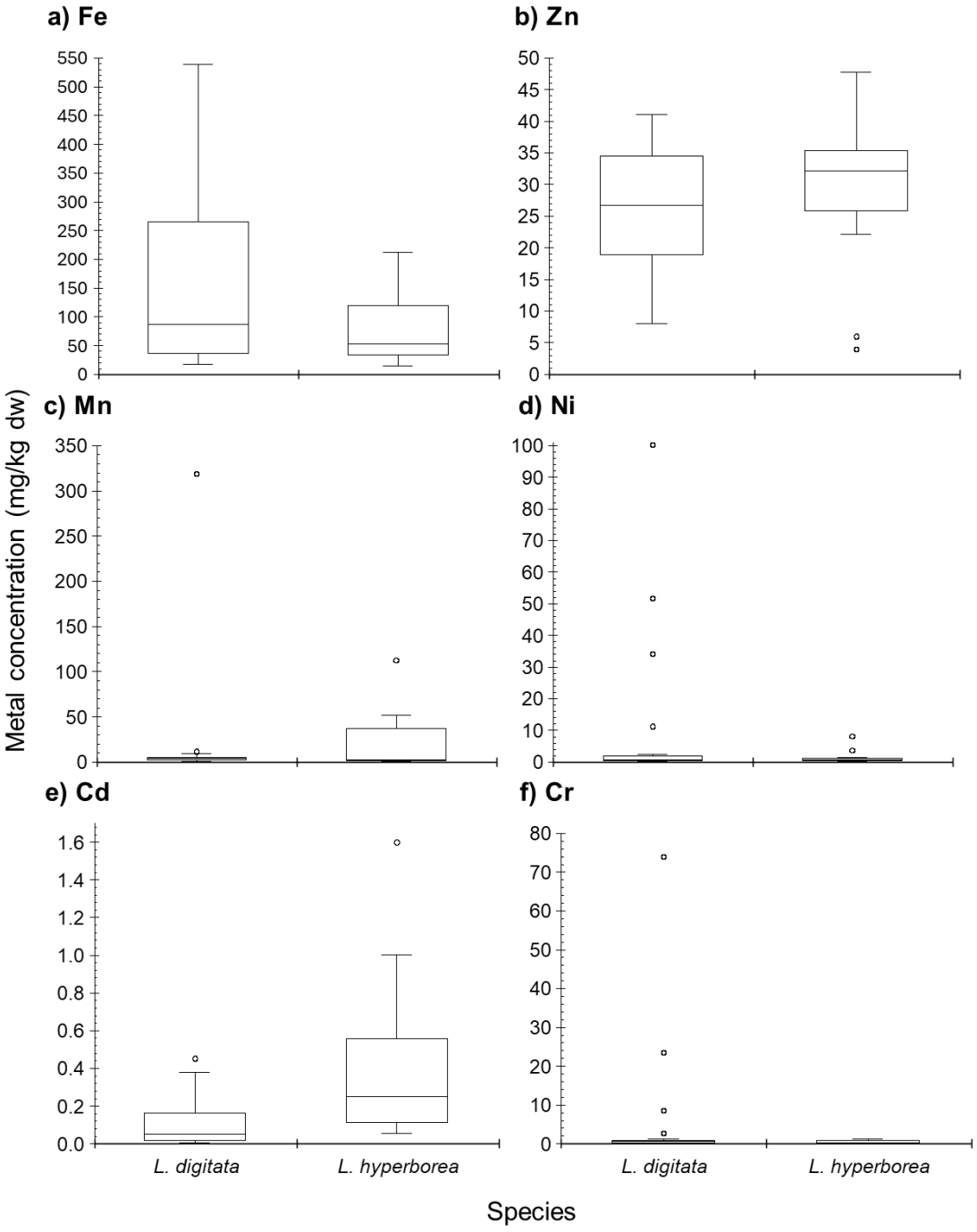

Figure 21 | Interspecific variation in trace metal concentrations in *Laminaria* spp. from Cullercoats Beach. Box plots comparing trace metal concentrations (mg/kg dry weight) between *L. digitata* (*n* = 33) and *L. hyperborea* (*n* = 17).

4.4. Implications of results

The aim of this study was to provide an updated, biologically relevant assessment of trace metal contamination along the northeast and North Yorkshire coastlines. This was achieved through five research objectives (section 1.3.), whose collective findings reveal a coastline shaped by the legacy of the Tees Estuary but buffered by environmental and biological variability.

4.4.1. Objectives 1 and 2: Spatial distribution of contamination relative to background levels

The spatial patterns observed in this study indicate that the Tees Estuary continues to act as a localised source of trace metals, with concentrations highest around South Gare and declining downcoast. However, the inconsistency of these distributions across different metals, combined with concentrations that largely fall within background ranges, suggests that estuarine influence is only one component of a more complex system. Hydrodynamic dispersion, metal-specific behaviour, and biological factors all modulate how contamination is expressed along the open coast. This reinforces the value of multi-metal, multi-site approaches, as reliance on single indicators may obscure broader patterns.

That most concentrations fall within background ranges has positive implications for regional water quality, suggesting that contamination may be largely contained within the estuary system. However, the use of background values derived from distant unpolluted sites introduces uncertainty (Brady *et al.*, 2015; Kowalska *et al.*, 2018), underscoring the need for locally derived baselines to support future assessments.

4.4.2. Objective 3: Temporal changes relative to historical data

The temporal stability of metal concentrations around South Gare since the late 1990s (Giusti, 2001) further supports the interpretation above. Despite regular maintenance dredging and recent industrial development (MMO, 2023a, 2023b), there is little evidence of increased contamination. This stability suggests that regulatory measures and natural attenuation processes have been effective in preventing deterioration of coastal water quality.

4.4.3. Objective 4: Influence of dredging and disposal of contaminated sediments

The combined findings from objectives 1–3 have nuanced implications for the role of dredging in shaping coastal metal distributions. The downcoast gradient in metal concentrations is consistent with an estuarine source and therefore suggests a possible dredging-related signal. However, the absence of concentrations above background levels, the lack of temporal increase despite recent industrial activity, and the inconsistent behaviour of individual metals weaken this interpretation.

Natural processes can exert effects similar to those of dredging. Tidal action, storms, and freshwater inputs can resuspend sediments and remobilise metals, making it difficult to distinguish anthropogenic disturbance from background variability (Todd *et al.*, 2015; Miró *et al.*, 2022). Seasonal shifts in temperature and salinity further influence metal partitioning between sediment and water (Ibhadon, Wright and Daniels, 2004; Hedge, Knott and Johnston, 2009), and the lack of synchronised sampling across seasons in this study may have obscured any dredging-related signal.

Dredging does not necessarily target the most contaminated sediments. Peak sediment metal concentrations occur in the middle and upper reaches of the Tees Estuary (Ibhadon, Wright and Daniels, 2004), whereas most maintenance dredging takes place in the approach channel and lower to middle stretches (Royal HaskoningDHV, 2025). If dredging does not disturb the most contaminated sediments, the potential for elevated coastal exposure is reduced.

Geochemical processes may constrain the residence time of dissolved metals in the water column. Resuspended particles readily adsorb dissolved metals and settle out again (Soetan *et al.*, 2023), removing them before macroalgae can take them up. Such behaviour has been documented in the Humber Estuary, where rapid scavenging of dissolved Pb reduced macroalgal uptake (Barnett and Ashcroft, 1985). Highly bioavailable species such as Cu^{2+} are quickly complexed or removed under high salinity conditions (Ibhadon, Wright and Daniels, 2004; Qian *et al.*, 2015; Hauser-Davis and Wosnick, 2022). Sediment plumes are also spatially localised and short-lived (Todd *et al.*, 2015), limiting the window during which macroalgae are exposed to elevated dissolved metals.

4.4.4. Objective 5: Trace metal variability in macroalgae and implications for biomonitoring

This study also has important implications for the use of macroalgae as biomonitors. The influence of species, season, shore level, and tissue type observed here aligns with recent research (e.g., García-Seoane *et al*., 2021; Rakib *et al*., 2021; Sim *et al*., 2023; Pacín *et al*., 2025) and reinforces the need for rigorous standardisation in biomonitoring programmes. When these factors are controlled, macroalgae remain highly effective indicators of bioavailable metals. Their observed global declines in metal concentrations since the 1970s, partly attributed to regulatory improvements (Aboal *et al.*, 2023; Pacín *et al.*, 2025), demonstrate their value for evaluating policy effectiveness.

However, the wider environmental context in which biomonitoring operates is evolving. Climate-driven shifts in rainfall patterns, storm frequency, and sea level rise are expected to increase metal inputs and remobilise contaminated sediments (Todd *et al.*, 2015; Hauser-Davis and Wosnick, 2022; Miró *et al.*, 2022; Soetan *et al.*, 2023). Ocean acidification may increase metal solubility whilst simultaneously reducing uptake through protonation of cell wall binding sites, creating uncertainty around net effects (Roberts *et al.*, 2013; Hauser-Davis and Wosnick, 2022; Aboal *et al.*, 2023; Soetan *et al.*, 2023). Interactions between changing seawater temperature, salinity, and pH and concurrent chemical stressors may also affect macroalgal physiology, abundance, and distribution (Roberts *et al.*, 2013; Hauser-Davis and Wosnick, 2022; Aboal *et al.*, 2023; Pacín *et al.*, 2025). This may alter their bioaccumulation capacity and, consequently, their suitability as biomonitors.

Dredging-related disturbances present a similar challenge. Increased turbidity, seabed smothering, and entrainment may affect local macroalgal populations, although these effects seem to be spatially limited and short-lived (Todd *et al.*, 2015; Miró *et al.*, 2022). As dredging intensity increases globally, driven by coastal development, port expansion, and large projects such as Teesworks (Todd *et al.*, 2015; Miró *et al.*, 2022), the need to understand how such disturbances interfere with biomonitoring purposes becomes increasingly important.

Despite these complexities, the broader implication of this study is that macroalgae remain a valuable tool for assessing trace metal contamination. Their ability to integrate bioavailable metals over ecologically meaningful timescales allows them to capture complex contamination dynamics that point-in-time water or

sediment samples cannot (Pacín *et al.*, 2025). As attention shifts towards emerging pollutants such as plastics, it is important that trace metal contamination remains a focus within coastal monitoring and policy (Hauser-Davis and Wosnick, 2022). Climate change and expanding coastal development are likely to alter metal dynamics in ways that are not yet fully understood, and environmental policy should consider contaminants within the context of these changing conditions (Roberts *et al.*, 2013). When applied rigorously, macroalgal biomonitoring offers a practical means of tracking these evolving risks and supporting evidence-based management of coastal environments.

5. Conclusions

- Trace metal concentrations along the northeast and North Yorkshire coasts generally reflect unpolluted conditions, falling within or below background and UK reference levels.
- A downstream decline in trace metal concentrations is observed from the Tees Estuary, although spatial distributions vary by metal.
- Two specimens from South Gare exhibit anomalously high Pb concentrations, substantially exceeding background thresholds and observations at other sites. Although the cause remains unclear, possible explanations include a transient influx of dissolved Pb in the area and surface contamination by fine particulate material, despite thorough cleaning.
- Elevated trace metal concentrations at Cullercoats Beach suggest a potential influence from the Tyne Estuary, consistent with its industrial legacy, which parallels that of the Tees Estuary.
- Contamination levels in the South Gare area appear broadly unchanged since the late 1990s, based on comparisons with historical data.
- Trace metal concentrations in macroalgae are influenced by several factors, including species, shore level, season and year of collection, thallus segment sampled, surface contamination by fine particulates, and local hydrodynamics. These variables must be carefully considered in future biomonitoring studies to ensure reliable assessment of trace metal pollution.
- Interspecific and intrathallus variation were explored in detail. Significant differences in trace metal concentrations were found between *L. digitata* and *L. hyperborea*, and between *F. vesiculosus* and *F. serratus*. Differences between genera could not be assessed. Several metals also showed significant variation between thallus segments, and most increased away from growing regions. Interspecific and intrathallus patterns appeared to be metal-specific.
- Collectively, results demonstrate that whilst the Tees Estuary remains a localised source of trace metals, its broader coastal impact is moderated by natural processes. In fulfilling the study's aim, macroalgae have shown strong potential as effective biomonitors, providing a biologically meaningful means of assessing trace metal contamination along this coastline.

6. Limitations

It is crucial to acknowledge the limitations of this study and emphasise that findings must be interpreted with caution. Confounding factors, mixed effects, and methodological constraints may contribute to trends that appear significant, potentially rendering results misleading.

6.1. Study design

The design of this study imposed constraints on the types of analyses that could be performed and the strength of conclusions that could be drawn. One key limitation is non-uniform sampling. Within the segmented sample set, some specimens hosted all four thallus segments, whilst others either completely lacked or did not have a large enough holdfast or stipe to subsample. Additionally, the number of meristem and blade samples varied between specimens, which made it challenging to reliably compare trace metal concentrations between segments. Further complexity arises from the inclusion of two species. The interaction of multiple factors makes it difficult to disentangle their individual effects, limiting the interpretability of significant results.

Similarly, in the blade/composite sample set, a number of variables were not controlled, making differences in trace metal concentrations difficult to interpret. Samples were collected from different sites, at different times of year, and even across years. Although four macroalgal species were sampled overall, not all species were collected at every site, preventing quantification of interspecific variation. Species differences also introduced variation in shore level and the temporal window represented by subsamples. *Laminaria* spp. blades are annual (Lee, 2018), meaning blade-only samples reflect metal accumulation since the start of the most recent growing season. *Fucus* spp. form new dichotomies several times per year (Lee, 2018; García-Seoane *et al.*, 2021), making the time window represented by composite subsamples uncertain and likely heterogeneous. Observed differences in trace metal concentrations between sites may reflect species, season, or subsampling strategy, rather than spatial variation in contaminant levels.

6.2. Sample preparation technique

Most samples in the segmented sample set were digested via microwave-assisted acid digestion, whereas blade/composite samples were digested on a hot plate. Direct comparison between the two techniques is not possible, as only one sample was prepared using both methods. However, trace metal concentrations in the microwave-prepared digest appeared consistently higher (by 12–34%, depending on the metal) compared to those obtained via hot plate digestion.

Preparation techniques for microwave-assisted digestion appeared less clean, as evidenced by elevated trace metal concentrations in the procedural blank. Consequently, many sample concentrations fell below MDLs and were instead substituted with half the MDLs. Whilst this substitution approach minimised data loss and enabled continued analysis, it introduced a substantial proportion of estimated values.

Additional evidence of reduced reliability in microwave-prepared samples comes from the greater variability observed in trace metal concentrations, despite all samples being collected from the same site and genus. However, this variability may alternatively reflect intrathallus variation, as the segmented set was sampled at a higher resolution than the blade/composite set.

7. Further work and recommendations

7.1. Improvements to study design

7.1.1. Standardising variables

Future investigations would benefit from a more rigorously controlled study design. In the present study, several uncontrolled variables and their interactions made it difficult to isolate significant influences on trace metal concentrations. A more effective approach would be to investigate a single variable (e.g., spatial distribution), whilst keeping all others (e.g., species, season, year, shore level, thallus segment) constant. García-Seoane *et al.* (2018) recommend sampling the apical parts of a single species collected at the same depth during June to facilitate interstudy comparisons.

Alternatively, variability across these factors could be incorporated through integrative sampling strategies. Fuge and James (1974) recommend using large sample masses to mitigate intrathallus variation. García-Seoane *et al.* (2018, 2019, 2021) describe ‘space-bulking’ and ‘time-bulking’ techniques, which involve pooling 30–40 specimens per site and conducting monthly collections to minimise intrasite and seasonal variability, respectively. Sampling multiple species across several tidal elevations on a monthly basis would enable confounding effects to be averaged out, although the associated financial and time costs may not be favourable.

The latter approach would also enable quantification of individual variables, provided sampling is balanced across groups. For example, to assess spatial and interspecific variation, as well as their interaction, equal numbers of all species should be collected at each site. The same principle applies to other factors such as season and shore level. Whilst multiple variables and their interactions may be assessed simultaneously, doing so adds increasing layers of complexity. Regardless of approach, standardising these variables remains essential.

7.1.2. Sample size

At several sites, only three specimens per species were collected, with a maximum of five. The thallus-segmented sample set consisted of subsamples from just four *L. digitata* and two *L. hyperborea* specimens. Only three holdfast samples

were analysed, and similarly low numbers of subsegments (e.g., basal stipe sections) were included. Increasing sample sizes would improve statistical power and enhance the reliability of results.

7.1.3. Spatial resolution

Spatial coverage could also be improved. Sampling was concentrated around South Gare and Redcar Beach, leaving extensive stretches of coastline to the north and south unsampled. Increasing the number of sample sites at regular intervals would enhance spatial resolution and help identify coastal trends. García-Seoane *et al.* (2018) recommend a sampling density of one site per 16 km or 32 km^2.

Sampling kelp beds further offshore, particularly near dredging disposal sites, could provide valuable insights into potential contamination sources. Given that results suggest the Tyne Estuary may contribute trace metal inputs to the coast, increased sampling density in this area would also be beneficial. This would enable comparison between the Tees and Tyne Estuaries.

7.1.4. Sample collection and processing

Additional recommendations by García-Seoane *et al.* (2018), not implemented in the present study but worth considering in future investigations to reduce sample contamination, enhance analytical accuracy, and improve interstudy comparability, include:

- Using precleaned, trace metal-free gloves during sample collection to minimise contamination from handling.
- Collecting only *in situ* specimens still attached to the substrate rather than washed up material (i.e., *L. hyperborea* from Cullercoats Beach) to ensure that samples are representative of their collection sites.
- Washing samples only with ambient seawater to preserve cellular osmotic equilibrium. In the laboratory, epiphytes and particulate material should only be removed manually (e.g., via scraping with a glass slide).
- Avoiding freezing samples before analysis to minimise intracellular metal loss due to cell lysis during freezing and thawing.
- Drying samples at low temperature (40 °C) to reduce volatilisation of metals.

- Using metal-free grinding mills (e.g., titanium, Teflon, or agate) with low heat generation to prevent contamination and volatile losses.
- Including a certified reference material for macroalgae (e.g., ERM-CD200 *Fucus vesiculosus*). An internal standard was used in this study instead.
- Correcting for fine particulate contamination on macroalgal surfaces by proportionally scaling metal concentrations in local sediments using Fe or Al as tracers.

7.2. Digestion methods

The microwave-assisted digestion method should be revisited. Elevated trace metal concentrations in the procedural blank introduced challenges in data processing and interpretation. This contamination likely stemmed from insufficiently clean sample preparation practices. Adopting the procedures used for hot plate digestion may help reduce contamination and improve data quality. Direct comparison of the two methods would be valuable. A suite of samples should be digested using both techniques and trace metal concentrations compared.

7.3. Avenues for future investigation

7.3.1. Interspecific relationships

Expanding the investigation to include a wider range of brown algal species (e.g., *Ascophyllum nodosum*, *Saccharina latissima*) and species from other macroalgal classes would enhance understanding of interspecific relationships in trace metal uptake. Where such relationships are well-characterised, it may be possible to infer trace metal concentrations in species absent from certain sites. This would improve the adaptability of biomonitoring programmes.

Although dissolved trace metals represent the most bioavailable fraction, particulate-bound metals may also contribute to metal accumulation in marine organisms (Bryan, 1980). Including other taxa such as bivalves would enable a more comprehensive assessment of metal pollution across multiple exposure pathways (Phillips, 1977; Bryan, 1980).

7.3.2. Tidal elevation

Higher trace metal concentrations were observed at Selwicks Bay Deep compared to Selwicks Bay Shallow. Investigating this trend with larger sample sizes and a broader range of depths would be valuable, particularly in conjunction with interspecific studies, given that different species occupy distinct tidal elevations.

7.3.3. Temporal and seasonal change

Monitoring changes in trace metal concentrations over time could provide important insights. Although comparison with Giusti (2001) revealed minimal change in macroalgal trace metals in the South Gare area, shorter-term fluctuations within this ~25-year interval are not evident. Annual sampling would enable construction of a long-term record and facilitate detection of temporal trends. This may be particularly relevant in the light of the ongoing Teesworks development and associated capital dredging.

Monthly sampling would additionally allow the quantification of seasonal change in macroalgal trace metal concentrations. For determination of seasonal variation, regular, high frequency (i.e., monthly) sampling over several years is recommended to account for interannual changes (García-Seoane *et al.*, 2018, 2021).

7.3.4. Experimental assessments

Controlled laboratory experiments investigating how biological and environmental factors affect trace metal uptake in macroalgae would allow for isolation of individual variables and the disentanglement of complex interactions that are difficult to resolve in field observations. For example, Bryan (1969) studied growth and Zn uptake in *L. digitata* under varying seawater concentrations and light regimes. Growth was inhibited and Zn uptake reduced at high Zn concentrations and under dark conditions. Furthermore, segment-level differences in Zn uptake were observed and the presence of other metals (Cu and Mn) was found to reduce or entirely inhibit Zn uptake.

Updated experimental data would be valuable. Assessing the effects of light, temperature, pH, and salinity on trace metal uptake would help predict macroalgal responses to different environments (e.g., at varying shore levels or along

estuaries). Understanding how dissolved trace metal concentrations and the coexistence of other metals in seawater affect uptake is also critical for identifying thresholds beyond which the reliability of macroalgae as biomonitors may start to diminish.

References

Aboal, J.R., Pacín, C., García-Seoane, R., Varela, Z., González, A.G. and Fernández, J.A. (2023) 'Global decrease in heavy metal concentrations in brown algae in the last 90 years', *Journal of Hazardous Materials*, 445, p. 130511. Available at: https://doi.org/10.1016/J.JHAZMAT.2022.130511.

Adams, J.M.M., Ross, A.B., Anastasakis, K., Hodgson, E.M., Gallagher, J.A., Jones, J.M. and Donnison, I.S. (2011) 'Seasonal variation in the chemical composition of the bioenergy feedstock *Laminaria digitata* for thermochemical conversion', *Bioresource Technology*, 102(1), pp. 226–234. Available at: https://doi.org/10.1016/J.BIORTECH.2010.06.152.

Ahn, I.Y., Choi, H.J., Ji, J., Chung, H. and Kim, J.H. (2004) 'Metal Concentrations in Some Brown Seaweeds from Kongsfjorden on Spitsbergen, Svalbard Islands', *Ocean and Polar Research*, 26(2), pp. 121–132. Available at: https://doi.org/10.4217/OPR.2004.26.2.121.

Alderton, S. (2012) *Heavy metal contamination along the coast of North-East England*. Durham University. Available at: https://etheses.dur.ac.uk/5918/ (Accessed: 29 October 2024).

Barnett, B.E. and Ashcroft, C.R. (1985) 'Heavy metals in *Fucus vesiculosus* in the Humber Estuary', *Environmental Pollution Series B, Chemical and Physical*, 9(3), pp. 193–213. Available at: https://doi.org/10.1016/0143-148X(85)90033-3.

Bartsch, I., Wiencke, C., Bischof, K., Buchholz, C.M., Buck, B.H., Eggert, A., Feuerpfeil, P., Hanelt, D., Jacobsen, S., Karez, R., Karsten, U., Molis, M., Roleda, M.Y., Schubert, H., Schumann, R., Valentin, K., Weinberger, F. and Wiese, J. (2008) 'The genus *Laminaria sensu lato*: recent insights and developments', *European Journal of Phycology*, 43(1), pp. 1–86. Available at: https://doi.org/10.1080/09670260701711376.

Baweja, P., Kumar, S., Sahoo, D. and Levine, I. (2016) 'Biology of Seaweeds', *Seaweed in Health and Disease Prevention*, pp. 41–106. Available at: https://doi.org/10.1016/B978-0-12-802772-1.00003-8.

Berry, A. and Plater, A.J. (1998) 'Rates of tidal sedimentation from records of industrial pollution and environmental magnetism: The Tees estuary, north-east

England', *Water, Air, and Soil Pollution*, 106(3–4), pp. 463–479. Available at: https://doi.org/10.1023/A:1005012813142/METRICS.

Biancarosa, I., Belghit, I., Bruckner, C.G., Liland, N.S., Waagbø, R., Amlund, H., Heesch, S. and Lock, E.J. (2018) 'Chemical characterization of 21 species of marine macroalgae common in Norwegian waters: benefits of and limitations to their potential use in food and feed', *Journal of the Science of Food and Agriculture*, 98(5), pp. 2035–2042. Available at: https://doi.org/10.1002/JSFA.8798.

Birkemeyer, C., Osmolovskaya, N., Kuchaeva, L. and Tarakhovskaya, E. (2019) 'Distribution of natural ingredients suggests a complex network of metabolic transport between source and sink tissues in the brown alga *Fucus vesiculosus*', *Planta*, 249(2), pp. 377–391. Available at: https://doi.org/10.1007/S00425-018-3009-4/FIGURES/1.

Black, W.A.P. (1950) 'The seasonal variation in weight and chemical composition of the common British Laminariaceae', *Journal of the Marine Biological Association of the United Kingdom*, 29(1), pp. 45–72. Available at: https://doi.org/10.1017/S0025315400056186.

Black, W.A.P. and Mitchell, R.L. (1952) 'Trace elements in the common brown algae and in sea water', *Journal of the Marine Biological Association of the United Kingdom*, 30(3), pp. 575–584. Available at: https://doi.org/10.1017/S0025315400012984.

Bolam, S., Mason, C., Hynes, C., Potter, K., Barber, J. and Warford, L. (2023) *Dredged Material Disposal Site Monitoring Round the Coast of England: Results of Sampling (2022-2023) North Tyne and Souter Point*. Available at: https://assets.publishing.service.gov.uk/media/64b1392999590000013002ad1/C6794_Disposal_site_monitoring_report_2023_v0.4.pdf (Accessed: 13 August 2025).

Bolam, S., Mason, C., Potter, K., Barber, J. and Hynes, C. (2024) *Dredged Material Disposal Site Monitoring Around the Coast of England: Results of Sampling (2023-2024) Tees (Inner and Outer)*. Available at: https://assets.publishing.service.gov.uk/media/667d290f4ae39c5e45fe4d08/C6794_Dredge_Disposal_Monitoring_Annual_Report_2023-2024_Tees_v2.0.pdf (Accessed: 15 July 2025).

Brady, J.P., Ayoko, G.A., Martens, W.N. and Goonetilleke, A. (2015) 'Development of a hybrid pollution index for heavy metals in marine and estuarine sediments',

Environmental Monitoring and Assessment, 187(5), p. 306. Available at: https://doi.org/10.1007/S10661-015-4563-X.

Bryan, G.W. (1969) 'The Absorption of Zinc and Other Metals by the Brown Seaweed *Laminaria digitata*', *Journal of the Marine Biological Association of the United Kingdom*, 49(1), pp. 225–243. Available at: https://doi.org/10.1017/S0025315400046531.

Bryan, G.W. (1971) 'The effects of heavy metals (other than mercury) on marine and estuarine organisms', *Proceedings of the Royal Society of London. Series B. Biological sciences*, 177(48), pp. 389–410. Available at: https://doi.org/10.1098/RSPB.1971.0037;PAGEGROUP:STRING:PUBLICATION.

Bryan, G.W. (1980) 'Recent trends in research on heavy-metal contamination in the sea', *Helgoländer Meeresuntersuchungen*, 33(1–4), pp. 6–25. Available at: https://doi.org/10.1007/BF02414731/METRICS.

Bryan, G.W. and Hummerstone, L.G. (1973) 'Brown Seaweed as an Indicator of Heavy Metals in Estuaries in South-West England', *Journal of the Marine Biological Association of the United Kingdom*, 53(3), pp. 705–720. Available at: https://doi.org/10.1017/S0025315400058902.

Cao, L., Lu, W., Mata, A., Nishinari, K. and Fang, Y. (2020) 'Egg-box model-based gelation of alginate and pectin: A review', *Carbohydrate Polymers*, 242. Available at: https://doi.org/10.1016/j.carbpol.2020.116389.

Carlson, L. (1991) 'Seasonal Variation in Growth, Reproduction and Nitrogen Content of *Fucus vesiculosus* L. in the Oresund Southern Sweden', *Botanica Marina*, 34(5), pp. 447–454. Available at: https://doi.org/10.1515/BOTM.1991.34.5.447/PDF/FIRSTPAGE.

Catarino, M.D., Silva, A.M.S. and Cardoso, S.M. (2018) 'Phycochemical Constituents and Biological Activities of *Fucus* spp.', *Marine Drugs*, 16(8), p. 249. Available at: https://doi.org/10.3390/MD16080249.

Chalkley, R., Child, F., Al-Thaqafi, K., Dean, A.P., White, K.N. and Pittman, J.K. (2019) 'Macroalgae as spatial and temporal bioindicators of coastal metal pollution following remediation and diversion of acid mine drainage', *Ecotoxicology and Environmental Safety*, 182, p. 109458. Available at: https://doi.org/10.1016/J.ECOENV.2019.109458.

Chung, I.K. and Lee, J.A. (1989) ‘The Effects of Heavy Metals in Seaweeds’, *Algae*, 4(2), pp. 221–238. Available at: http://www.e-algae.org/journal/view.php?number=1929 (Accessed: 21 July 2025).

Davies, C.A.L., Tomlinson, K. and Stephenson, T. (1991) ‘Heavy Metals in River Tees Estuary Sediments’, *Environmental Technology*, 12(11), pp. 961–972. Available at: https://doi.org/10.1080/09593339109385095.

Davis, T.A., Volesky, B. and Mucci, A. (2003) ‘A review of the biochemistry of heavy metal biosorption by brown algae’, *Water Research*, 37(18), pp. 4311–4330. Available at: https://doi.org/10.1016/S0043-1354(03)00293-8.

DEFRA (2023) *Environmental Improvement Plan 2023*. Available at: https://www.gov.uk/government/publications/environmental-improvement-plan (Accessed: 31 August 2025).

Eastabrook, C.L., Maqueda, M.M., Vagg, C., Idomeh, J., Nasif-Whitestone, T.A., Lawrence, P., Bronowska, A.K., Bothwell, J.H., Sallach, B.J., Redfern, J. and Caldwell, G.S. (2022) ‘Determining the toxicity and potential for environmental transport of pyridine using the brown crab *Cancer pagurus* (L.)’, *bioRxiv* [Preprint]. Available at: https://doi.org/10.1101/2022.11.17.516169.

Environment Agency (2023) *Tees Management Catchment*. Available at: https://environment.data.gov.uk/catchment-planning/ManagementCatchment/3093 (Accessed: 23 April 2025).

Environment Agency (2025a) *Abandoned metal mines in England: baseline length of rivers and estuaries polluted by harmful metals*. Available at: https://www.gov.uk/government/publications/abandoned-metal-mines-in-england-baseline-length-of-rivers-and-estuaries-polluted-by-harmful-metals/abandoned-metal-mines-in-england-baseline-length-of-rivers-and-estuaries-polluted-by-harmful-metals (Accessed: 16 September 2025).

Environment Agency (2025b) *Catchment Data Explorer*. Available at: https://environment.data.gov.uk/catchment-planning/WaterBody/GB510302509900 (Accessed: 15 July 2025).

Environment Agency (2025c) *Tyne management catchment: baseline length of rivers and estuaries polluted by abandoned metal mines*. Available at: https://www.gov.uk/government/publications/abandoned-metal-mines-in-england-

baseline-length-of-rivers-and-estuaries-polluted-by-harmful-metals/tyne-management-catchment-baseline-length-of-rivers-and-estuaries-polluted-by-abandoned-metal-mines (Accessed: 13 August 2025).

Environment Agency (2025d) *Water quality data archive*. Available at: https://environment.data.gov.uk/water-quality/view/landing (Accessed: 1 September 2025).

Espinoza, D., González, A., Pizarro, J., Segura, R., Laporte, D., Rodríguez-Rojas, F., Sáez, C.A. and Moenne, A. (2021) '*Ulva compressa* from copper-polluted sites exhibits intracellular copper accumulation, increased expression of metallothioneins and copper-containing nanoparticles in chloroplasts', *International Journal of Molecular Sciences*, 22(19), p. 10531. Available at: https://doi.org/10.3390/IJMS221910531/S1.

Evans, D.W., Cutshall, N.H., Cross, F.A. and Wolfe, D.A. (1977) 'Manganese Cycling in the Newport River Estuary, North Carolina', *Estuarine and Coastal Marine Science*, 5(1), pp. 71–80. Available at: https://doi.org/10.1016/0302-3524(77)90074-3.

Fletcher, H.R., Biller, P., Ross, A.B. and Adams, J.M.M. (2017) 'The seasonal variation of fucoidan within three species of brown macroalgae', *Algal Research*, 22, pp. 79–86. Available at: https://doi.org/10.1016/J.ALGAL.2016.10.015.

Ford, A.T., Fitzsimons, M.F. and Halsall, C. (2024) 'Why there is no evidence that pyridine killed the English crabs', *Environmental Science: Advances*, 3(10), pp. 1385–1391. Available at: https://doi.org/10.1039/D4VA00006D.

Forsberg, Å., Söderlund, S., Frank, A., Petersson, L.R. and Pedersén, M. (1988) 'Studies on metal content in the brown seaweed, *Fucus vesiculosus*, from the Archipelago of Stockholm', *Environmental Pollution*, 49(4), pp. 245–263. Available at: https://doi.org/10.1016/0269-7491(88)90091-7.

Foster, P. (1976) 'Concentrations and concentration factors of heavy metals in brown algae', *Environmental Pollution (1970)*, 10(1), pp. 45–53. Available at: https://doi.org/10.1016/0013-9327(76)90094-X.

Fuge, R. and James, K.H. (1973) 'Trace metal concentrations in brown seaweeds, Cardigan Bay, Wales', *Marine Chemistry*, 1(4), pp. 281–293. Available at: https://doi.org/10.1016/0304-4203(73)90018-2.

Fuge, R. and James, K.H. (1974) ‘Trace Metal Concentrations in *Fucus* from the Bristol Channel’, *Marine Pollution Bulletin*, 5(1), pp. 9–12. Available at: https://doi.org/10.1016/0025-326X(74)90026-5.

García-Seoane, R., Fernández, J.A., Villares, R. and Aboal, J.R. (2018) ‘Use of macroalgae to biomonitor pollutants in coastal waters: Optimization of the methodology’, *Ecological Indicators*, 84, pp. 710–726. Available at: https://doi.org/10.1016/J.ECOLIND.2017.09.015.

García-Seoane, R., Fernández, J.A., Varela, Z., Real, C., Boquete, M.T. and Aboal, J.R. (2019) ‘Sampling optimization for biomonitoring metal contamination with marine macroalgae’, *Environmental Pollution*, 255, p. 113349. Available at: https://doi.org/10.1016/J.ENVPOL.2019.113349.

García-Seoane, R., Fernández, J.A., Boquete, M.T. and Aboal, J.R. (2021) ‘Analysis of intra-thallus and temporal variability of trace elements and nitrogen in *Fucus vesiculosus*: Sampling protocol optimization for biomonitoring’, *Journal of Hazardous Materials*, 412, p. 125268. Available at: https://doi.org/10.1016/J.JHAZMAT.2021.125268.

Garcia-Vaquero, M., Rajauria, G., Miranda, M., Sweeney, T., Lopez-Alonso, M. and O’Doherty, J. (2021) ‘Seasonal Variation of the Proximate Composition, Mineral Content, Fatty Acid Profiles and Other Phytochemical Constituents of Selected Brown Macroalgae’, *Marine Drugs*, 19(4), p. 204. Available at: https://doi.org/10.3390/MD19040204/S1.

Gibbon, S. (2023) ‘How Teesworks dredges the Tees’, *North East Bylines*, 5 July. Available at: https://northeastbylines.co.uk/news/teesworks-the-shadow-inquiry/how-teesworks-dredges-the-tees/ (Accessed: 24 April 2025).

Giusti, L. (2001) ‘Heavy metal contamination of brown seaweed and sediments from the UK coastline between the Wear River and the Tees River’, *Environment International*, 26(4), pp. 275–286. Available at: https://doi.org/10.1016/S0160-4120(00)00117-3.

Giusti, L., Williamson, A.C. and Mistry, A. (1999) ‘Biologically available trace metals in *Mytilus edulis* from the coast of Northeast England’, *Environment International*, 25(8), pp. 969–981. Available at: https://doi.org/10.1016/S0160-4120(99)00066-5.

Grant, G.T., Morris, E.R., Rees, D.A., Smith, P.J.C. and Thom, D. (1973) ‘Biological interactions between polysaccharides and divalent cations: The egg-box model’, *FEBS Letters*, 32(1), pp. 195–198. Available at: https://doi.org/10.1016/0014-5793(73)80770-7.

Hardy, F.G., Evans, S.M. and Tremayne, M.A. (1993) ‘Long-term changes in the marine macroalgae of three polluted estuaries in north-east England’, *Journal of Experimental Marine Biology and Ecology*, 172(1–2), pp. 81–92. Available at: https://doi.org/10.1016/0022-0981(93)90090-B.

Haug, A. (1961) ‘The Affinity of Some Divalent Metals for Different Types of Alginates’, *Acta Chemica Scandinavica*, 15, pp. 1794–1795. Available at: https://doi.org/10.3891/ACTA.CHEM.SCAND.15-1794.

Haug, A. and Smidsrød, O. (1965) ‘The Effect of Divalent Metals on the Properties of Alginate Solutions. II. Comparison of Different Metal Ions’, *Acta Chemica Scandinavica*, 19(2), pp. 341–351. Available at: https://doi.org/10.3891/acta.chem.scand.19-0341.

Hauser-Davis, R.A. and Wosnick, N. (2022) ‘Climate Change Implications for Metal and Metalloid Dynamics in Aquatic Ecosystems and its Context within the Decade of Ocean Sciences’, *Water*, 14(15), p. 2415. Available at: https://doi.org/10.3390/w14152415.

Hedge, L.H., Knott, N.A. and Johnston, E.L. (2009) ‘Dredging related metal bioaccumulation in oysters’, *Marine Pollution Bulletin*, 58(6), pp. 832–840. Available at: https://doi.org/10.1016/J.MARPOLBUL.2009.01.020.

Herman, K.S., Iskandarova, M. and Sovacool, B.K. (2025) ‘Imagining a net-zero Teesside: actors, networks, and expectations in industrial decarbonisation megaprojects’, *Environmental Research Communications*, 7(1), p. 015007. Available at: https://doi.org/10.1088/2515-7620/AD8F99.

Hill, J.M. (2008) *Oarweed (*Laminaria digitata*)*, *Marine Life Information Network: Biology and Sensitivity Key Information Reviews*. Available at: https://www.marlin.ac.uk/species/detail/1386 (Accessed: 3 April 2025).

Huang, L., Lee, J.Y., Park, Y.K. and Lee, J. (2025) ‘Heavy metals in seaweed: Implications for health benefits, risks, and safety regulations’, *Journal of Agriculture*

and Food Research, 21, p. 101830. Available at: https://doi.org/10.1016/J.JAFR.2025.101830.

Hudson-Edwards, K., Macklin, M. and Taylor, M. (1997) 'Historic metal mining inputs to Tees River sediment', *Science of The Total Environment*, 194–195, pp. 437–445. Available at: https://doi.org/10.1016/S0048-9697(96)05381-8.

Hudson-Edwards, K.A., Macklin, M.G., Curtis, C.D. and Vaughan, D.J. (1996) 'Processes of Formation and Distribution of Pb-, Zn-, Cd-, and Cu-Bearing Minerals in the Tyne Basin, Northeast England: Implications for Metal-Contaminated River Systems', *Environmental Science and Technology*, 30(1), pp. 72–80. Available at: https://doi.org/10.1021/ES9500724/ASSET/IMAGES/MEDIUM/ES9500724E00010.GIF.

Ibhadon, A.O., Wright, P. and Daniels, R. (2004) 'Trace metal speciation and contamination in an intertidal estuary', *Journal of Environmental Monitoring*, 6(8), pp. 679–683. Available at: https://doi.org/10.1039/B315954J.

IDRIC (2022) *Tees Valley Industrial Cluster*. Available at: https://idric.org/stakeholders/teesside-industrial-cluster/#toggle-id-1 (Accessed: 23 April 2025).

Jackson, A. (2008) *Toothed wrack (*Fucus serratus*)*, *Marine Life Information Network: Biology and Sensitivity Key Information Reviews*. Available at: https://www.marlin.ac.uk/species/detail/1326 (Accessed: 1 April 2025).

Jones, B. and Turki, A. (1997) 'Distribution and speciation of heavy metals in surficial sediments from the Tees Estuary, north-east England', *Marine Pollution Bulletin*, 34(10), pp. 768–779. Available at: https://doi.org/10.1016/S0025-326X(97)00047-7.

Karaouzas, I., Kapetanaki, N., Mentzafou, A., Kanellopoulos, T.D. and Skoulikidis, N. (2021) 'Heavy metal contamination status in Greek surface waters: A review with application and evaluation of pollution indices', *Chemosphere*, 263, p. 128192. Available at: https://doi.org/10.1016/J.CHEMOSPHERE.2020.128192.

Konstantin, B., Anastasia, P., Nikolay, I. and Daria, P. (2023) 'Seasonal variations in the chemical composition of Arctic brown macroalgae', *Algal Research*, 72, p. 103112. Available at: https://doi.org/10.1016/J.ALGAL.2023.103112.

Kowalska, J.B., Mazurek, R., Gąsiorek, M. and Zaleski, T. (2018) 'Pollution indices as useful tools for the comprehensive evaluation of the degree of soil

contamination–A review', *Environmental Geochemistry and Health*, 40(6), pp. 2395–2420. Available at: https://doi.org/10.1007/S10653-018-0106-Z.

Lee, R.E. (2018) *Phycology*. 5th ed. Cambridge University Press. Available at: https://doi.org/10.1017/9781316407219.

Li, B., Lu, F., Wei, X. and Zhao, R. (2008) 'Fucoidan: Structure and Bioactivity', *Molecules*, 13(8), pp. 1671–1695. Available at: https://doi.org/10.3390/MOLECULES13081671.

Losada, S., Pitchers, E.P., Potter, K., Katsiadaki, I. and Barber, J.L. (2025) 'Quantitative Determination of Pyridine Content in Crustacean Tissues and Marine Sediments by Headspace Gas Chromatography/Tandem Mass Spectrometry (HS-GC-MS/MS)', *Analytical Letters*, 58(17), pp. 3011–3027. Available at: https://doi.org/10.1080/00032719.2025.2451182.

Miramand, P. and Bentley, D. (1992) 'Heavy metal concentrations in two biological indicators (*Patella vulgata* and *Fucus serratus*) collected near the French nuclear fuel reprocessing plant of La Hague', *Science of The Total Environment*, 111(2–3), pp. 135–149. Available at: https://doi.org/10.1016/0048-9697(92)90352-S.

Miró, J.M., Megina, C., Donázar-Aramendía, I. and García-Gómez, J.C. (2022) 'Effects of maintenance dredging on the macrofauna of the water column in a turbid estuary', *Science of The Total Environment*, 806, p. 151304. Available at: https://doi.org/10.1016/J.SCITOTENV.2021.151304.

MMO (2019) *Dredging*. Available at: https://www.gov.uk/guidance/dredging (Accessed: 24 April 2025).

MMO (2023a) *South Bank Quay marine licence applications*. Available at: https://www.gov.uk/government/publications/south-bank-quay-marine-licence-applications (Accessed: 15 July 2025).

MMO (2023b) *Tees and Hartlepool Maintenance Dredge Disposal Licence*. Available at: https://www.gov.uk/government/publications/tees-and-hartlepool-maintenance-dredge-disposal-licence (Accessed: 15 July 2025).

Morillo, J., Usero, J. and Gracia, I. (2004) 'Heavy metal distribution in marine sediments from the southwest coast of Spain', *Chemosphere*, 55(3), pp. 431–442. Available at: https://doi.org/10.1016/J.CHEMOSPHERE.2003.10.047.

Murrey, L.A. and Norton, M.G. (1979) *Fisheries Research Technical Report No. 52 The composition of dredged spoils dumped at sea from England and Wales*. Available at: https://www.cefas.co.uk/publications/techrep/tech52.pdf (Accessed: 14 April 2025).

Office for National Statistics (2025) *Regions (December 2024) Boundaries EN BGC*, *Open Geography portalx*. Available at: https://geoportal.statistics.gov.uk/datasets/125a1e3fca4940e5941d85c585b96aba_0/explore (Accessed: 14 August 2025).

OSPAR Commission (2008) *Assessment of the environmental impact of dredging for navigational purposes*. Available at: https://www.ospar.org/documents?v=7124 (Accessed: 24 April 2025).

Ownsworth, E., Selby, D., Ottley, C.J., Unsworth, E., Raab, A., Feldmann, J., Sproson, A.D., Kuroda, J., Faidutti, C. and Bücker, P. (2019) 'Tracing the natural and anthropogenic influence on the trace elemental chemistry of estuarine macroalgae and the implications for human consumption', *Science of The Total Environment*, 685, pp. 259–272. Available at: https://doi.org/10.1016/J.SCITOTENV.2019.05.263.

Pacín, C., Fernández, J.A., Conde-Amboage, M., Lazzari, M., García-Seoane, R., Viana, I.G., Varela, Z., Real, C., Villares R. and Aboal, J.R. (2025) 'Three Decades of Change in Potentially Toxic Elements in Brown Algae in the Northeast Atlantic Ocean', *Environmental Science & Technology*, 59(21), pp. 10476–10487. Available at: https://doi.org/10.1021/ACS.EST.4C14013.

Phillips, D.J.H. (1977) 'The use of biological indicator organisms to monitor trace metal pollution in marine and estuarine environments — a review', *Environmental Pollution (1970)*, 13(4), pp. 281–317. Available at: https://doi.org/10.1016/0013-9327(77)90047-7.

Plater, A.J., Ridgway, J., Appleby, P.G., Berry, A. and Wright, M.R. (1999) 'Historical Contaminant Fluxes in the Tees Estuary, UK: Geochemical, Magnetic and Radionuclide Evidence', *Marine Pollution Bulletin*, 37(3–7), pp. 343–360. Available at: https://doi.org/10.1016/S0025-326X(99)00052-1.

Preston, A., Jeffries, D.F., Dutton, J.W.R., Harvey, B.R. and Steele, A.K. (1972) 'British Isles coastal waters: The concentrations of selected heavy metals in sea water, suspended matter and biological indicators — A pilot survey', *Environmental*

Pollution (1970), 3(1), pp. 69–82. Available at: https://doi.org/10.1016/0013-9327(72)90018-3.

Qian, Y., Zhang, W., Yu, L. and Feng, H. (2015) 'Metal Pollution in Coastal Sediments', *Current Pollution Reports*, 1(4), pp. 203–219. Available at: https://doi.org/10.1007/S40726-015-0018-9.

Raab, A., Stengel, D.B. and Feldmann, J. (2025) 'Differential prevalence of arsenic speciation in the kelps *Laminaria digitata* and *L. hyperborea*', *Marine Pollution Bulletin*, 211, p. 117473. Available at: https://doi.org/10.1016/J.MARPOLBUL.2024.117473.

Rakib, R.J., Jolly, Y.N., Dioses-Salinas, D.C., Pizarro-Ortega, C.I., De-la-Torre, G.E., Khandaker, M.U., Alsubaie, A., Almalki, A.S.A. and Bradley, D. A. (2021) 'Macroalgae in biomonitoring of metal pollution in the Bay of Bengal coastal waters of Cox's Bazar and surrounding areas', *Scientific Reports*, 11(1), pp. 20999-. Available at: https://doi.org/10.1038/s41598-021-99750-7.

Riget, F., Johansen, P. and Asmund, G. (1997) 'Baseline levels and natural variability of elements in three seaweed species from West Greenland', *Marine Pollution Bulletin*, 34(3), pp. 171–176. Available at: https://doi.org/10.1016/S0025-326X(96)00084-7.

Roberts, D.A., Birchenough, S.N., Lewis, C., Sanders, M.B., Bolam, T. and Sheahan, D. (2013) 'Ocean acidification increases the toxicity of contaminated sediments', *Global Change Biology*, 19(2), pp. 340–351. Available at: https://doi.org/10.1111/gcb.12048.

Rowbotham, J.S., Dyer, P.W., Greenwell, H.C. and Theodorou, M.K. (2012) 'Thermochemical processing of macroalgae: A late bloomer in the development of third-generation biofuels?', *Biofuels*, 3(4), pp. 441–461. Available at: https://doi.org/10.4155/BFS.12.29;JOURNAL:JOURNAL:TBFU20;WGROUP:STRING:PUBLICATION.

Rowbotham, J.S., Dyer, P.W., Greenwell, H.C., Selby, D. and Theodorou, M.K. (2013) 'Copper(II)-mediated thermolysis of alginates: a model kinetic study on the influence of metal ions in the thermochemical processing of macroalgae', *Interface Focus*, 3(1). Available at: https://doi.org/10.1098/RSFS.2012.0046.

Rowbotham, J.S., Greenwell, C.H. and Dyer, P.W. (2021) ‘Opening the Egg Box: NMR spectroscopic analysis of the interactions between s-block cations and kelp monosaccharides’, *Dalton Transactions*, 50(38), pp. 13246–13255. Available at: https://doi.org/10.1039/D0DT04375C.

Rowlatt, S.M. and Lovell, D.R. (1994) ‘Lead, zinc and chromium in sediments around England and Wales’, *Marine Pollution Bulletin*, 28(5), pp. 324–329. Available at: https://doi.org/10.1016/0025-326X(94)90159-7.

Royal HaskoningDHV (2025) *Tees Maintenance Dredge Protocol (MDP) Baseline Document*. Available at: https://northeastfc.uk/RiverTees/TeesMaintenanceAnnualDredgeReview/Tees (Accessed 3 May 2026).

Ryan, S., McLoughlin, P. and O’Donovan, O. (2012) ‘A comprehensive study of metal distribution in three main classes of seaweed’, *Environmental Pollution*, 167, pp. 171–177. Available at: https://doi.org/10.1016/J.ENVPOL.2012.04.006.

Sawidis, T., Brown, M.T., Zachariadis, G. and Sratis, I. (2001) ‘Trace metal concentrations in marine macroalgae from different biotopes in the Aegean Sea’, *Environment International*, 27(1), pp. 43–47. Available at: https://doi.org/10.1016/S0160-4120(01)00052-6.

Schiener, P., Black, K.D., Stanley, M.S. and Green, D.H. (2015) ‘The seasonal variation in the chemical composition of the kelp species *Laminaria digitata*, *Laminaria hyperborea*, *Saccharina latissima* and *Alaria esculenta*’, *Journal of Applied Phycology*, 27(1), pp. 363–373. Available at: https://doi.org/10.1007/S10811-014-0327-1/TABLES/2.

Sharp, G.J., Samant, H.S. and Vaidya, O.C. (1988) ‘Selected metal levels of commercially valuable seaweeds adjacent to and distant from point sources of contamination in Nova Scotia and New Brunswick’, *Bulletin of Environmental Contamination and Toxicology*, 40(5), pp. 724–730. Available at: https://doi.org/10.1007/BF01697522/METRICS.

Sim, R., Feldmann, J., Stengel, D.B. and Pétursdóttir, Á.H. (2023) ‘Temporal and intra-thallus variation in arsenic species in the brown macroalga *Laminaria digitata*’, *Environmental Chemistry*, 20(2), pp. 55–65. Available at: https://doi.org/10.1071/EN22123.

Smurthwaite, R. (2006) *Diet and heavy metal uptake by two top predator species in the Tees Estuary*. Durham University. Available at: https://etheses.dur.ac.uk/2651/ (Accessed: 16 September 2025).

Soetan, O., Nie, J., Viteritto, M. and Feng, H. (2023) 'Evaluation of sediment dredging in remediating toxic metal contamination — a systematic review', *Environmental Science and Pollution Research*, 30(27), pp. 69837–69856. Available at: https://doi.org/10.1007/S11356-023-27489-X.

Stengel, D.B., Macken, A., Morrison, L. and Morley, N. (2004) 'Zinc concentrations in marine macroalgae and a lichen from western Ireland in relation to phylogenetic grouping, habitat and morphology', *Marine Pollution Bulletin*, 48(9–10), pp. 902–909. Available at: https://doi.org/10.1016/J.MARPOLBUL.2003.11.014.

Stengel, D.B., McGrath, H. and Morrison, L.J. (2005) 'Tissue Cu, Fe and Mn concentrations in different-aged and different functional thallus regions of three brown algae from western Ireland', *Estuarine, Coastal and Shelf Science*, 65(4), pp. 687–696. Available at: https://doi.org/10.1016/J.ECSS.2005.07.003.

Stiger-Pouvreau, V., Bourgougnon, N. and Deslandes, E. (2016) 'Carbohydrates from Seaweeds', *Seaweed in Health and Disease Prevention*, pp. 223–274. Available at: https://doi.org/10.1016/B978-0-12-802772-1.00008-7.

Taylor, D. (1982) 'Distribution of heavy metals in the water of a major industrialized estuary', *Environmental Technology*, 3(1–11), pp. 137–144. Available at: https://doi.org/10.1080/09593338209384109.

Todd, V.L.G., Todd, I.B., Gardiner, J.C., Morrin, E.C.N., MacPherson, N.A., DiMarzio, N.A. and Thomsen, F. (2015) 'A review of impacts of marine dredging activities on marine mammals', *ICES Journal of Marine Science*, 72(2), pp. 328–340. Available at: https://doi.org/10.1093/ICESJMS/FSU187.

Tomlinson, D.L., Wilson, J.G., Harris, C.R. and Jeffrey, D.W. (1980) 'Problems in the assessment of heavy-metal levels in estuaries and the formation of a pollution index', *Helgoländer Meeresuntersuchungen*, 33(1–4), pp. 566–575. Available at: https://doi.org/10.1007/BF02414780/METRICS.

Tyler-Walters, H. (2007) *Tangle or cuvie (*Laminaria hyperborea*)*, *Marine Life Information Network; Biology and Sensitivity Key Information Reviews*. Available at: https://www.marlin.ac.uk/species/detail/1309 (Accessed: 3 April 2025).

Vázquez-Arias, A., Pacín, C., Ares, Á., Fernández, J.Á. and Aboal, J.R. (2023) ‘Do we know the cellular location of heavy metals in seaweed? An up-to-date review of the techniques’, *Science of The Total Environment*, 856, p. 159215. Available at: https://doi.org/10.1016/J.SCITOTENV.2022.159215.

Viana, I.G., Aboal, J.R., Fernández, J.A., Real, C., Villares, R. and Carballeira, A. (2010) ‘Use of macroalgae stored in an Environmental Specimen Bank for application of some European Framework Directives’, *Water Research*, 44(6), pp. 1713–1724. Available at: https://doi.org/10.1016/J.WATRES.2009.11.036.

van Weelden, G., Bobi, M., Okła, K., van Weelden, W.J., Romano, A. and Pijnenborg, J.M.A. (2019) ‘Fucoidan Structure and Activity in Relation to Anti-Cancer Mechanisms’, *Marine Drugs*, 17(1), p. 32. Available at: https://doi.org/10.3390/MD17010032.

Whitcombe, B. and Forster, R. (2023) ‘An investigation into water quality: A case study on crustacean mass mortalities along the northeast coast of England in 2021 and 2022’. [Preprint]. Available at: https://doi.org/10.13140/RG.2.2.14128.53769.

White, N. (2008) *Bladder wrack (*Fucus vesiculosus*)*, *Marine Life Information Network: Biology and Sensitivity Key Information Reviews*. Available at: https://www.marlin.ac.uk/species/detail/1330 (Accessed: 1 February 2024).

Zhang, G., Bai, J., Xiao, R., Zhao, Q., Jia, J., Cui, B. and Liu, X. (2017) ‘Heavy metal fractions and ecological risk assessment in sediments from urban, rural and reclamation-affected rivers of the Pearl River Estuary, China’, *Chemosphere*, 184, pp. 278–288. Available at: https://doi.org/10.1016/J.CHEMOSPHERE.2017.05.155.

Appendices

Appendix A: Sample collection details

Site name (site ID)	Latitude	Longitude	Elevation (m, RSL)	Date(s) of collection	Collector(s)	Species
Cullercoats Beach (C)	55.0354	-1.4297	-5 to -1*	22/01/2025	D. Gröcke	*L. digitata* (*n*=4)
					F. Alldred	*L. hyperborea* (*n*=2)
						F. vesiculosus (*n*=4)
						F. serratus (*n*=5)
South Gare 1 (SG1)	54.6383	-1.1411	2.67	03/03/2025	E. Brendler-Spaeth	*F. vesiculosus* (*n*=3)
South Gare 3 (SG3)	54.6451	-1.1370	-8 to -7*	27/04/2024	J. Pealing	*L. digitata* (*n*=5)
South Gare 4 (SG4)	54.6464	-1.1332	-8 to -7*	11/05/2024	J. Pealing	*L. hyperborea* (*n*=3)
				07/07/2024		
South Gare 2 (SG2)	54.6431	-1.1339	0.00	03/03/2025	E. Brendler-Spaeth	*F. vesiculosus* (*n*=3)
Redcar Beach 1 (R1)	54.6186	-1.0598	6.00	03/03/2025	E. Brendler-Spaeth	*F. vesiculosus* (*n*=3)
Redcar Beach 2 (R2)	54.6187	-1.0573	3.00	03/03/2025	E. Brendler-Spaeth	*F. vesiculosus* (*n*=3)
Cayton Bay (CB)	54.2630	-0.3691	-4.50	13/08/2024	R. Forster	*L. digitata* (*n*=5)
						L. hyperborea (*n*=5)
Selwicks Bay Deep (SD)	54.1218	-0.0778	-8.50	15/08/2024	R. Forster	*L. hyperborea* (*n*=4)
Selwicks Bay Shallow (SS)	54.1184	-0.0787	-4.50	15/08/2024	R. Forster	*L. hyperborea* (*n*=5)

Table A1 | Summary of collection sites, sampling dates, and species collected.

* Retrospectively estimated.

Sample ID	Species	Digestion method	Metal concentration (mg/kg dw)							
			Cr	Mn	Fe	Ni	Cu	Zn	Cd	Pb
C-1-S1 rep 1	*L. digitata*	Microwave	128.77	9.90	648.95	90.27		23.69	0.05	
C-1-S1 rep 2	*L. digitata*	Microwave	19.22	2.10	121.57	13.23		29.84*	0.04	
C-1-S2	*L. digitata*	Microwave	0.44*	1.50*	37.93	0.36		24.97	0.06	
C-1-S3	*L. digitata*	Microwave	0.75*	0.95	41.65	0.42		39.57*	0.03	
C-1-M1	*L. digitata*	Microwave	0.46*	1.27	17.44	0.35		29.27*	0.13	
C-1-M2	*L. digitata*	Microwave	0.04*	1.57	17.81	0.25*		22.47	0.16	
C-1-M3	*L. digitata*	Microwave	23.54	3.76	226.46	100.24		26.61	0.19	
C-1-B1	*L. digitata*	Microwave	0.75	2.08	90.39	1.88		21.60	0.05	
C-1-B2 rep 1	*L. digitata*	Microwave	0.69*	2.13	67.99	0.32		18.51	0.02	
C-1-B2 rep 2	*L. digitata*	Microwave	0.91*	2.05	69.75	0.59		14.80*	0.01	
C-1-B3	*L. digitata*	Microwave	2.74	2.44	83.49	34.15		31.42*	0.01	
C-1-B4	*L. digitata*	Microwave	0.94	3.34	119.02	2.55		36.32*	0.01	
C-1-B5	*L. digitata*	Microwave	0.75	2.60	73.18	0.78		34.67	0.01	
C-1-B6	*L. digitata*	Microwave	1.24*	4.68	199.26	0.76		41.01	0.01	
C-2-H	*L. digitata*	Microwave	0.84*	318.62	186.87	2.53		12.42*	0.09	

Sample ID	Species	Digestion method	Metal concentration (mg/kg dw)							
			Cr	Mn	Fe	Ni	Cu	Zn	Cd	Pb
C-2-S1	*L. digitata*	Microwave	0.56*	2.22	35.34	0.38		18.87*	0.09	
C-2-S2	*L. digitata*	Microwave	0.64*	1.71*	36.49	0.46		8.06*	0.10	
C-2-S3	*L. digitata*	Microwave	0.16*	1.49*	25.82	0.29*		8.80*	0.28	
C-2-M1	*L. digitata*	Microwave	0.33*	1.81	22.32	0.58*		18.76*	0.45	
C-2-M2	*L. digitata*	Microwave	0.27*	2.68	32.88	0.41		37.14*	0.38	
C-2-B1 rep 1	*L. digitata*	Microwave	0.70*	4.38	163.15	0.66		29.87	0.05	
C-2-B1 rep 2	*L. digitata*	Microwave	0.49*	4.16	167.24	0.61		37.83	0.04	
C-2-B2	*L. digitata*	Microwave	0.60*	4.73	194.67	0.64		39.33*	0.01	
C-2-B3	*L. digitata*	Microwave	0.94*	6.10	267.20	1.15		34.08	0.05	
C-2-B4	*L. digitata*	Microwave	0.75*	4.80	259.44	0.80		26.67	0.06	
C-3-M1	*L. digitata*	Microwave	0.24*	2.85	23.36	0.33*		11.32*	0.20	
C-3-B1	*L. digitata*	Microwave	0.41*	4.68	82.88	0.42*		23.95*	0.16	
C-3-B2 rep 1	*L. digitata*	Microwave	16.94	12.52	408.68	21.91		37.67*	0.04	
C-3-B2 rep 2	*L. digitata*	Microwave	0.16*	5.94	206.85	0.54*		28.51	0.04	
C-3-B3	*L. digitata*	Microwave	0.51*	5.88	507.35	0.40		25.36	0.02	

Sample ID	Species	Digestion method	Metal concentration (mg/kg dw)							
			Cr	Mn	Fe	Ni	Cu	Zn	Cd	Pb
C-3-B4	*L. digitata*	Microwave	0.51*	13.97	539.18	1.25		40.86	0.02	
C-4-M1	*L. digitata*	Microwave	0.26*	4.06	52.45	0.58*		33.92*	0.29	
C-4-M2 rep 1	*L. digitata*	Microwave	0.23*	4.96	44.57	0.49*		32.98*	0.23	
C-4-M2 rep 2	*L. digitata*	Microwave		5.99	92.82	0.40*		40.51*	0.11	
C-4-M3	*L. digitata*	Microwave	0.04*	4.24	291.89	1.81		19.08*	0.02	
C-4-M4	*L. digitata*	Microwave	0.69*	5.06	520.21	0.52		17.80*	0.01	
C-4-B1	*L. digitata*	Microwave	8.62	11.51	458.72	12.60		34.23	0.03	
C-5-H rep 1	*L. hyperborea*	Microwave	0.82	47.70	74.10	7.22		4.90*	0.41	
C-5-H rep 2	*L. hyperborea*	Microwave	1.71	56.03	122.06	9.10		3.07*	0.68	
C-5-M1	*L. hyperborea*	Microwave	0.03*	1.00	16.95	0.47*		27.43	0.39	
C-5-S1	*L. hyperborea*	Microwave	1.09*	35.44	191.24	3.70		28.16*	0.17	
C-5-S2	*L. hyperborea*	Microwave	0.26*	46.09	70.63	1.44		31.86*	0.11	
C-5-S3	*L. hyperborea*	Microwave	0.13*	1.59	50.13	0.62*		32.40	0.24	
C-5-B1	*L. hyperborea*	Microwave	0.13*	1.81	41.28	0.43		33.44*	0.16	
C-5-B2	*L. hyperborea*	Hot plate	0.16	1.87	43.82	0.27		25.32	0.07	

Sample ID	Species	Digestion method	Metal concentration (mg/kg dw)							
			Cr	Mn	Fe	Ni	Cu	Zn	Cd	Pb
C-5-B3	*L. hyperborea*	Microwave	0.95*	3.30	98.86	1.22		35.22	0.05	
C-5-B4	*L. hyperborea*	Microwave	0.54*	3.74	181.04	1.33		47.73	0.06	
C-6-H	*L. hyperborea*	Microwave	0.35*	112.56	203.87	0.56		5.97*	1.00	
C-6-S1	*L. hyperborea*	Microwave	0.88*	42.88	212.32	0.83		22.08	0.39	
C-6-S2	*L. hyperborea*	Microwave	0.78*	5.60	17.05	0.87		36.57*	0.16	
C-6-S3	*L. hyperborea*	Microwave	0.16*	1.64*	32.86	0.34*		26.05*	0.91	
C-6-M1	*L. hyperborea*	Microwave	0.21*	1.75*	14.79	0.36*		33.29*	1.60	
C-6-B1	*L. hyperborea*	Hot plate	0.17	1.29	34.26	0.35		34.56	0.59	
C-6-B2	*L. hyperborea*	Hot plate	0.12	1.21	33.65	0.35		27.78	0.45	
C-6-B3	*L. hyperborea*	Hot plate	0.22	1.86	55.29	0.59		35.69	0.26	
C-6-B4 rep 1	*L. hyperborea*	Microwave	0.86*	3.44	119.46	1.45		50.01	0.12	
C-6-B4 rep 2	*L. hyperborea*	Hot plate	0.32	2.67	78.73	0.96		43.81	0.11	
C-7	*F. vesiculosus*	Hot plate	0.10	110.05	86.84	3.18	2.15	51.43	0.46	0.33
C-8	*F. vesiculosus*	Hot plate	0.09	83.24	90.68	3.71	2.39	41.24	0.32	0.47
C-9	*F. vesiculosus*	Hot plate	0.10	142.22	109.34	4.82	2.45	50.20	0.39	0.63

Sample ID	Species	Digestion method	Metal concentration (mg/kg dw)							
			Cr	Mn	Fe	Ni	Cu	Zn	Cd	Pb
C-10	*F. vesiculosus*	Hot plate	0.11	133.47	87.78	4.09	2.06	46.83	0.47	0.37
C-11	*F. serratus*	Hot plate	0.07	45.72	45.36	1.84	1.93	60.44	0.72	0.32
C-12	*F. serratus*	Hot plate	0.08	88.68	52.61	2.22	2.48	62.75	0.78	0.55
C-13	*F. serratus*	Hot plate	0.06	64.64	49.62	2.13	2.00	40.12	0.52	0.33
C-14	*F. serratus*	Hot plate	0.08	54.64	52.00	1.78	1.93	54.24	0.60	0.31
C-15 rep 1	*F. serratus*	Hot plate	0.13	90.92	77.39	2.81	3.03	65.50	0.90	0.76
C-15 rep 2	*F. serratus*	Hot plate	0.08	73.36	55.19	2.27	2.48	65.34	0.81	0.55
C-15 rep 3	*F. serratus*	Hot plate	0.09	81.85	70.03	2.59	2.93	68.82	0.90	0.71
CB-1 rep 1	*L. hyperborea*	Hot plate	0.67	39.00	43.15	0.66	1.26	18.31	0.12	0.61
CB-1 rep 2	*L. hyperborea*	Hot plate	0.13	36.49	32.14	0.60	1.15	17.18	0.12	0.52
CB-1 rep 3	*L. hyperborea*	Hot plate	0.14	35.86	27.71	0.59	1.15	16.70	0.11	0.49
CB-1 rep 4	*L. hyperborea*	Hot plate	0.09	32.21	26.32	0.50	1.12	15.38	0.11	0.57
CB-1 rep 5	*L. hyperborea*	Hot plate	0.17	39.89	30.29	0.79	1.91	18.08	0.11	0.68
CB-2 rep 1	*L. hyperborea*	Hot plate	0.11	8.16	18.62	0.42	0.94	17.80	0.18	0.18
CB-2 rep 2	*L. hyperborea*	Hot plate	0.12	10.01	23.22	0.49	0.97	21.88	0.21	0.30

Sample ID	Species	Digestion method	Metal concentration (mg/kg dw)							
			Cr	Mn	Fe	Ni	Cu	Zn	Cd	Pb
CB-2 rep 3	*L. hyperborea*	Hot plate	0.18	9.18	26.68	0.58	1.10	20.12	0.20	0.22
CB-2 rep 4	*L. hyperborea*	Hot plate	0.06	7.05	19.22	0.30	0.91	16.96	0.18	0.26
CB-3	*L. hyperborea*	Hot plate	0.15	15.34	28.45	0.23	0.86	16.52	0.08	0.47
CB-4	*L. hyperborea*	Hot plate	0.18	22.52	41.44	0.67	1.43	18.73	0.20	0.65
CB-5	*L. hyperborea*	Hot plate	0.15	7.34	27.06	0.21	1.01	16.90	0.12	0.21
CB-6	*L. digitata*	Hot plate	0.10	5.12	44.08	0.17	2.32	35.14	0.03	0.33
CB-7	*L. digitata*	Hot plate	0.31	5.27	37.63	0.24	1.79	23.07	0.03	0.35
CB-8	*L. digitata*	Hot plate	0.19	5.11	55.77	0.20	1.91	25.40	0.03	0.28
CB-9	*L. digitata*	Hot plate	0.13	3.82	48.43	0.20	1.91	34.30	0.03	0.31
CB-10 rep 1	*L. digitata*	Hot plate	0.20	4.13	35.50	0.22	1.70	20.54	0.02	0.44
CB-10 rep 2	*L. digitata*	Hot plate	0.17	4.73	34.50	0.21	1.88	23.06	0.03	0.56
CB-10 rep 3	*L. digitata*	Hot plate	0.18	5.03	42.06	0.20	1.96	23.98	0.03	0.49
R1-1	*F. vesiculosus*	Hot plate	0.07	28.14	34.24	2.50	1.94	36.99	0.40	0.16
R1-2	*F. vesiculosus*	Hot plate	0.09	46.32	53.96	4.29	2.29	45.43	0.42	0.32
R1-3	*F. vesiculosus*	Hot plate	0.08	48.56	35.21	4.02	2.21	50.42	0.52	0.24

Sample ID	Species	Digestion method	Metal concentration (mg/kg dw)							
			Cr	Mn	Fe	Ni	Cu	Zn	Cd	Pb
R2-1	*F. vesiculosus*	Hot plate	0.09	30.45	56.44	3.30	2.23	43.56	0.28	0.31
R2-2	*F. vesiculosus*	Hot plate	0.07	35.59	49.40	3.71	2.34	44.95	0.27	0.29
R2-3	*F. vesiculosus*	Hot plate	0.08	17.31	30.07	1.61	1.42	23.68	0.22	0.17
SD-1	*L. hyperborea*	Hot plate	0.23	26.05	103.31	0.57	1.73	23.62	0.25	0.85
SD-2	*L. hyperborea*	Hot plate	0.18	37.45	65.45	1.23	2.64	23.96	0.21	0.99
SD-3	*L. hyperborea*	Hot plate	0.24	30.29	67.85	1.16	4.02	37.39	0.35	1.05
SD-4 rep 1	*L. hyperborea*	Hot plate	0.19	28.69	68.62	0.48	2.66	34.02	0.35	2.08
SD-4 rep 2	*L. hyperborea*	Hot plate	0.23	30.86	89.16	0.59	2.90	36.25	0.40	2.25
SD-4 rep 3	*L. hyperborea*	Hot plate	0.22	26.41	73.50	0.48	2.44	31.41	0.33	1.90
SG1-1	*F. vesiculosus*	Hot plate	0.37	112.21	194.70	2.34	5.77	88.42	0.19	2.68
SG1-2	*F. vesiculosus*	Hot plate	0.28	104.51	152.51	2.71	5.13	76.73	0.29	2.15
SG1-3	*F. vesiculosus*	Hot plate	0.34	58.53	146.63	0.65	4.42	40.40	0.15	1.62
SG2-1	*F. vesiculosus*	Hot plate	0.11	61.31	120.83	4.25	2.54	54.50	0.53	0.43
SG2-2	*F. vesiculosus*	Hot plate	0.10	69.35	119.94	4.28	2.54	47.93	0.44	0.54
SG2-3	*F. vesiculosus*	Hot plate	0.12	92.92	128.56	5.71	3.26	70.76	0.70	0.57

Sample ID	Species	Digestion method	Metal concentration (mg/kg dw)							
			Cr	Mn	Fe	Ni	Cu	Zn	Cd	Pb
SG3-1 rep 1	*L. digitata*	Hot plate	0.46	18.64	967.39	0.39	4.03	45.11	0.04	6.99
SG3-1 rep 2	*L. digitata*	Hot plate	0.49	18.76	896.50	0.47	4.31	52.11	0.04	8.10
SG3-2 rep 1	*L. digitata*	Hot plate	0.26	12.62	459.94	0.26	2.81	35.54	0.02	3.90
SG3-2 rep 2	*L. digitata*	Hot plate	0.28	15.19	429.30	0.32	3.68	46.91	0.04	4.27
SG3-3	*L. digitata*	Hot plate	0.24	13.97	621.72	0.36	3.99	56.02	0.04	5.92
SG3-4	*L. digitata*	Hot plate	0.24	10.26	505.61	0.27	2.84	32.78	0.04	4.20
SG3-5	*L. digitata*	Hot plate	0.19	14.10	361.28	0.29	2.98	34.86	0.04	3.31
SG4-1 rep 1	*L. hyperborea*	Hot plate	0.16	18.74	78.72	0.27	2.89	49.25	0.14	32.26
SG4-1 rep 2	*L. hyperborea*	Hot plate	0.12	14.20	60.54	0.21	2.04	35.73	0.11	24.74
SG4-2 rep 1	*L. hyperborea*	Hot plate	0.29	9.75	472.36	0.20	4.67	42.63	0.03	40.96
SG4-2 rep 2	*L. hyperborea*	Hot plate	0.27	9.73	464.97	0.18	4.48	41.43	0.04	42.99
SG4-3	*L. hyperborea*	Hot plate	0.25	15.86	66.79	0.29	1.94	27.48	0.22	1.61
SS-1	*L. hyperborea*	Hot plate	0.15	9.52	37.71	0.48	1.67	21.25	0.14	0.29
SS-2	*L. hyperborea*	Hot plate	0.12	21.11	29.00	0.34	1.36	17.17	0.19	0.44
SS-3	*L. hyperborea*	Hot plate	0.16	15.08	40.55	0.35	1.75	20.62	0.20	0.38

Sample ID	Species	Digestion method	Metal concentration (mg/kg dw)							
			Cr	Mn	Fe	Ni	Cu	Zn	Cd	Pb
SS-4	*L. hyperborea*	Hot plate	0.18	17.34	74.84	0.28	1.63	20.33	0.16	0.67
SS-5	*L. hyperborea*	Hot plate	0.21	8.55	93.71	0.49	1.80	21.50	0.17	0.41

Table B1 | Sample trace metal concentrations (mg/kg dry weight). Values have been corrected for instrumental drift, dilution, procedural blank concentrations (microwave samples only), and sample mass. Replicate numbers are provided where applicable.

* Substituted values (half sample-specific MDLs).

Blank number	Digestion batch number	Digestion method	Metal concentration (ppb)							
			Cr	Mn	Fe	Ni	Cu	Zn	Cd	Pb
1	1	Microwave	2.06	1.48	19.97	1.01	6.64	64.69	0.01	5.30
2	2	Microwave	20.91	1.45	95.26	13.51	-1.62	13.47	0.00	0.65
3	3	Hot plate	0.09	-0.10	-0.67	-0.05	0.09	-0.42	-0.01	-0.16
4	3	Hot plate	53.14	2.33	278.00	466.90	1.07	8.30	0.00	0.16
5	3	Hot plate	-0.01	-0.10	-0.73	-0.02	-0.06	-0.53	0.00	-0.16
6	3	Hot plate	-0.01	-0.10	-0.72	-0.06	0.03	-0.27	0.00	-0.15
7	4	Hot plate	-0.03	-0.08	-1.02	-0.08	0.32	-0.34	0.00	-0.10
8	4	Hot plate	-0.02	-0.09	-1.13	-0.08	0.20	-0.21	0.00	-0.11
9	4	Hot plate	-0.02	-0.10	-1.19	-0.08	0.20	-0.55	0.00	-0.11
10	4	Hot plate	-0.03	-0.10	-1.16	-0.07	0.21	-0.48	0.00	-0.11
11	5	Hot plate	-0.02	-0.07	-0.85	-0.06	0.22	-2.71	0.00	-0.04
12	5	Hot plate	-0.02	-0.11	-1.01	-0.05	-0.25	-2.77	0.00	-0.05
13	5	Hot plate	-0.02	-0.09	-1.08	-0.06	-0.25	-2.75	0.00	-0.05

Table B2 | Procedural blank concentrations (ppb). Blank 1 was used to correct microwave results for batches 1 and 2, as Blank 2 exhibited extremely high concentrations. For batch 3, only Blanks 3, 5, and 6 were used to calculate MDLs. Blank 4 was excluded due to anomalously high values.

Appendix C: Evaluation of data normality

Metal	*W*	*p*-value	Normality
Cr	0.895	< 0.001	Violated
Mn	0.844	< 0.001	Violated
Fe	0.573	< 0.001	Violated
Ni	0.819	< 0.001	Violated
Cu	0.891	< 0.001	Violated
Zn	0.940	0.016	Violated
Cd	0.901	0.001	Violated
Pb	0.336	< 0.001	Violated

Table C1 | Shapiro–Wilk normality test results for blade/composite dataset (*n* = 48). $p \geq 0.05$ for normality to be met.

Metal	*W*	*p*-value	Normality
Cr	0.243	< 0.001	Violated
Mn	0.303	< 0.001	Violated
Fe	0.792	< 0.001	Violated
Ni	0.320	< 0.001	Violated
Zn	0.963	0.124	Met
Cd	0.662	< 0.001	Violated

Table C2 | Shapiro–Wilk normality test results for thallus-segmented dataset (*n* = 50). $p \geq 0.05$ for normality to be met.

Appendix D: Statistical test results

Metal	*ρ*	*p*-value	Trend downcoast
Cr	-0.265	0.103	No clear trend
Mn	-0.308	0.056	No clear trend
Fe	-0.591	< 0.001	Decreasing
Ni	-0.176	0.283	No clear trend
Cu	-0.685	< 0.001	Decreasing
Zn	-0.720	< 0.001	Decreasing
Cd	0.027	0.870	No clear trend
Pb	-0.464	0.003	Decreasing

Table D1 | Spearman's rank correlation coefficients assessing downcoast trends in trace metal concentrations from South Gare 1. Sample sizes: South Gare 1 (n = 3), South Gare 3 (n = 5), South Gare 4 (n = 3), South Gare 2 (n = 3), Redcar Beach 1 (n = 3), Redcar Beach 2 (n = 3), Cayton Bay (n = 10), Selwicks Bay Deep (n = 4), Selwicks Bay Shallow (n = 5).

Metal	*W*	*p*-value
Cr	18	0.064
Mn	20	0.020
Fe	15	0.270
Ni	20	0.020
Cu	18	0.066
Zn	20	0.020
Cd	20	0.020
Pb	20	0.020

Table D2 | Wilcoxon rank-sum test results assessing differences in trace metal concentrations between two depths. Sample sizes: Selwicks Bay Deep (n = 4), Selwicks Bay Shallow (n = 5).

Metal	*W*	*p*-value
Cr	14	0.916
Mn	0	0.012
Fe	23	0.037
Ni	3	0.046
Cu	25	0.012
Zn	25	0.012
Cd	0	0.007
Pb	11	0.835

Table D3 | Wilcoxon rank-sum test results assessing differences in trace metal concentrations between *Laminaria* spp. from Cayton Bay. Sample sizes: *L. digitata* (*n* = 5), *L. hyperborea* (*n* = 5).

Metal	*W*	*p*-value
Cr	2	0.061
Mn	1	0.037
Fe	0	0.020
Ni	0	0.020
Cu	8	0.712
Zn	16	0.178
Cd	20	0.020
Pb	8	0.623

Table D4 | Wilcoxon rank-sum test results assessing differences in trace metal concentrations between *Fucus* spp. from Cullercoats Beach. Sample sizes: *F. vesiculosus* (*n* = 4), *F. serratus* (*n* = 5).

Metal	Segment 1	Segment 2	*z*	Adjusted *p*-value*
Cr	Blade	Meristem	-2.383	0.103
Cr	Blade	Holdfast	0.564	0.642
Cr	Blade	Stipe	-0.465	0.642
Cr	Holdfast	Meristem	-1.874	0.183
Cr	Holdfast	Stipe	-0.793	0.642
Cr	Meristem	Stipe	1.667	0.191
Mn	Blade	Meristem	-1.138	0.383

Mn	Blade	Holdfast	2.539	0.022
Mn	Blade	Stipe	-0.584	0.629
Mn	Holdfast	Meristem	-3.042	0.014
Mn	Holdfast	Stipe	-2.737	0.019
Mn	Meristem	Stipe	0.483	0.629
Fe	Blade	Meristem	-2.618	0.053
Fe	Blade	Holdfast	0.353	0.724
Fe	Blade	Stipe	-2.088	0.110
Fe	Holdfast	Meristem	-1.780	0.150
Fe	Holdfast	Stipe	-1.488	0.205
Fe	Meristem	Stipe	0.462	0.724
Ni	Blade	Meristem	-1.777	0.227
Ni	Blade	Holdfast	0.893	0.441
Ni	Blade	Stipe	-0.894	0.441
Ni	Holdfast	Meristem	-1.829	0.227
Ni	Holdfast	Stipe	-1.342	0.359
Ni	Meristem	Stipe	0.770	0.441
Zn	Blade	Meristem	-1.904	0.068
Zn	Blade	Holdfast	-3.265	0.007
Zn	Blade	Stipe	-2.081	0.068
Zn	Holdfast	Meristem	2.055	0.068
Zn	Holdfast	Stipe	1.957	0.068
Zn	Meristem	Stipe	-0.154	0.878
Cd	Blade	Meristem	2.880	0.024
Cd	Blade	Holdfast	2.427	0.046
Cd	Blade	Stipe	2.245	0.050
Cd	Holdfast	Meristem	-0.719	0.567
Cd	Holdfast	Stipe	-1.069	0.428
Cd	Meristem	Stipe	-0.554	0.579

Table D5 | Dunn's test results assessing differences in trace metal concentrations between thallus segments. Sample sizes: holdfast (*n* = 3), stipe (*n* = 12), meristem (*n* = 12), blade (*n* = 23).

* Adjusted *p*-values calculated using Benjamini-Hochberg correction.

Metal	*ρ*	*p*-value	Trend along thallus
Cr	-0.758	< 0.001	Decreasing
Mn	-0.686	0.001	Decreasing
Fe	-0.818	< 0.001	Decreasing
Ni	-0.564	0.012	Decreasing
Zn	0.418	0.075	No clear trend
Cd	0.350	0.142	No clear trend

Table D6 | Spearman's rank correlation coefficients assessing trends in trace metal concentrations from holdfast to meristem 1. Sample sizes: holdfast (*n* = 3), stipe 1 (*n* = 4), stipe 2 (*n* = 4), stipe 3 (*n* = 4), meristem 1 (*n* = 4).

Metal	*ρ*	*p*-value	Trend along thallus
Cr	0.670	< 0.001	Increasing
Mn	0.435	0.009	Increasing
Fe	0.672	< 0.001	Increasing
Ni	0.615	< 0.001	Increasing
Zn	0.368	0.030	Increasing
Cd	-0.766	< 0.001	Decreasing

Table D7 | Spearman's rank correlation coefficients assessing trends in trace metal concentrations from meristem 1 to blade tip. Sample sizes: meristem 1 (*n* = 6), meristem 2 (*n* = 3), meristem 3 (*n* = 2), meristem 4 (*n* = 1), blade 1 (*n* = 6), blade 2 (*n* = 5), blade 3 (*n* = 5), blade 4 (*n* = 5), blade 5 (*n* = 1), blade 6 (*n* = 1).

Metal	*W*	*p*-value
Cr	402	0.013
Mn	328	0.341
Fe	368	0.075
Ni	318	0.455
Zn	214	0.176
Cd	110	<0.001

Table D8 | Wilcoxon rank-sum test results assessing differences in trace metal concentrations between *Laminaria* spp. from Cullercoats Beach. Sample sizes: *L. digitata* (*n* = 33), *L. hyperborea* (*n* = 17).